The C9orf72 dipeptide repeat protein poly-glycine-alanine sequesters nucleoporins and disrupts nuclear membranes

Karl Richter

PSL
UNIVERSITÉ PARIS

THÈSE DE DOCTORAT
DE L'UNIVERSITÉ PSL

Préparée à l'Institut Curie et Biogen

La protéine répétée dipeptidique poly-glycine-alanine de C9orf72 séquestre les nucléoporines et perturbe les membranes nucléaires.

The C9orf72 dipeptide repeat protein poly-glycine-alanine sequesters nucleoporins and disrupts nuclear membranes.

Soutenue par
Karl RICHTER
Le 28 novembre 2022

Ecole doctorale n° 562
Bio Sorbonne Paris Cité

Spécialité
Biologie cellulaire et moléculaire
UMR 144

Composition du jury :

Fen-Biao, GAO Professor, U. Massachusetts	*Président/Rapporteur*
Leonard, PETRUCELLI Professor, Mayo Clinic	*Rapporteur*
Alex, BAFFET Directeur de Research, Institut Curie	*Examinateur*
Morwena, LATOUCHE Professeur adjoint, EPHE/ICM	*Examinateur*
Graça, RAPOSO Directeur de Research, Institut Curie	*Directrice de thèse*
Sophie, PARMENTIER BATTEUR Vice-president, Biogen	Co-*Directrice de thèse*

institut Curie | PSL

1. Summary

The most common cause of familial amyotrophic lateral sclerosis (ALS) and a frequent cause of frontotemporal dementia (FTD) is a mutation in the non-coding region of the gene known as C9ORF72. The mutation is an expansion of GGGGCC hexanucleotide repeat between exons 1A and 1B in the C9ORF72 gene, but how this mutation causes neurodegeneration is unknown. Three different mechanisms have been hypothesized for the role of the C9ORF72 expansion mutation in the pathophysiology of the disease. First, the presence of the expansion reduces the amount of full-length protein produced (haploinsufficiency). Second, the repeat DNA sequence is transcribed into repeat RNA, which forms abnormal tertiary structures and can cause damage by binding and sequestering RNA binding proteins. Finally, despite being in a non-coding region, the repeat RNA is translated into five distinct dipeptide repeat proteins (DPR) from sense [poly-GA (glycine–alanine), poly-GP (glycine–proline), poly-GR (glycine–arginine) and antisense poly-GP (glycine–proline), poly-PR (proline–arginine), and poly-PA (proline–alanine)] strands. These DPRs accumulate in various parts of the central nervous system of C9ORF72 ALS/FTD patients. However, the pathogenic contribution of DPR-associated toxicity to disease progression is still unknown. In addition, the relative contribution of each individual DPR remains unclear. This work particularly focuses on the role of one of these dipeptides repeats, poly-GA, for several reasons. First, poly-GA is the most abundant DPR found in postmortem tissues from C9ORF72 ALS/FTD patients. Second, other than the arginine-containing DPRs, poly-GA is the most toxic of the five DPRs in both in vitro and in vivo disease models. Finally, targeting poly-GA protein with an antibody increased survival and rescued neurodegeneration in a study of transgenic mice expressing human C9ORF72 from a bacterial artificial chromosome (BAC).

My thesis research aimed to investigate how poly-GA may cause damage to neurons in the course of C9ORF72-related ALS pathology. In particular, I examined the effect of poly-GA on elements of nucleocytoplasmic transport machinery and nuclear membrane health in a simple cell line system, then in a disease relevant C9ORF72 ALS patient-derived iPSC motor neuron model.

Finally, I tested the effect of an antibody-based therapeutic strategy targeting the specific reduction of poly-GA in the C9ORF72 ALS motor neurons in an effort to understand how poly-GA may impact neurodegeneration.

In the first part of my research work, I established a cellular model of poly-GA accumulation in a HEK293 cell line. This model was used to test a hypothesized mechanism of toxicity related to the direct impairment of nuclear pores. The study revealed that poly-GA sequesters a subset of nucleoporins away from the nuclear membrane. I then used a more disease-relevant model of C9ORF72 ALS patient-derived motor neurons that integrates the complexity of the C9ORF72-associated pathology. The characterization of this model led to the evidence of disruption of nuclear membranes with ectopic nuclear pores not previously described in ALS motor neurons. Moreover, two of the nuclear pore proteins found to be sequestered in the HEK293 cells were positively correlated with the amount of poly-GA expressed by the C9ORF72 motor neurons. These data suggest that poly-GA in the nuclear membrane could led to the dysfunction of nuclear pores. In a third part, I examined the consequences of poly-GA on neurodegeneration in C9ORF72 motor neurons. Since patient-derived motor neurons did not exhibit spontaneous neurodegeneration under basal growth conditions, the cells were treated with a protein synthesis inhibitor, challenging the homeostatic ability of the neurons. This cellular stress revealed an increased susceptibility of the C9ORF72 motor neurons to neurodegeneration as compared to control cultures derived from healthy donors. In this model, chronic treatment with an antibody targeting poly-GA DPRs did not produce a protective effect.

In conclusion, the results from these two cellular models provide some insight on cells' abilities to process large, mature poly-GA protein aggregates in HEK cells versus misfolded but not yet aggresome-located poly-GA DPRs in immature neurons. Perspectives of this work speculate on potential additional ways that C9ORF72 repeat expansion causes neurodegeneration in ALS and thoughts about which research lines might be productive.

Table of Contents

Table of Figures and Tables

2. Abbreviations

Gene and protein names and abbreviations follow conventional nomenclature, with the OMIM (Online Mendelian Inheritance in Man) and UniProt (www.uniprot.org) as references.

ALS…….Amyotrophic lateral sclerosis
BAC……..Bacterial artificial chromosome
C9orf72..HGNC approved gene symbol for “Chromosome 9, open reading frame 72”
C9 ALS/FTD……C9orf72-linked amyotrophic lateral sclerosis/frontotemporal dementia
CNS……..Central nervous system
CSF…….Cerebrospinal fluid
DIV ……Days *in vitro*
DPR……..Dipeptide repeat protein
ER……..Endoplasmic reticulum
fALS……..Familial ALS
GA……..Glycine–alanine
GR……..Glycine–arginine
GP……..Glycine–proline
IF……..Immunofluorescence
IPS…….Induced pluripotent stem
Nups…….Nucleoporins
PBS…….Phosphate buffered saline
PLA…….Proximity ligation assay
PA……..Proline–alanine
PR……..Proline–arginine
sALS……..Sporadic ALS
SOD1…….Superoxide dismutase 1
SQSTM1..Sequestosome 1, also known as P62
STED……..Stimulated-emission depletion (microscopy)
TBS…….Tris-buffered saline
TDP-43…..Transactive response DNA-binding protein 43

3. Introduction

Amyotrophic lateral sclerosis (ALS), also known as motor neuron disease, is a rare, progressive, and fatal neurodegenerative disease characterized by the degeneration of motor neurons of the brain and spinal cord. This loss of functioning motor neurons gradually results in paralysis. Patient survival is highly variable, but the average time from symptom onset to death is 3-4 years (Couratier et al., 2016). There is no approved treatment to reverse damage to motor neurons or cure ALS. However, symptomatic treatments can help prevent unnecessary complications, and make living with the disease easier.

The first symptoms noted by patients are often muscle stiffness or weakness in the limbs, gradually followed by increasing weakness, wasting, and paralysis of the muscles (Traxinger, Kelly, Johnson, Lyles, & Glass, 2013). Symptoms usually begin with limb muscle weakness (spinal onset) but can begin with difficulty speaking or swallowing (bulbar onset, referring to the brain's medulla, which is also known as the bulb). Rarely, symptoms begin with muscles of the torso (Grad, Rouleau, Ravits, & Cashman, 2017). The disease is highly heterogenous in the location of first symptom, rate of progression, and underlying neuropathology, but always involves loss of motor neurons. In general, ALS is characterized by a loss of both upper and lower motor neurons. Specifically, "upper motor neurons" are the Betz cells in layer V of the primary motor cortex that are essential for voluntary movement. "Lower motor neurons" refers to the alpha motor neurons in the anterior horn of the spinal cord and motor neurons of the motor nuclei in the brainstem. Axonal degeneration is often detectable in the pathways projecting to the lower motor neurons from the cell bodies of the cortex and in the lower motor neuron projections of the peripheral nerves innervating the muscle (Grad et al., 2017).

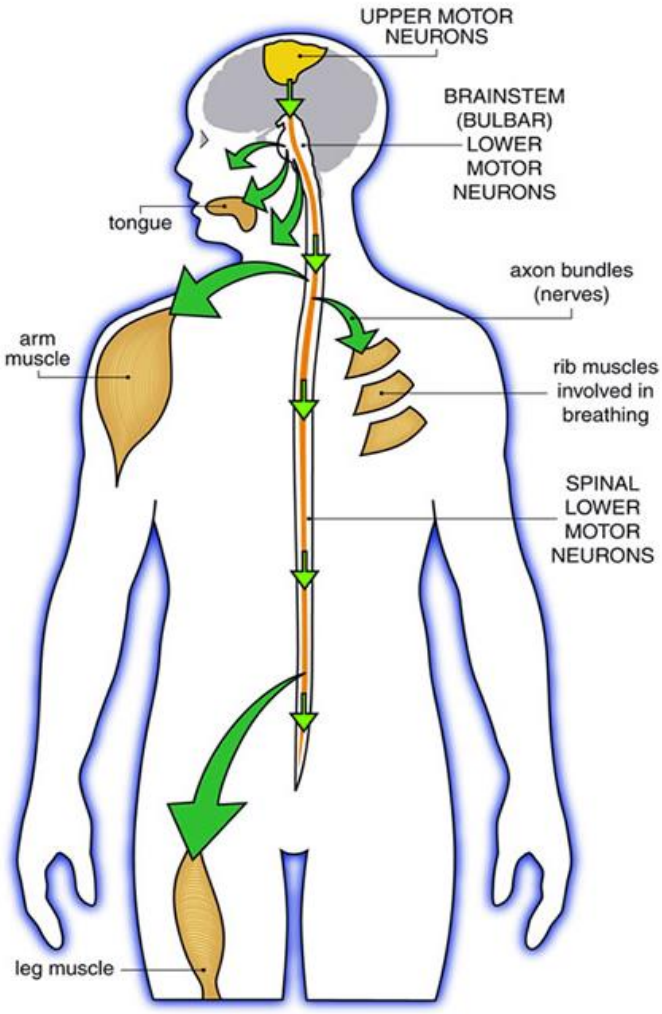

Source: tabletsmanual.com

Figure 3 . Upper and lower motor neurons. Upper motor neurons' cell bodies lie in the cortex and innervate lower motor neurons. The lower motor neurons, whether in the brainstem or spinal cord, innervate the muscles of the body.

3.1. ALS Disease overview

3.1.1. ALS Disease progression.

Early stages

Muscles

Muscles may be weak and soft, or they may be stiff and tight. Muscle cramping and twitching (fasciculation) occurs, as does atrophy. Symptoms may be limited to a single body region or mild symptoms may affect more than one region.

Physical effects

The person may experience fatigue, poor balance, slurred words, a weak grip, or tripping when walking. This stage may occur before a diagnosis is made.

Middle stages

Muscles

Symptoms become more widespread. Some muscles are paralyzed, while others are weakened or unaffected. Fasciculations may continue.

Physical effects

Unused muscles may cause contractures, in which the joints become rigid, painful, and sometimes deformed. If a fall occurs, the person may not be able to stand back up alone. Weakness in swallowing muscles may cause choking and greater difficulty eating and managing saliva. Weakness in breathing muscles can cause respiratory insufficiency, especially when lying down. Some people experience bouts of uncontrolled and inappropriate laughing or crying (pseudobulbar affect). Despite behavior, the person usually reports not feeling particularly sad or happy.

Late stages

Muscles

Most voluntary muscles are paralyzed. The muscles that help move air in and out of the lungs are severely compromised.

Physical effects

Mobility is extremely limited, and help is needed in caring for most personal needs. Poor respiration may cause fatigue, cognitive loss, headaches, and susceptibility to pneumonia. Speech, or eating and drinking by mouth, may not be possible. Respiratory insufficiency is the leading cause of death in ALS.

[This stage table is modified from information provided by the muscular dystrophy association. www.mda.org/disease/amyotrophic-lateral-sclerosis]

Table 1: Progressive disease stages in ALS

The rate at which patients suffer more severe symptoms is highly variable. Although mean survival time is 3-4 years, approximately 10–20% of ALS patients survive longer than 10 years (Chiò et al., 2009). Substantial effort has been devoted to improving prediction of disease progression for individual patients, and to categorizing known mutations with respect to their implications for prognosis. There are overall trends that can be applied generally by neurologists based on symptoms before more detailed genetic or biomarker tests are performed.

Predictors of progression include:

1) site of symptom onset, with bulbar or respiratory onset predicting faster deterioration,

2) the speed of symptom progression before neurological clinical assessment, with fast initial progression predicting a faster decline,

3) impaired cognitive executive function, also predicting a faster decline (Elamin et al., 2015).

Several rating scales have been developed to assess patient status. Currently, the most widely used and validated is the ALS Functional Rating Scale-Revised (ALS-FRS(R)) (Beswick et al., 2022). Change in the ALS-FRS(R) score over time is the most frequent way of defining disease progression. Several biomarkers have been proposed, with varying utility in diagnosis or prognosis, including plasma siRNA from extracellular vesicles (Banack, Dunlop, Stommel, Mehta,

& Cox, 2022), compound muscle action potential (CMAP) in the thenar muscle of the hand (Lu et al., 2022) and neurofilament light chain in cerebrospinal fluid (T. M. Miller et al., 2022). The latter may have utility in drug development (Carvalho, 2022).

The disease progresses with increasingly more muscle groups affected. Over time this progresses to muscles of respiration. Ultimately, most ALS patients die of respiratory failure (O. Hardiman et al., 2017).

3.1.2. Treatments

In the U.S., there are three approved treatments for ALS, riluzole (Rilutek™ and other formulations of riluzole), edaravone (Radicava™) and a combination of sodium phenylbutyrate and taurursodiol (Relyvrio™). All are considered to have only modest efficacy (R. G. Miller, Mitchell, & Moore, 2012; Witzel et al., 2022) (Fagan, 2022).

Riluzole is 6-(trifluoromethoxy)-2-benzothiazolamine

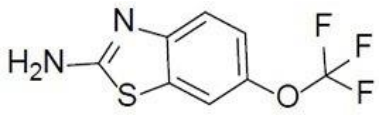

Riluzole has a complex pharmacology. *In vitro*, it is both an indirect and a direct glutamate antagonist and inhibitor of sodium channel NaV1.4 (Doble, 1996). It is believed to act *in vivo* as sodium channel blocker, an inhibitor of glutamate release, and a blocker of glutamate receptors (Doble, 1996; Nagoshi, Nakashima, & Fehlings, 2015). The rationale for its use in treating ALS is its anti-glutamatergic action in preclinical models. A review of trials of the compound in about 1500 patients (across three trials) found a 9% gain in the probability of surviving one year (49% placebo *vs.* 58% riluzole) and increased median survival from 11.8 to 14.8 months (R. G. Miller et al., 2012).

Edaravone is 3-methyl-1-phenyl-2-pyrazolin-5-one

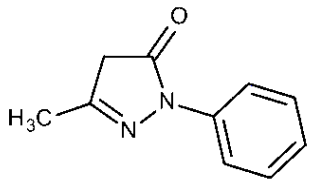

Edaravone is a purported free radical scavenger and inhibitor of the mitochondrial permeability transition pore (Rajesh, Sasaguri, Suzuki, & Maeda, 2003). It was in use in Japan as a treatment for ischemic stroke before its adoption as a potential treatment for ALS. Based on an apparent reduction in a marker of oxidation reaction products, 3-nitrotyrosine, in the CSF of treated patients in a small study (Yoshino & Kimura, 2006), the compound was advanced to a larger, placebo-controlled trial. In that study (K. Abe et al., 2014), a total of 200 patients were infused intravenously once per day with 60 mg edaravone or placebo for 24 weeks. The primary endpoint, the revised ALS functional rating scale (ALSFRS-R), was not significantly different in the treated group as compared with controls, but the results showed that disease progression in controls was slower than originally anticipated, thus reducing the power of the trial to detect a change. The sponsors then launched a new study with more strictly defined inclusion criteria, treating with the same dose of compound (Koji Abe et al., 2017). That study *did* find a statistically significant slower disease progression in edaravone-treated as compared with placebo-treated patients. The beneficial effect of edaravone in patients as measured by the ALSFRS-R was replicated in another study extending the treatment duration in some patients to 48 weeks. Nevertheless, the benefit is relatively modest and there are questions about the applicability to most ALS patients (Orla Hardiman & van den Berg, 2017) (Turnbull, 2018). Riluzole, but not edaravone, has been shown in randomized clinical trials to prolong survival.

The two-drug cocktail, Relyvrio™, was conditionally approved in Canada in June, 2022, and in the U.S. by the Food and Drug Administration (FDA) on 28 September, 2022, on the basis of a clinical trial published in 2022 (Sabrina Paganoni et al., 2022) and 2020 (S. Paganoni et al., 2020). Relyvrio is composed of active ingredients sodium phenylbutyrate and taurursodiol.

Sodium phenylbutyrate is 4-phenylbutyric acid, sodium salt.

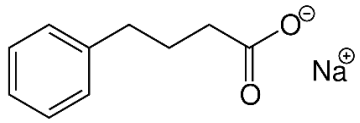

Taurursodiol is ursodoxicoltaurine a.k.a. tauroursodeoxycholic acid, a bile acid derivative.

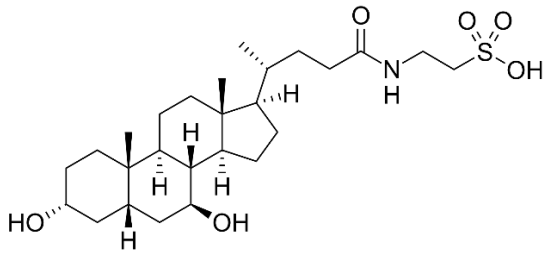

The proposed mechanism of action of the mixture was summarized by the company in three sentences in an appendix to (S. Paganoni et al., 2020) as follows:

"Endoplasmic reticulum stress or dysfunction associated with protein misfolding and aggregation has been implicated in the pathogenesis of ALS (Jaronen, Goldsteins, & Koistinaho, 2014), as has disruption of mitochondrial function and structure (Mehta et al., 2019). Sodium phenylbutyrate is a histone deacetylase inhibitor that has been shown to upregulate heat shock proteins and act as a small molecular chaperone, thereby ameliorating toxicity from endoplasmic reticulum stress (Kaur et al., 2018), (Suaud et al., 2011). Taurursodiol recovers mitochondrial bioenergetic deficits through several mechanisms, including by preventing translocation of the Bax protein into the mitochondrial membrane, thus reducing mitochondrial permeability and increasing the apoptotic threshold of the cell (Rodrigues, Solá, Sharpe, Moura, & Steer, 2003)."

There is also other support for the use of tauroursodeoxycholic acid. It has been shown to promote the outgrowth of neurites in human iPSC-derived motor neurons and mouse motor neurons challenged with the ER stress-inducing compound, cyclopiazonic acid (Thams et al., 2019). It was also active *in vivo* at reducing denervation of the tibialis muscle in mice expressing $hSOD1^{G93A}$, a mouse model of human ALS caused by a mutation in the SOD1 gene (Thams et al., 2019). Other mechanisms have been proposed for a general neuroprotective effect in other neurodegenerative disease models (Khalaf, Tornese, Cocco, & Albanese, 2022). The basis of approval was the clinical findings produced in a trial supported by the Northeast Amyotrophic Lateral Sclerosis Consortium and the drug sponsor, Amylyx Pharmaceuticals. In the trial (S. Paganoni et al., 2020), the mean rate of change in the ALSFRS-R score was −1.24 points per month with the drug and −1.66 points per month with placebo (difference=0.42 points per month; 95% confidence interval=0.03 to 0.81; P = 0.03). For context, the overall rate of decline in the patients before the trial was 0.94 points per month. In an open-label extension of the trial, active drug administration prolonged survival time free of tracheostomy or permanent assisted ventilation by 7.3 months as compared with placebo (Sabrina Paganoni et al., 2022). A phase III trial, PHOENIX (NCT05021536), is ongoing as of October, 2022.

3.1.3. Causes of disease

In most patients, the cause of the disease is unknown. In approximately 10% of patients, there is a known family history, so the disease in these cases is often called familial ALS (fALS). Beginning with the discovery of a mutation in the gene SOD1 (Rosen et al., 1993), specific mutations have been identified in some ALS kindreds with recognized inheritance patterns, further establishing the idea of familial ALS. It is important to note that there can be incomplete penetrance and an only probabilistic effect of genotype on phenotype (O. Hardiman et al., 2017), making the understanding of inheritance pattern more difficult. The categorization into “sporadic” and “familial” arose from the observation of clear inheritance patterns of the disease without the knowledge of the underlying genetics. However, the use of the sporadic vs. familial suggests a distinction that is an oversimplification. If approached from the point of view of “what is the risk that this person will develop ALS?” there is in fact a range of risk associated with a

variety of known genetic markers (Al-Chalabi et al., 2010), (Ryan, Heverin, McLaughlin, & Hardiman, 2019), (Trabjerg et al., 2020), (S. Zhang et al., 2022). Recent evidence suggests that in all ALS cases, whether categorized as sporadic or familial, about 50% of the risk of developing ALS is heritable (Wingo, Cutler, Yarab, Kelly, & Glass, 2011), (Ryan et al., 2019), (Trabjerg et al., 2020). An interaction of genes with environment is also possible, with some genes possibly contributing to an increased risk factor. The role of environmental toxins, head trauma and other non-genetic factors in ALS generally is possible and is also an active area of research (O. Hardiman et al., 2017).

The most common genes clearly associated with ALS, as summarized in 2017 (O. Hardiman et al., 2017), are summarized below:

Gene symbol	Name, synonym, or description	Speculated role
ALS2	alsin	Endosomal trafficking
ANG	angiogenin	RNA metabolism
ATXN2	ataxin 2	RNA metabolism
C9orf72	Chromosome 9 open reading frame 72	RNA metabolism and autophagy
CHCHD10	coiled-coil-helix-coiled-coil-helix domain-containing 10	Mitochondrial maintenance
CHMP2B	charged multivesicular body protein 2B	Endosomal trafficking
ERBB4	receptor tyrosine-protein kinase erbB 4	Neuronal development
FIG4	polyphosphoinositide phosphatase	Endosomal trafficking
FUS	fused-in-sarcoma	RNA metabolism
HNRNPA1	heterogeneous nuclear ribonucleoprotein A1	RNA metabolism
MATR3	matrin 3	RNA metabolism
OPTN	optineurin	Autophagy
PFN1	profilin 1	Cytoskeleton
SETX	senataxin	RNA metabolism
SIGMAR1	sigma non-opioid intracellular receptor 1	UPS and autophagy
SOD1	superoxide dismutase 1	Oxidative stress
SQSTM1	sequestosome 1	Autophagy
TARDBP	TAR DNA-binding protein 43	RNA metabolism
TBK1	serine/threonine-protein kinase TBK1	Autophagy
TUBA4A	tubulin α4A	Cytoskeleton
UBQLN2	ubiquilin-2	UPS and autophagy
VAPB	vesicle-associated membrane protein-associated protein B/C	Endoplasmic reticulum stress
VCP	valosin-containing protein	Autophagy

Table 2: ALS risk genes

However, using genome-wide association studies (GWAS), machine learning, and profiling of patient-derived stem cells, a more recent analysis has detected **690** genes contributing to the risk of ALS (S. Zhang et al., 2022).

Of familial ALS cases, the most common cause is a mutation in the gene C9orf72 (chromosome 9, open reading frame 72)**.** This mutation is responsible for approximately 40% of fALS and 7% of sALS (Renton, Chiò, & Traynor, 2014). Not only does this mutation cause ALS, it is also responsible for about 25% of cases of frontotemporal dementia (FTD) (Van Langenhove, van der Zee, & Van Broeckhoven, 2012). Frontotemporal dementia is a form of early-onset dementia caused by degeneration in the frontal and anterior temporal lobes (Bang, Spina, & Miller, 2015), resulting in deficits in language and cognitive and executive function. In fact, C9orf72 mutations cause a spectrum of disease, with motor neuron degeneration leading to motor dysfunction at one end and purely cognitive and behavioral dysfunction at the other, with many patients suffering from a combination of these symptoms (Starr & Sattler, 2018). Such patients are typically first diagnosed with ALS or FTD depending on their presenting symptoms.

3.2. Physiology and pathology of C9orf72

3.2.1. C9orf72 Gene

The mutation in C9orf72 that causes ALS or FTD is a hexanucleotide GGGGCC (G4C2) repeat expansion in an intron of the gene between exons 1a and 1b (DeJesus-Hernandez et al., 2011; Ian R. Mackenzie et al., 2013; Renton et al., 2011). C9orf72 refers to the gene's location on chromosome 9 in open reading frame 72. The gene consists of 11 exons with two alternative start sites.

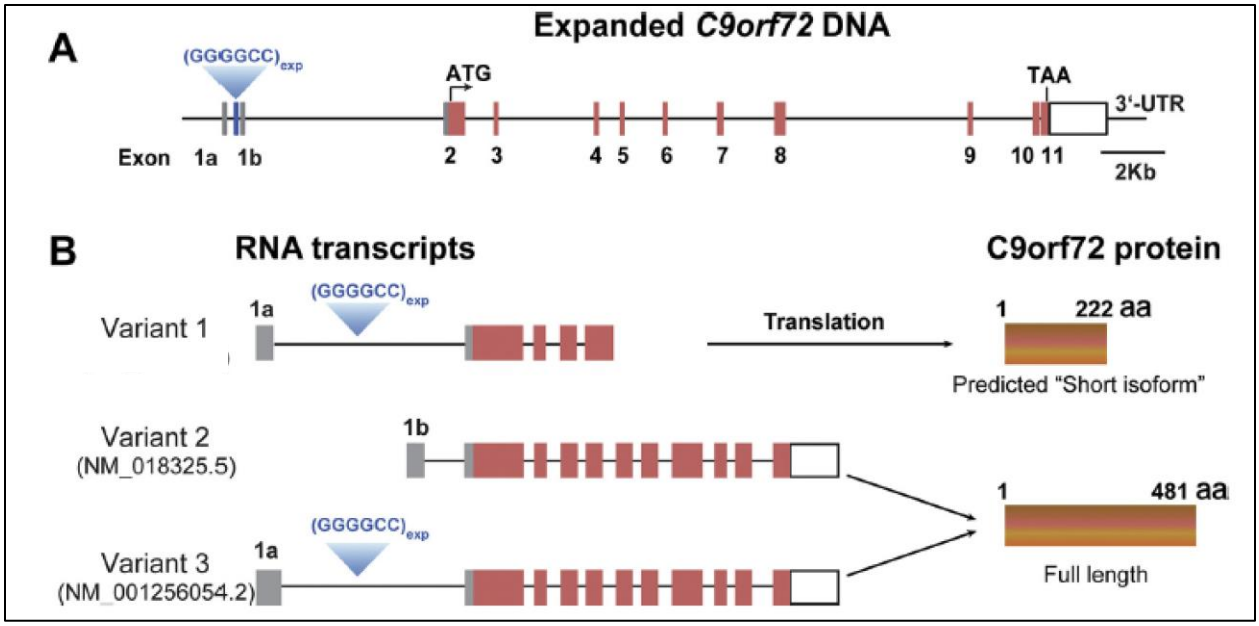

Figure 4. C9orf72 gene with repeat expansion produces at least three transcripts resulting in at least two protein isoforms. Modified from (McEachin, Parameswaran, Raj, Bassell, & Jiang, 2020).

C9orf72 is highly conserved across vertebrate species. The human gene is 99% similar to dog gene and 97% similar to the opossum gene ((Safran et al., 2021) www.genecards.org), 84% similar to Xenopus; but only 15% similar to C. elegans and with no known similarity in the Drosophila genome (Smeyers, Banchi, & Latouche, 2021). C9orf72 is expressed at similar levels in most tissues in humans ((Uhlén et al., 2015) www.proteinatlas.org). It is expressed in the CNS, with the highest CNS expression in the retina. Highest expression by cell type is in CD14+ monocytes (Rizzu et al., 2016). Its expression is reduced in carriers of the hexanucleotide repeat expansion (Rizzu et al., 2016), a fact that may be important for understanding the pathophysiology of the disease.

3.2.2. Role of C9orf72 protein

The physiological roles of the C9orf72 proteins are incompletely understood. The longer isoform of approximately 54 kDa forms a complex with proteins SMCR8 and WDR41. Together, this trimer regulates autophagy at several steps in the autophagic pathway (Corbier & Sellier, 2017). The trimer also acts as a GTPase Activator Protein (GAP), which in turn regulates several small GTPases (Tang, Sheng, Xu, Yan, & Qi, 2020). These GTPases play a role not only in autophagy, but also other processes, such as actin dynamics and vesicular trafficking (reviewed

by (Pang & Hu, 2021) and (Smeyers et al., 2021), thus greatly expanding the possible physiological roles of C9orf72. One or both isoforms are also important in several processes in inflammation (Smeyers et al., 2021). Knockout of C9orf72 in mouse models has repeatedly produced an inflammatory phenotype (Burberry et al., 2016; O'Rourke et al., 2016), including splenomegaly, increased neutrophils, increased cytokines, and premature death. The short isoform has been reported only in humans, where it was localized to the nuclear membrane and appeared to be mislocalized to the cell membrane in a small sample of ALS cases (Xiao et al., 2015).

3.2.3. The mutation: C9orf72 repeat expansion

In healthy individuals, the G4C2 repeat in C9orf72 comprises most frequently from two to 25 repeats (DeJesus-Hernandez et al., 2011). In ALS-FTD patients with C9orf72 expansion mutation, the number of repeated units can be in the order of hundreds to thousands (DeJesus-Hernandez et al., 2011), (Renton et al., 2011).

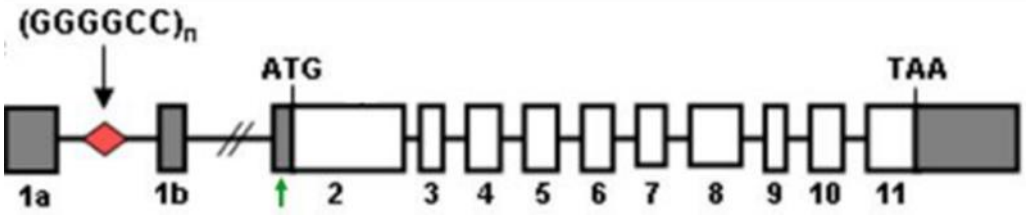

Figure 3. Hexanucleotide repeat expansion in C9orf72. The repeat expansion is in a normally noncoding region of the gene between exons 1a and 1b. From (DeJesus-Hernandez et al., 2011).

The repeat expanded region is transcribed in the absence of an ATG start site in both the sense and anti-sense direction. RNA transcripts from both directions accumulate in patient CNS (Zu et al., 2013). Despite being located in an intron, these sense and anti-sense transcripts were found to produce dipeptide repeat-containing proteins (DPRs) (Zu et al., 2011), (Zu, Liu et al. 2013). The sense transcript (containing 5'-G4C2-3' hexanucleotide repeats) was found to be translated through repeat-associated non-ATG (RAN) translation to produce poly-(Gly-Ala) (GA), poly-(Gly-

Pro) (GP), and poly-(Gly-Arg) (GR) proteins. The antisense transcript (containing 5'-G2C4-3' hexanucleotide repeats) was found to be translated through repeat-associated non-ATG (RAN) translation to produce poly-(Pro-Ala) (PA), poly-(Pro-Arg) (PR), poly-(Gly-Pro) (GP) proteins.

3.2.4. Possible mechanisms of pathophysiology

There are at least three mechanisms by which an intronic repeat expansion in C9 could cause disease. First, the intronic mutation could cause a reduction in the amount of full-length, canonical C9orf72 gene product (haploinsufficiency). Second, the repeat region is transcribed, forming GC-rich RNA transcripts that may cause toxicity (Xu et al., 2013). Finally, abnormal dipeptide repeat (DPR) proteins accumulate in patient brain early in disease. There has been much research to understand the relative roles these proteins play in the disease. We focus our work in studying the role of poly-GA primarily because of its high expression levels in the disease. Poly-GA was found to be the most abundant of the dipeptide repeat proteins (DPR) inclusions in patient tissue at autopsy (Lee et al., 2017; I. R. Mackenzie et al., 2015). In addition, in two animal models producing endogenous RAN translation of the C9 repeat sequence, poly-GA was the most common inclusion (J. Chew, Tania F. Gendron, Mercedes Prudencio, Hiroki Sasaguri, Yong-Jie Zhang, et al., 2015). The possible roles of poly-GA and the other DPRs will be discussed below.

3.2.4.1. Evidence for haploinsufficiency and its role in disease

Several lines of evidence show that the repeat expansion in the intron between exon 1A and 2 could cause a loss of canonical C9 mRNA and protein. The first report from DeJesus-Hernandez and collaborators (DeJesus-Hernandez et al., 2011) detected a change in transcript levels but not in protein. These results were confirmed by other authors describing a decrease of the long isoform of C9 protein in frontal cortex (but not motor cortex or spinal cord) of C9 ALS patients (Saberi et al., 2018; Xiao et al., 2015) associated with an increase of the short C9 protein isoform in frontal and temporal cortex using western blot (Xiao et al., 2015). The decreased amount of

long form C9 protein was further validated using an antibody-free method to prevent any uncertainty due to the lack of highly specific, validated antibodies (Viodé et al., 2018).

The question of the role of the C9 protein in the disease has been investigated using a range of techniques from genetic human data to transgenic rodent and patient-derived iPSC models. In a cohort of 389 ALS patients, no evidence for LOF mutations was found other than the repeat expansion (Harms et al., 2013). Two human cases of homozygous mutations in C9 have been reported, and their symptoms or disease progression were not substantially worse than that of heterozygotes (Cooper-Knock et al., 2013; Fratta et al., 2013). In mice, several groups saw little or no effect of C9 reduction on motor behavior or neuron loss, either by knock-out (Koppers et al.) or using antisense oligonucleotides (ASO). However, the loss of C9 protein could still play a role in the disease in the presence of repeat expansion or other insult. Dong and collaborators created a rat model of C9 knocked down using CRISPR of portions of exon2 and intron2 (W. Dong et al., 2021). Rats with C9 knockdown had enlarged spleens and cervical lymph nodes but no detected motor deficit. When chronically treated with 4 mg/kg kainic acid, a glutamate agonist, for 4 or 6 weeks, these rats suffered a loss of muscle coordination and grip strength. These deficits were not seen in wild type rats treated with the same kainic acid protocol or in the C9 knockout rats treated with vehicle. In fact, Shi and collaborators found that motor neurons differentiated from induced pluripotent stem cells derived from C9 ALS patients (iPSCMN-C9) were more susceptible to glutamate toxicity than iPSC MN derived from heathy individuals (iPSC MN-WT) (Y. Shi et al., 2018). This phenotype could be rescued by restoring the level of C9orf72 expression of in the iPSC MN-C9, showing that the survival deficit during the glutamate exposure was due to a loss of C9 protein. In addition, knockdown of C9 protein in iPSC MN-WT reproduced the deficit. Both the *in vitro* experiments on human iPSC MN and the rat model suggest a synergistic effect of C9 haploinsufficiency and excitotoxicity. This is consistent with earlier attempts to model ALS by reducing C9 protein in that loss of C9 alone did not cause deficits, but loss of C9 in combination with another insult synergize to produce a degenerative process in neurons. The functions of C9orf72 and evidence for its role in ALS-FTD was recently reviewed by (Smeyers et al., 2021), who concluded that there is substantial evidence for a role of C9 loss of function in ALS.

3.2.4.2. Evidence for the role of RNA foci in disease

Another mechanism by which a repeat expansion in the first intron of C9orf72 could harm the nervous system is the production of RNA transcripts from the G4C2 repeat region. RNA transcripts are produced in both the sense and anti-sense direction (DeJesus-Hernandez et al., 2011) and found in nucleus and cytoplasm of neurons and other cell types in several brain and spinal cord areas, including frontal cortex, hippocampus and cerebellum (Mizielinska et al., 2013). Both sense and anti-sense transcripts have been found in anterior horn neurons in cases of C9-ALS, with (Vatsavayai, Nana, Yokoyama, & Seeley, 2019) finding 78% of anterior horn neurons positive for antisense transcripts and a smaller proportion with sense transcripts.

There are several possible ways in which RNA foci could damage cells. One proposed mechanism is the sequestration, and therefore depletion, of RNA binding proteins. This has precedent in the case of myotonic dystrophy, in which RNA transcripts from a repeat CTG expansion in the DM1 gene are known to bind and deplete MBNL1 protein (J. W. Miller et al., 2000). In ALS, there is evidence for the binding or sequestration of ADARB2, ALYREF, nucleolin, pur-alpha, SRSF1 and SRSF2, and Zfp106 (McEachin, Parameswaran, et al., 2020), though none of these has been proven to be causative for ALS-FTD. The G4C2 RNA sequence also adopts a tertiary structure that confers unusual properties. In addition to RNA hairpins, the sequence forms a G-quadruplex, a three-dimensional aggregate that is particularly long-lasting and can interfere with normal RNA metabolism (Reddy, Zamiri, Stanley, Macgregor, & Pearson, 2013). G4C2 RNA in this configuration has been shown to bind RanGAP1 (K. Zhang et al., 2015), a key regulator of nucleocytoplasmic transport. This would lead to a relative loss of RanGAP1 in the cytoplasm near the nucleus, causing a reduction in nuclear import of proteins. This has been shown for TDP-43 in C9 ALS-derived iPSC neurons (K. Zhang et al., 2015). On the other hand, some have proposed that nuclear RNA foci could be protective by sequestering the repeat RNA in the nucleus and preventing its translation into more toxic dipeptide repeat proteins in the cytosol (Tran et al., 2015).

It is also possible that the aberrant RNA species could produce toxicity through a gain-of-toxic-function not involving sequestration of known RNA binding proteins. It is conceivable, for

example, that RNA transcribed from the repeat expansion forms a stable structure that inhibits the export of properly spliced mRNA out of the nucleus, or impairs nucleolar function, possibly by disrupting the phase separation that characterizes healthy nucleoli. In fact, nucleolin has been found to bind G-quadruplexes (Santos, Salgado, Cabrita, & Cruz, 2022).

3.2.4.3. Evidence for the role of dipeptide repeat proteins in disease

The five RAN dipeptide repeat proteins vary in their regional expression and protein properties.

DPR	Physical /chemical properties	Cellular toxicity
GA	Uncharged, forms aggregates	Moderate
GP	Uncharged, polar, highly soluble	Non-toxic
GR	Highly charged, polar	High
PA	Uncharged, polar	Non-toxic
PR	Highly charged, polar	High

Table 3: Properties of dipeptide repeat proteins

(Kwon & Xian, 2014), (Gill, Wang, Levine, Premasiri, & Vieira, 2019), (Freibaum & Taylor, 2017)

There is uncertainty about which of the DPR may be the most important for the disease process. The arginine-containing proteins (poly-GR, poly-PR) have been shown to be acutely toxic in cells and when expressed in *Drosophila* eye (Mizielinska, Grönke, & Niccoli, 2014) or when added exogenously to neurons (Wen et al., 2014). Poly-GP and Poly-PA have rarely produced toxicity (Mizielinska et al., 2014). Poly-GA is the most abundant of the DPRs in the CNS of ALS patients

(Mackenzie, Frick et al. 2015) (Lee, Baskaran et al. 2017). It is less rapidly toxic that GR or PR in some systems (Mizielinska et al., 2014), but its toxicity may be more relevant for the disease. For example, when expressed in mice, poly-GA but not poly-PR produced ALS-like symptoms (LaClair et al., 2020).

3.2.4.4. Role of repeat proteins vs. RNA foci in the disease

Regardless of the exact species of DPR, there have been several efforts to determine the relative importance of RAN translated proteins vs. repeat-containing RNA in the disease process. To do this, several groups have prepared RNAs with an ATG start sequence with codons that avoid G4C2 content, but still code for a long sequence of any one of the DPRs, sometimes called "codon optimized" constructs. These are designed to produce DPRs with no repeat RNA. Conversely, other sequences have been designed that contain a large amount of G4C2, but contain stop codons in all three reading frames in both directions, so that at most short sequences of a few amino acids could be produced, but much of the tertiary structure of the RNA remains. Using this method in *Drosophila*, it was found that long repeat RNA did not produce DPR, but could bind RNA binding proteins without any associated toxicity (Moens et al., 2018). These data suggested that repeat RNA was unlikely to play a key role in disease. Using different methods but still in *Drosophila* model, other authors reached a similar conclusion (Tran et al., 2015). However, these results were challenged by the findings in other models such as zebrafish (Swinnen et al., 2018) and SH-SY5Y cells (Lee et al., 2013) showing toxicity of repeat RNA in the absence of RAN-translated DPR. Therefore, the relative roles of repeat RNA and dipeptide repeat proteins in the progression of human ALS and FTD are still unclear.

3.2.4.5. Role of the various DPRs – Evidence of poly-GA toxicity

The relative contribution of each DPR to disease pathogenesis remains unclear. However, several lines of evidence from both *in vitro* and *in vivo* experiments suggest that the toxicity of poly-GA repeat peptides in particular could be a major mechanism of C9-induced pathology.

In vitro models

When all five dipeptide proteins with 125 repeats were expressed in HEK cells, only poly-GA produced PARP cleavage and resulted in the formation of TDP-43 fragments in a dose-responsive manner (Lee et al., 2017). When the same constructs were electroporated into embryonic chick spinal cord, poly-GA was the most toxic of the dipeptide repeat proteins when assessed 24 hrs. later. Poly-GA has also been reported to cause damage *in vitro* in primary neurons. When a GA149 repeat was expressed via lentivirus in rat hippocampal neurons, the poly-GA produced not only the SQSTM-positive aggregates reported in many cell types, but also reduced the dendritic branching of the neurons, and increased the number of caspase-positive cells in culture (May et al., 2014).

In vivo models

In mice, the expression of moderate amounts of CFP-tagged poly-GA149 resulted in GA inclusions in deep cerebellar nuclei, and in motor neurons and interneurons of the spinal cord and brain stem (Schludi et al., 2017). However, there was no associated neuronal loss at six months of age. Pathological changes included an increase in TDP-43 phosphorylation, but no modification in motor neuron morphology or loss of choline acetyltransferase (ChAT) staining, a marker of motor neurons. The mice developed microglial activation but no astrogliosis in the spinal cord. Despite no apparent loss of motor neurons, the mice developed gait and balance impairments, but no loss of grip strength or rotarod performance (Schludi et al., 2017). Vaccinating these mice with ovalbumin-tagged poly-GA10 reduced inflammation, poly-GA aggregates in spinal cord anterior horn, and largely protected against motor deficits (Zhou et al., 2020).

Consistent with *in vitro* findings of acute toxicity of arginine-containing DPR, LaClair and collaborators compared congenic lines of mice expressing 175 repeats of poly-GA and poly-PR (LaClair et al., 2020). The PR mice developed two distinct phenotypes: either they showed ataxia and seizures but not muscle weakness; or they transcriptionally downregulated the transgene; in which case had no obvious phenotype and a normal lifespan. The poly-GA mice, by contrast, showed selective motor neuron loss, denervation of muscle and increased inflammation, all characteristics of human ALS. All the models just mentioned rely on DPR expressed from a

construct deliberately created to avoid G4C2 repeat RNA sequences. This methodology rules out a contribution of RNA toxicity; but also means that phenotypes observed potentially could result from toxic mechanisms not present in the human disease.

The most compelling evidence for the toxicity of poly-GA in an *in vivo* context was provided by the results using a BAC transgenic mouse with the full human C9orf72 sequence including a 500 repeat G4C2 expansion (Y. Liu et al., 2016). The transgene included a promoter region, including substantial flanking sequences. This mouse line developed neurodegeneration in the anterior horn of the spinal cord, in hippocampus, and cortex. Full-length C9orf72 and both sense and anti-sense transcripts were produced. These mice also displayed GA and GP DPR proteins and TDP-43 deposits. The mice developed motor deficits leading to paralysis (Y. Liu et al., 2016). When treated with an antibody against poly-GA (αGA1), these mice had reduced poly-GA protein. The antibody also reduced inflammation, reduced neurodegeneration in the anterior horn; partly protected against motor deficits, and prolonged survival (Nguyen et al., 2020).

In summary, Poly-GA is the most abundant DPR in the CNS of C9 expansion patients. Poly-GA can also co-aggregate with other DPR (McEachin, Gendron, et al., 2020), and is responsible for ALS-like degeneration in mouse models (LaClair et al., 2020). Finally, antibodies against poly-GA reduced not only poly-GA but also GP and GR and protected against motor neuron loss in a transgenic mouse model using a repeat-expanded human C9orf72 gene (Nguyen et al., 2020). For all these reasons, our work focuses on the mechanism of action of poly-GA and subsequent role in ALS disease pathology.

3.3. Poly-GA toxicity

3.3.1. Intrinsic Properties of poly-GA

Poly-GA is highly insoluble: a sequence of 100 GA units is predicted to have no probability of aqueous solubility when expressed in E. coli as calculated by U. Oklahoma algorithm (Harrison, 2009). Synthetic poly-GA with 15 repeats (GA(15)) rapidly formed fibrils in aqueous solvent

(Chang, Jeng, Chiang, Hwang, & Chen, 2016) which were shown to form beta pleated sheet conformation and stain with thioflavin and Congo Red as is common for amyloid proteins. Primary neurons transduced with a GA(175)-GFP fusion construct produced poly-GA that formed flat, twisted ribbons of 13–15 nm thickness, 20–80 nm width and highly variable length when examined in situ with cryo-EM (Guo et al., 2018). In human C9 patients at autopsy, (Y. J. Zhang et al., 2014) found poly-GA aggregates in several regions of the CNS, including hippocampus, cortex, cerebellum, thalamus, and spinal cord. In cerebellum, 15-17 nm wide GA+ filaments were found in cerebellar granule cells, most frequently in cytoplasm but also in the nucleus.

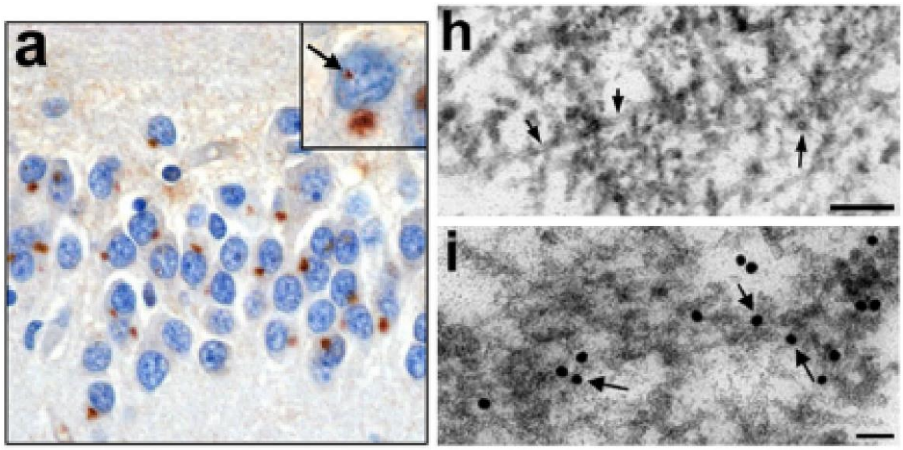

Figure 4. Poly-GA aggregates in brain of C9orf72 repeat expansion patient. Left (a) Immunohistochemical stain of poly-GA aggregates in the dentate fascia of hippocampus. Note both cytoplasmic and nuclear inclusions. **Right (h)** Conventional EM of granule cells of cerebellar cortex reveals 15-17 nm filaments. **(i)** Immuno-EM of the same tissue shows filaments labeled with poly-GA antibody coupled to 18 nm gold beads. From (Y. J. Zhang et al., 2014).

3.3.2. Anatomical location of poly-GA in human ALS/FTD

Poly-GA is the most abundant DPR inclusion in ALS/FTD. This is true both in frontal cortex and in spinal cord (I. R. Mackenzie et al., 2015). DPR have been found in neurons and ependymal cells lining the central canal, but not in astrocytes, oligodendrocytes, or microglia (Schludi et al., 2015).

DPR, including GA, can occur in pinealocytes and SCN neurons in ALS/FTD in the absence of TDP-43 pathology (Dedeene, Van Schoor et al. 2019). One cell can even contain more than one species of DPR (Mori et al., 2013).

Poly-GA is found in hippocampus, particularly the dentate gyrus, frontal cortex, temporal cortex, and granule cell and molecular cell layers of the cerebellum (Y.-J. Zhang et al., 2014); (I. R. Mackenzie et al., 2015). It is more abundant in these regions than in anterior horn neurons.

On a regional basis, poly-GA is not well spatially correlated with areas of degenerating neurons (Vatsavayai et al., 2019), but there is evidence of GA spreading from one cell to another (Westergard et al., 2016), (Chang et al., 2016). In fact, poly-GA promoted the ubiquitinylation and mislocalization of TDP-43 via a mechanism involving cell-to-cell transmission in a cell culture system (Khosravi et al., 2020). Therefore, a lack of spatial correlation between poly-GA aggregates and neuron loss when viewed at the end stage of the disease may not mean that poly-GA is unrelated to the disease process.

3.3.3. Subcellular localization of poly-GA in ALS/FTD patients

In C9 ALS-FTD patients**,** poly-GA-positive inclusions have been found within cells either with or without TDP-43 pathology. Inclusions occur more frequently in the cytoplasm but also in the nucleus (Y. J. Zhang et al., 2014).

TDP-43 is mislocalized from nucleus to cytoplasm in nearly all cases of ALS, and loss or mislocalization of nuclear transport factors have been detected in C9 ALS patients. Because the mutation is located in a gene whose protein product is found in the nuclear membrane, and most of the DPR proteins are found close to the nuclear membrane, there are reasons to examine the impact of C9-related mechanisms on nucleocytoplasmic trafficking.

3.4. Role of Nucleoporins and Transport Receptors in Cell Function

Eukaryotes must be able to move macromolecules such as proteins and RNA into and out of the nucleus in a controlled fashion. This is achieved by selective movement through nuclear pores, which are passageways across the double-membrane nuclear envelope (see details on nuclear pore structure and function in section 3.5). Small molecules move freely through the pore. Proteins smaller than about 30 KDa appear to diffuse passively through the pore, whereas larger objects require facilitated transport to move rapidly across the nuclear envelope (Mohr, Frey, Fischer, Güttler, & Görlich, 2009). This facilitation is provided by the importin and exportin families of proteins.

1- Nucleocytoplasmic transport process

Transport proteins are known as karyopherins.

Proteins destined for transport (cargo proteins) usually contain one or more specific consensus sequences that allow binding to one of the karyopherins (Kabachinski & Schwartz, 2015). Importins recognize a nuclear localization sequence (NLS). The NLS is a lysine-rich motif with certain other sequence characteristics (Kalderon, Roberts, Richardson, & Smith, 1984) Consensus sequences are not restricted to specific, sequential series of permissible amino acids, but instead are regions that present similar binding characteristics that depend on the tertiary structure, electronegativity, hydrophobicity, and H-bonding of the peptide. As an example, the exporter protein XPO1 binds cargo proteins with one or more nuclear export sequences (NES). These sequences consist of certain patterns of hydrophobic amino acids with short, intervening residue(s) (X. Dong et al., 2009). Both NLS and NES have subcategories of these sequences that allow for specific binding of families of cargoes to particular transporters (Fung, Fu, & Chook, 2017).

Transport through the pore itself does not require ATP, but is driven by the RAN/GDP gradient. RAN (ras-related nuclear protein) is a small GTPase essential to nucleocytoplasmic transport. The cell maintains a higher concentration of G**T**P (guanosine triphosphate) in the nucleus than in the

cytoplasm. Conversely, G**D**P (guanosine diphosphate) is higher in the cytoplasm than in the nucleus.

Transporting a protein into the nucleus proceeds according to the following process.

First, an importin or complex of importins recognizes and binds to the NLS of a cargo. The importin(s)-cargo complex moves rapidly through the nuclear pore. Upon arriving in the nucleus, the importin binds RAN-GTP. This binding serves a signal to the importin, causing unbinding of the cargo, which is deposited in the nucleus. The importin-RAN-GTP complex moves back through the pore into the cytoplasm, where the GTP is hydrolyzed to GDP. Export proceeds in a reciprocal fashion: A cargo protein with a NES is bound by an exportin that recognizes the NES, and by RAN-GTP. This heterotrimeric complex then moves through the pore into the cytoplasm, where the GTP is hydrolyzed by RAN-GTPase Activating Proteins (RanGAPs) in the cytoplasm, causing the dissociation of the complex, leaving the cargo protein in the cytoplasm. The gradient is maintained by Ran guanine nucleotide exchange factor (GEF) that is abundant in the nucleus and the RanGAPs that are abundant in the cytoplasm (figure 5). Thus, the transport cycle uses the energy from GTP hydrolysis and the cell's maintenance of the GTP/GDP gradient and the RanGAP/RanGEF gradient. These gradients maintain the direction of import and export.

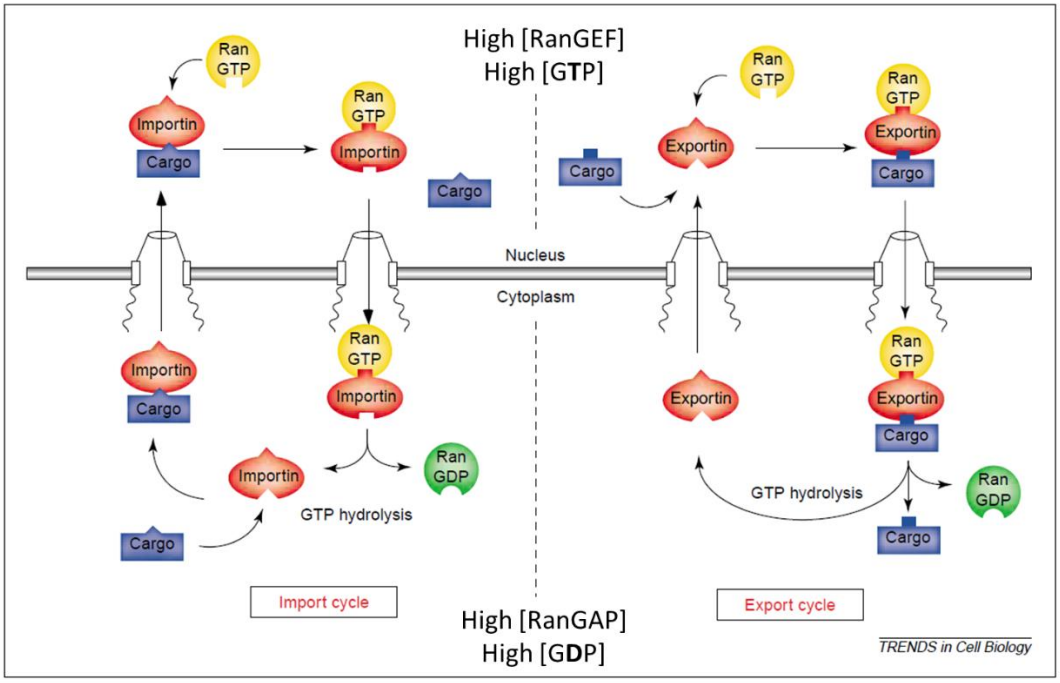

Figure 5. Outline of nucleocytoplasmic transport. Transport is not directly dependent on ATP, but uses RAN gradient to move proteins into and out of the nucleus. Modified from (Kuersten, Ohno, & Mattaj, 2001).

3.5. Nuclear Pores

Nuclear pores have been observed in the nuclear membrane since at least the mid-1950s (Afzelius, 1955; Watson, 1959). The nuclear pore is a channel-like complex bridging the inner and outer nuclear membrane (the nuclear envelope) that provides a passageway for macromolecules between the cytoplasm and the nucleoplasm of eukaryotes. It is a roughly cylindrical structure with radial symmetry. The total structure is approximately 125 MDa in human cells and is composed of multiple copies of over 30 different proteins called nucleoporins, which form the pore and the surrounding complex. The nucleoporins (Nups) are grouped into several different structural and functional categories.

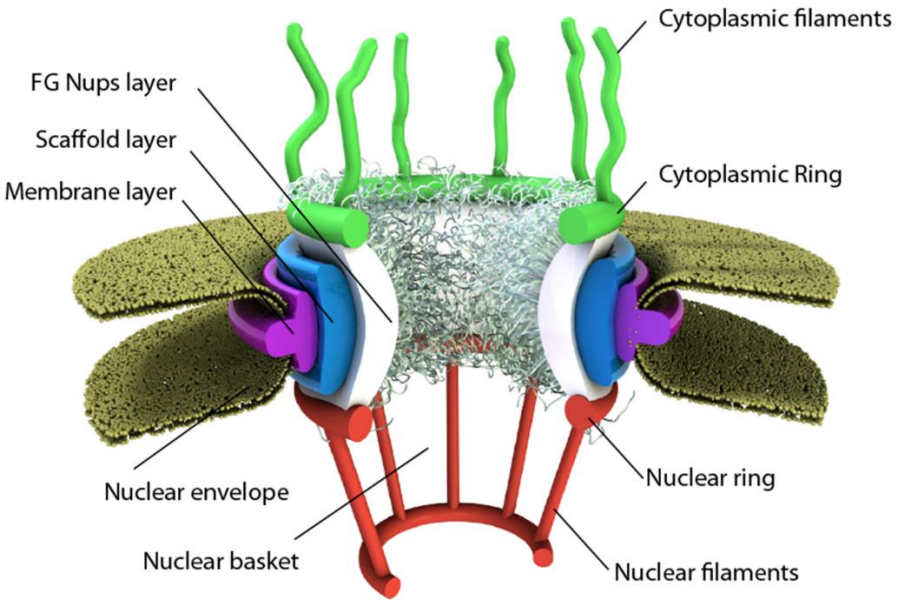

Figure 6. Structure of the nuclear pore. Overall structure of the nuclear pore with structural elements but not proteins indicated (Azimi & Mofrad, 2013).

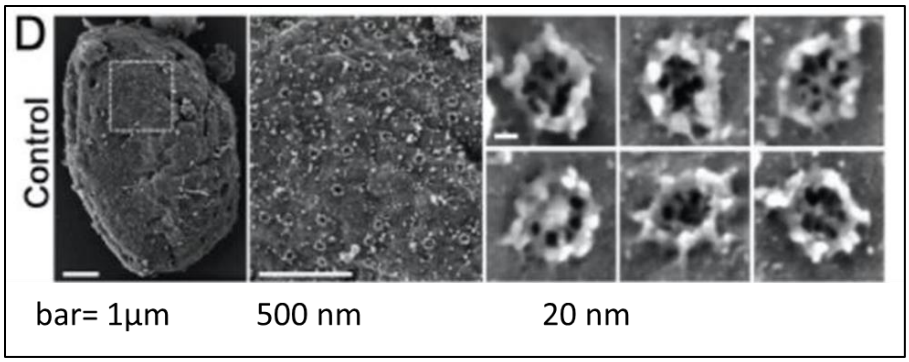

Figure 7. Scanning EM views of the nuclear pore. Scanning EM views of the nuclear pore at increasing magnification. From supplemental information to (Coyne et al., 2020).

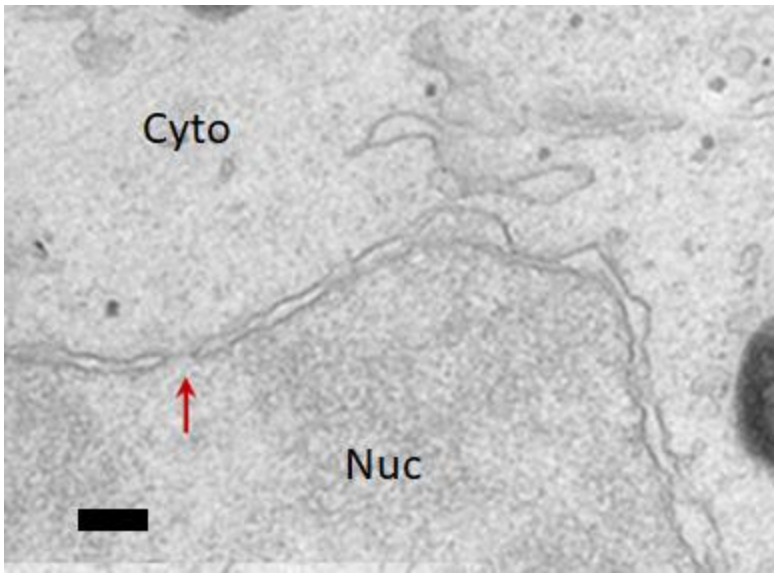

Figure 8. Conventional transmission EM of a nuclear pore. The inner and outer nuclear membrane are visible as dark lines with light gap between. Red arrow indicates nuclear pore. Scale bar = 200 nm. Romao, M., Richter, K., Raposo, G., previously unpublished.

Organization of the nuclear pores

Facing the cytoplasm are the cytoplasmic Nups that form filament-like structures reaching into the cytoplasm (Kabachinski & Schwartz, 2015). Passing through the nuclear envelope are structural Nups that, among other functions, anchor the complex to the inner and outer nuclear membranes, regulate the size and shape of the pore, and serve as assembly points during reorganization of the nuclear membrane, such as during cell division (Hartono et al., 2019). Lining the center of the pore are Nups forming a central pore that regulates the passage of molecules between the nuclear and cytoplasmic compartments of the cell. Finally, there are Nups that protrude from the pore into the nucleoplasm, forming what is known as the nuclear basket (Kim et al., 2018).

The nuclear pore family

Cytoplasmic Nups include Nup88, Nup214 and Nup358. Structural, or scaffold Nups, include Nup35, Nup85, Nup93, Nup107, Nup155, Nup160, and Nup205. POM121 and GP210 are two nucleoporins that extend from the inner to the outer nuclear membranes and contain classical

transmembrane domains found in most membrane-spanning proteins (Kabachinski & Schwartz, 2015), (Kim et al., 2018). Nuclear basket nucleoporins are critical for binding and transport of cargo out of the nucleus. Nup50, Nup153, and Tpr are components of the nuclear basket and are necessary for the binding and export of mRNA (Li, Aksenova, et al., 2021)

The structure and functions of nuclear pores

The structure of the individual proteins and the complex as a whole has been the focus of research using many techniques, including crystallography, electron microscopy, atomic force microscopy (Stanley et al.), and cryo-electron tomography (Kim et al., 2018). Some of the functions of each of the Nups and nucleoporin categories have been elucidated, although of course one protein or complex can serve several functions under different circumstances. One of the key functions of the nuclear pore is its ability to selectively permit or exclude large molecules from moving through the central channel. The central channel comprises nucleoporins that contain long sequences of phenylalanine-glycine repeats. These FG Nups are thought to be essential to forming the selectivity barrier of the pore (Denning, Patel, Uversky, Fink, & Rexach, 2003), although exactly how they accomplish this remains mysterious (Aramburu & Lemke, 2017). Movement through the pore is thought to require nuclear transport receptors complexed with cargo to bind and release stretches of FG repeats in the pore. This must occur extremely rapidly, as individual cargoes have been shown to move through the pore in milliseconds (Aramburu & Lemke, 2017). These hydrophobic FG repeats are also thought to contribute to the accumulation of nucleoporins in phase-separated membraneless organelles, such as stress granules. FG Nups include Nup58, Nup62, and Nup98.

3.6. Nucleocytoplasmic transport is implicated in ALS

Several lines of evidence point to nucleocytoplasmic transport (NCT) as playing a role in ALS.

3.6.1. Human genetics

The protein Gle1 isoform B is a nuclear pore component that facilitates export of mRNA from the nucleus, as well as translation initiation and termination. Deleterious mutations in GLE1 gene

were found in several individuals with ALS, resulting in a net accumulation of GLE1 away from the nuclear membrane in the cytoplasm (Kaneb et al., 2015) and a change in isoform expression. Mutations in GLE1 were confirmed and additional nonsense and missense mutations were identified in another population of ALS patients (Li, Sun, et al., 2021).

Mutations in the human gene fused-in-sarcoma (FUS) were discovered to be a cause of familial ALS in several kindreds (Kwiatkowski et al., 2009; Vance et al., 2009). As with TDP-43, FUS is an RNA-binding protein that moves between the nucleus and the cytosol but is found mostly in the nucleus. Many of the mutations lie in or near the NLS in the C-terminal nuclear localization sequence of the protein where they have been shown to impair nuclear import in *in vitro* systems (Dormann et al., 2010).

Thus, human genetic changes that cause ALS implicate nucleocytoplasmic transport as a process closely involved with the pathogenesis of ALS.

3.6.2. Human pathology

In all known forms of ALS except for those caused by mutations in SOD1 or FUS (~3% of cases), TDP-43 is found mislocalized from nucleus to cytoplasm in post-mortem CNS. TDP-43 accumulates and forms various types of inclusions. The TDP-43 modifications include aggregation, misfolding, phosphorylation, and other post-translational modifications (reviewed in (Keating, San Gil, Swanson, Scotter, & Walker, 2022). The ultimate cause of TDP-43 mislocalization is unknown, but, again, the finding of a nuclear protein in the cytosol suggests a failure of proper nucleocytoplasmic sorting.

The hypothesized mechanisms of TDP-43 pathology include the loss of properly functioning TDP-43 from the nucleus, (loss of function) and/or the extranuclear accumulation of misfolded, phosphorylated, cleaved, or otherwise modified TDP-43, i.e. gain of toxic function. Both of these mechanisms may play a role, but strong evidence suggest that loss of TDP-43's nuclear function leads to RNA mis-splicing events that cause damage to motor neurons (Melamed et al.,

2019). Because of the prominent mislocalization of TDP-43 observed in post-mortem histopathological studies from ALS patients, it has been speculated that TDP-43 nucleocytoplasmic transport function might be impaired (Winton et al., 2008). Models have been created to study the impact of mutating the Nuclear Location Signal (NLS) and Nuclear Export Signal (NES) of TDP-43. The small size of TDP-43 (molecular weight ~43 kDa) could allow transport through passive nuclear export (Schwartz, 2022). Indeed, recent work showed that NES-mediated export by XPO1 plays no role in the normal movement of TDP-43 out of the nucleus (Archbold et al., 2018), (Ederle et al., 2018), (Pinarbasi et al., 2018). Therefore, while TDP-43 pathology may be impacted by nucleocytoplasmic transport changes, it is not directly due to a failure of XPO1-mediated export. Very recent evidence suggests the TDP-43 gradient may be maintained by TDP-43's binding to GU-rich RNA in the nucleus (Duan et al., 2022). This may provide clues to ways to prevent the loss of TDP-43 from the nucleus of aging neurons.

Other studies have reported a potential role of the importin family proteins involved in chaperoning protein molecules from the cell's cytoplasm to the nucleus via binding to specific NLS region. Dysregulation of the expression levels of importin proteins have been reported to be altered in ALS patients such as i) loss of importin β1 from the nucleus in spinal cord anterior horn cells (Kinoshita et al., 2009), and ii) a loss of importin α4 in C9 ALS and FTD cases associated with TDP43 pathology (Solomon et al., 2018). These data could suggest that the importin system could participate in the mechanism(s) of TDP-43 mislocalization. However, these data have been challenged by others who showed no changes in importin β1 in ALS patients (Saberi et al., 2018).

Abnormal expression and distribution of nucleoporins have also been observed in ALS patient tissues. Specifically, nucleoporin Nup205 was abnormally distributed in brain tissues from ALS patients without C9 repeat expansion, specifically one TDP-43 and 10 sporadic ALS cases, in addition to C9 cases (Chou et al., 2018). In the motor cortex, Nup205 has been found to be aggregated with pTDP43 suggesting nuclear pore abnormalities accompanying TDP-43 pathology in ALS patients with and without C9ORF72 repeat expansion.

3.6.3. Experimental models

Several experimental models of C9orf72 ALS-FTD implicate defects in nucleocytoplasmic transport.

3.6.3.1. Drosophila screens

Morphological abnormalities in the nuclear membrane have been found in *Drosophila* expressing G4C2 repeats without an AUG start site (i.e., RAN translation (Freibaum et al., 2015). Using this fly model as a genetic screen, they identified 18 genetic modifiers of the phenotype. Many of those were nuclear pore components, including (gene symbols listed by human ortholog): Nucleoporins Nup153, Nup98, Nup160, Nup107 and Nup50; nuclear export chaperone XPO1; transport factor RAN; RNA export factors Gle1, NXF1 and CHTOP; and RNA transcription and export protein ALYREF.

Using a screen for modifiers of DPR protein PR15, Boeynaems and collaborators identified several nucleoporins, including TPR, NUP50, NUP62, NUP93, and NUP155, among others (Boeynaems et al., 2016). They also identified four exportin or importin proteins. Similarly, nuclear transport factors were also identified in a screen of modifiers of TDP-43 and FUS toxicity (Kankel et al., 2020).

3.6.3.2. Mammalian cell models

In rodent primary neuron cultures, low doses of XPO1 inhibitor were found to protect against cell death induced by overexpression of wild-type or ALS mutant TDP-43 (Archbold et al., 2018). However, the protective concentrations were below detectable XPO1 inhibition, and an unrelated XPO1 inhibitor, leptomycin B, did not provide protection, leaving the question of mechanism of action unresolved. The same compounds also provided some protection *in vivo* in mice expressing human TDP-43 (Archbold et al., 2018).

In neurons derived from C9 ALS patient iPSC, specific loss of a subset of nucleoporins was found (Coyne et al., 2020). Later, the authors extended this observation to sALS derived iPSC neurons

(Coyne et al., 2021). The proposed mechanism was the following. First, a mislocalization to the nucleus of the protein CHMP7, a member of the ESCRT (endosomal sorting complex required for transport) system for ubiquitinated cargo. CHMP7 is known to be involved in nuclear membrane sealing and nuclear pore maintenance (Webster et al., 2016). The mislocalization to or retention in the nucleus results in an increased abundance of CHMP7 at or near the nuclear membrane, where its activity causes a loss of nucleoporin POM121. The loss of POM121 then leads to a reduction in expression of a subset of other Nups (Coyne et al., 2021). The loss of Nups then results in, by an unknown mechanism, the mislocalization of TDP-43.

A separate line of evidence implicates nucleocytoplasmic transport in TDP-43 mislocalization. In the brains of FTD patients, Nishimura and colleagues found not only cytoplasmic TDP-43 accumulations, but also detected a loss of importin karyopherin α2 and transporter CSE1L (also called CAS or XPO2) (Nishimura et al., 2010). CSE1L is involved in the return of cargo-free karyopherin α2 to the cytoplasm (Kutay, Bischoff, Kostka, Kraft, & Görlich, 1997). Karyopherin α2 (a.k.a. importin alpha), in turn, is required for nuclear import of TDP-43. These data suggest the loss of both proteins leads to a net loss of TDP-43 transport into the nucleus.

Objectives of Experimental Work

The understanding of the toxic mechanisms of C9ORF72 expansion mutation responsible for neurodegeneration in ALS and FTD patients is critical to the discovery of novel therapeutic strategies. One anti-C9 strategy consisted of either active or passive immunization against poly-GA ((Zhou et al., 2020), (Nguyen et al., 2020)). Nguyen et al. used an anti-GA antibody that reduced soluble GFP-GA protein in a cellular system and provided neuroprotection and increased survival in C9 BAC transgenic mice with DPR-associated pathology. The present PhD project focused on the role of poly-GA DPRs and aimed at elucidating the activity of poly-GA on key pathways of nucleocytoplasmic transport that could explain the beneficial effect of the anti-GA antibody. To address this question, there was a critical need to generate and characterize reliable in vitro cell-based system. Therefore, the three main specific objectives were:

1- The development and validation of a HEK cell model that rapidly accumulates poly-GA protein in the absence of any repeat RNA. This model was used to characterize the structures that the cell forms with the production of poly-GA. The model also allowed investigation of whether the GA aggregates directly block transport through nuclear pores, as well as the consequences of poly-GA accumulation on expression and distribution of nuclear pores, and individual nuclear pore proteins at the nuclear membrane.

2- The characterization of a model that more closely reflects the C9 pathology in ALS by using induced pluripotent stem cell-derived motor neurons (iPSC MN) derived from C9 ALS patients. The formation and cellular distribution of accumulations of poly-GA was examined in addition to potential correlation in expression levels and colocalization with nucleoporin and TDP-43.

3- The development and validation of a model of neurodegeneration using C9 iPSC MN. Since C9 iPSC MN did not exhibit a phenotype substantially different from control motor neurons under basal growth conditions, I showed that specific treatment with a protein synthesis inhibitor, puromycin, resulted in an increase sensitivity of C9 iPSC MN to neurodegeneration. This model was used to evaluate the impact of anti poly-GA antibody to understand relative contribution of poly-GA to the downstream degeneration.

4. Results

4.1. Role of poly-GA in cytoplasmic transport, nuclear membrane integrity, and TDP-43 mislocalization in an inducible HEK cell model.

Objective and plans of the experimental studies:

In order to study the processing of poly-GA in a cellular context, we chose a reliable cell system in which to express poly-GA protein only. We used HEK-293, a system used in other studies of repeat expansion toxicity ((Mori et al., 2013),(May et al., 2014), (Frottin, Perez-Berlanga, Hartl, & Hipp, 2021)). We created a cell line (HEK-GA161) that produced poly-GA dipeptide repeat protein using an inducible promoter with a sequence lacking G4C2 content, precluding the possibility of G4C2-containing RNA foci. Patient genomes contain between 70 and several thousand repeats (Renton et al., 2011), (DeJesus-Hernandez et al., 2011), therefore we chose a construct greater than the minimum known to cause disease. The construct coded for 161 repeated GA subunits with a V5 sequence tag at the N-terminal (figure 9) under a tet-sensitive promoter. Poly-GA aggregates could then be labeled using either an antibody to the V5 tag or an antibody to GA repeats. We specifically chose the V5 (14 amino acids) tag because it is much smaller than protein tags such as GFP (238 amino acids) which could cause interactions that poly-GA alone might not make. We validated the model by examining the location, appearance, and clearance of the poly-GA aggregates. We further sought markers of protein degradation systems, including the ubiquitin/proteasome and autophagy pathways.

Finally, we employed electron microscopy to dissect the molecular architecture of poly-GA protein aggregates within intact HEK cells at high resolution.

4.1.1. Validation of an inducible model of poly-GA production in HEK cells.

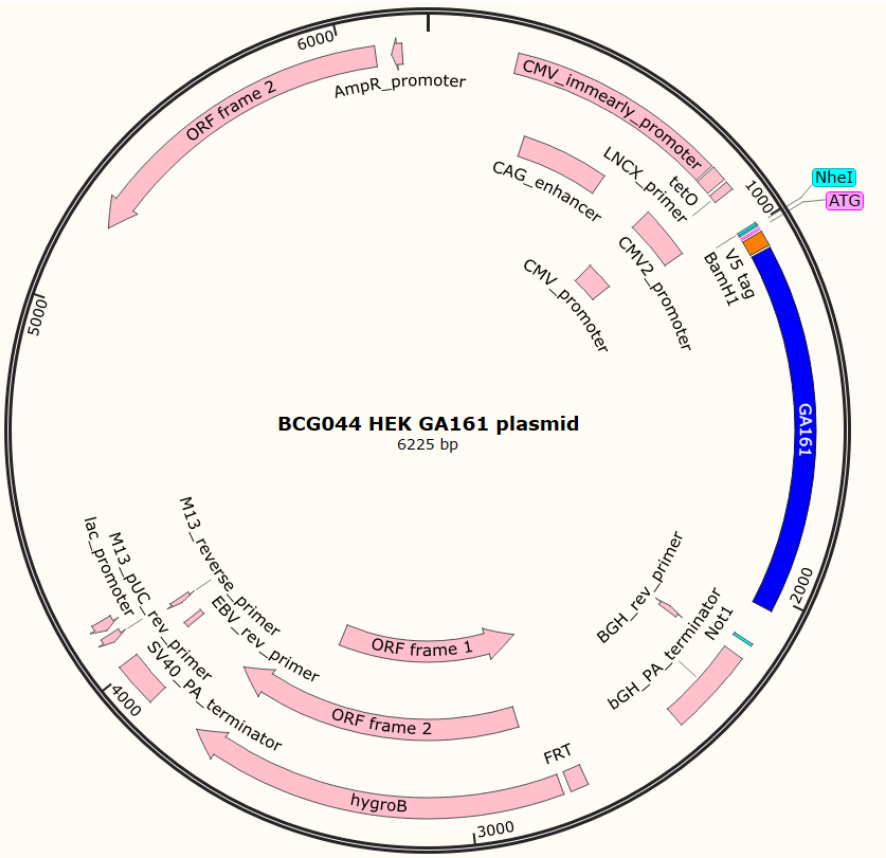

Figure 9. Map of expression plasmid. The plasmid coding for tet-dependent expression of poly-GA(161 repeat) was designed to allow doxycycline-dependent expression of a poly-GA sequence of disease-relevant length.

4.1.1.1. Appearance and subcellular localization of poly-GA aggregates after induction

When treated with doxycycline, these cells rapidly produced poly-GA that accumulated in the cytoplasm and the nucleus of the HEK cells, without causing overt cell death. Cell death was measured by counting healthy nuclei 48 hours after doxycycline and poly-GA induction; cell number was normalized as a ratio of cell number in the doxycycline *versus* vehicle treated wells and expressed as percentage. No difference in cell number was found after doxycycline treatment at 105±18%. The poly-GA aggregates were labeled using either an antibody to the V5 tag or an antibody to GA repeats (figure 10A). Quantification of the GA aggregates was performed with high-content imaging using area in microns occupied by V5 staining (figure 10B).

Using V5 immunolabeling, we showed that poly-GA aggregates appeared as early as two hours after treatment with doxycycline. In some instances, poly-GA accumulation appeared in both the nucleus and adjacent cytoplasm visualized using a maker of the nuclear membrane, the anti-lamin antibody (figure 10B). The aggregates often appeared apposed to the nuclear membrane (figure 10C).

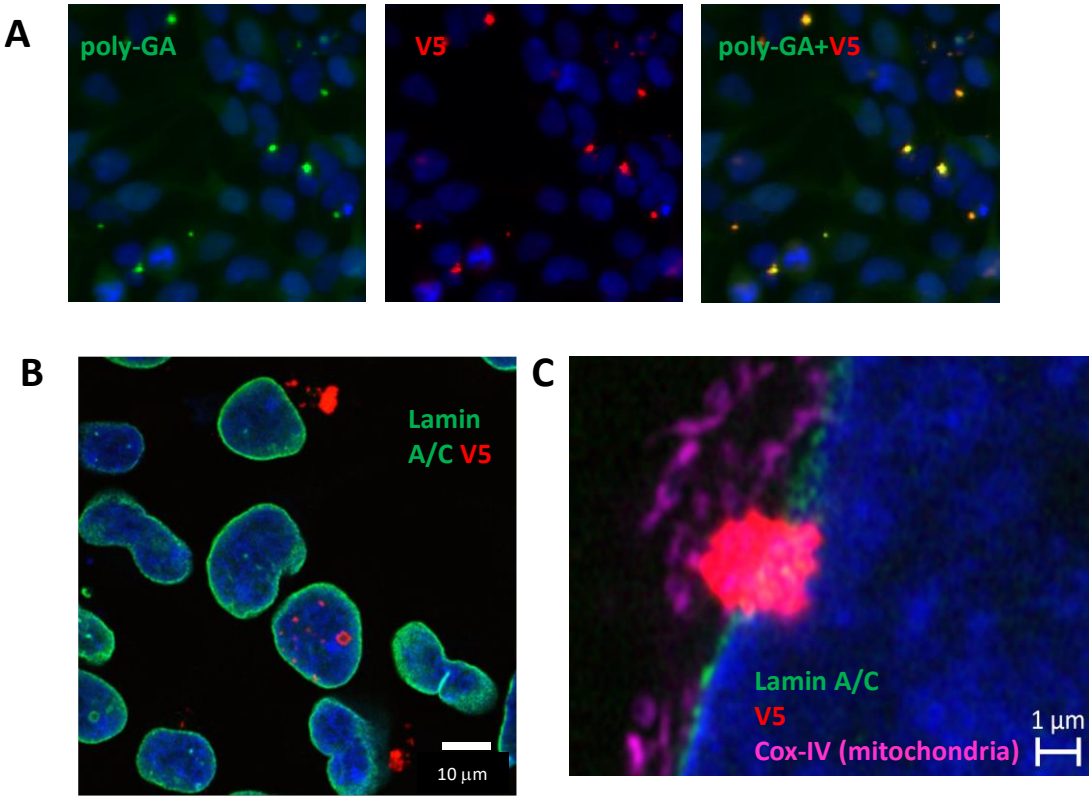

Figure 10. Poly-GA rapidly forms aggregates in HEK-GA161 cells in the presence of doxycycline.

A) Aggregates were detected with either an antibody directed against polymeric GA, αGA4 (green, left) or V5 (red, middle). **B)** Aggregates found within both cytosol and nucleus. **C)** One instance of an aggregate interacting with the nuclear membrane. Single z-plane collected with Zeiss Airyscan.

4.1.1.2. Poly-GA aggregates colocalized with markers of aggresomes in HEK cells

Cellular aggregates that are not membrane enclosed are usually surrounded by cages of intermediate filaments, notably vimentin, and HDAC6. Vimentin accumulation and HDAC6 are characteristic of so-called aggresomes (Kopito, 2000), (Watanabe et al., 2020). Therefore, to examine the potential colocalization of poly-GA aggregates with aggresomes, we selected some previously validated markers including 1) SQSTM1/p62 closely involved in the macroautophagy process, 2) HDAC6 known to regulate aggresome formation, 3) vimentin that can sequester unfolded proteins in aggresomes. At 48 hours after doxycycline induction, aggregated poly-GA protein in the cell was highly colocalized with puncta immunoreactive for SQSTM1/p62 (figure 11A). We also found that HDAC6 (figure 11B) and vimentin (11C) were often found close to poly-GA aggregates near the nucleus.

Conventional EM revealed electron-dense material in aggregates that were not surrounded by a membrane (figure 11D, 11E). Immunogold labeling on ultrathin cryosections (immuno-EM) using the Tokuyasu method revealed large aggregates of accumulated poly-GA (figure 8). Poly-GA was also detected associated with other cell compartments, such as endoplasmic reticulum (ER), as expected, but it was not found ubiquitously throughout the cell. For example, it was never detected with mitochondria (not shown).

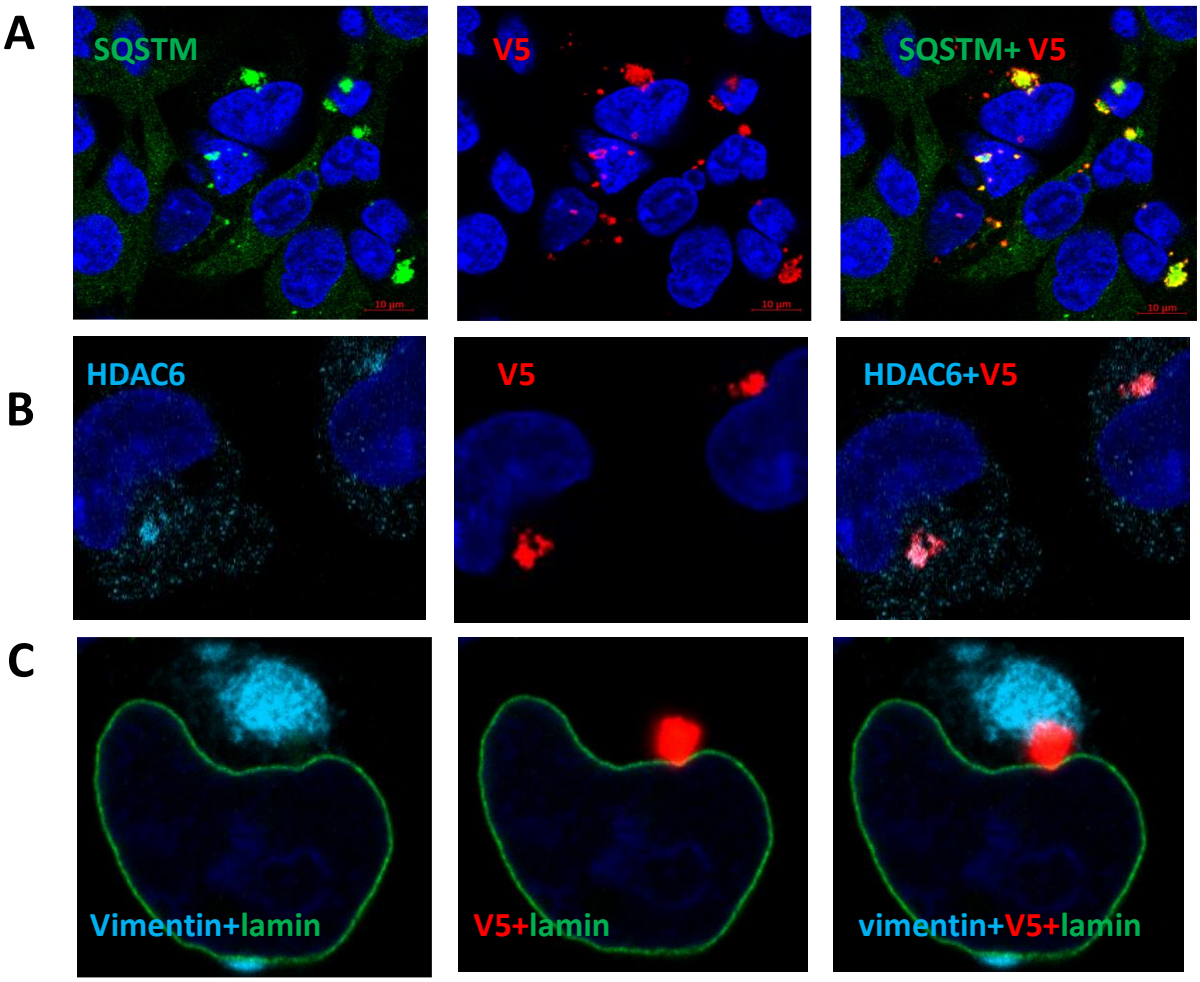

Figure 11. Poly-GA in HEK-GA161 is found in aggresome-like structures. A) Many aggregates were also positive for SQSTM/P62. **B)** HDAC6 staining was found near poly-GA aggregates. **C)** poly-GA aggregates near the nucleus were often found close to condensed vimentin staining.

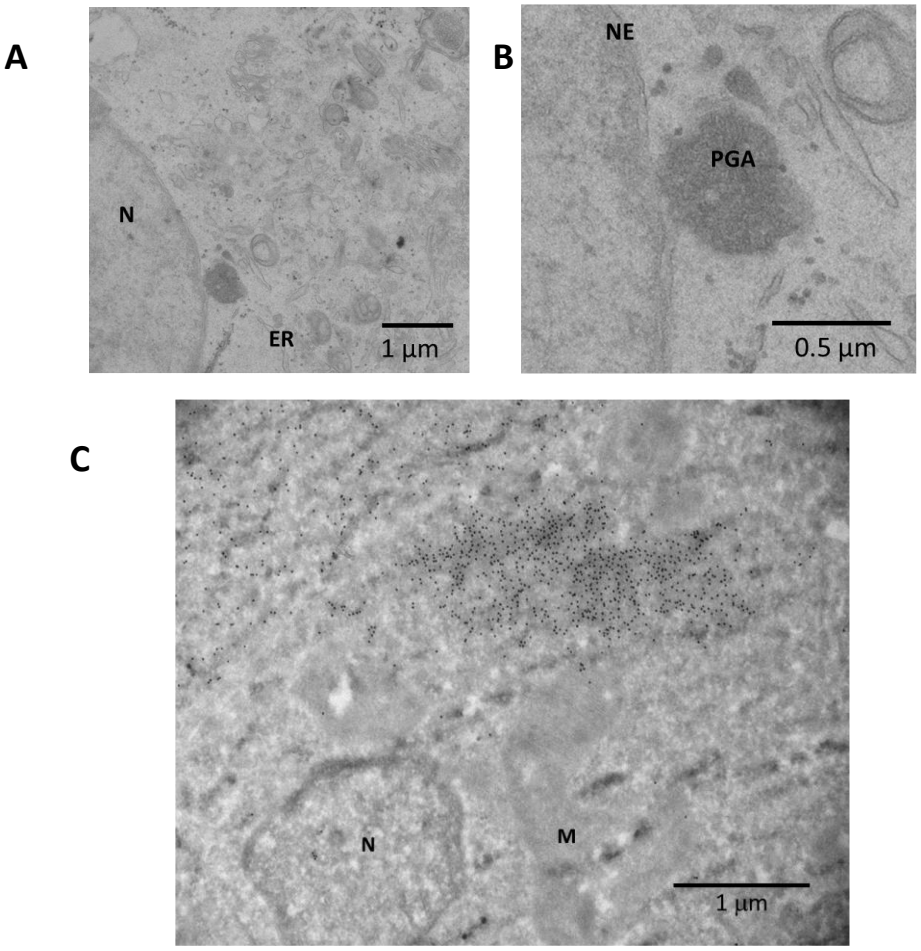

Figure 12. Poly-GA in HEK-GA161 is found in membrane-less structures.

A) Conventional electron micrograph with electron-dense probable GA accumulation near the nucleus. The dense area is not membrane-bound. **B)** higher magnification of A. N=nucleus ER=endoplasmic reticulum NE=nuclear envelope PGA=putative GA aggregate. **C)** Immuno-EM using αGA3 detected with gold-labeled secondary antibody. M=mitochondrion, N=nucleus

4.1.1.3. Mechanism of clearance of Poly-GA aggregates in inducible HEK cell models is still undetermined.

The clearance mechanism, if any, of poly-GA aggregates is still unknown. Endogenously produced poly-GA has no lysine, cysteine, serine, or threonine residues that could potentially act as sites of ubiquitination. Aggregates of GFP-tagged poly-GA(175) have been detected associated with the proteasome in cultured neurons (Guo et al., 2018), where it caused proteasome stalling. Pre-aggregated poly-GA(34) tagged with V5 and labeled with Atto fluorophores, when added to cultured neurons, was found mainly associated with lysosomes in axonal swellings (Marchi et al., 2022). Dipeptide repeat aggregates *in vitro* and *in vivo* are often found to be positive for SQSTM1 as shown previously. From our data, both the SQSTM1 positivity and the presence of aggresome markers suggest a possible role of autophagy in poly-GA clearance. To determine how V5-only tagged poly-GA is cleared, HEK-GA161 cells were treated with modulators of autophagy. Autophagy in HEK-293 cells has been previously characterized using pharmacological tools such as bafilomycin A1 and Torin1. Bafilomycin inhibits the completion of autophagy, thus revealing the basal autophagic flux. Torin1 stimulates the initiation of (mTor dependent) autophagy (Musiwaro, Smith, Manifava, Walker, & Ktistakis, 2013).

Treating HEK cells with bafilomycin A1 (100 nM, 2 hrs.) after 24 hrs. of induction had no effect on the amount of poly-GA detected in the RIPA-soluble lysate (figure 11A). This result suggests no involvement of basal autophagy in the clearance of poly-GA aggregates. To investigate the potential contribution of mTOR-related induced autophagy and to reveal changes in clearance that may be apparent only in the absence of new poly-GA protein synthesis, HEK cells were induced for 24 hours followed by a 24-hour washout period during which the cells were exposed to an mTor-mediated stimulator of autophagy, Torin1 in the absence of doxycyline. We showed that Torin1 treatment at low (20 μM) and high (40 μM) concentrations had no effect on poly-GA aggregate levels (figure 13A). The activity of Torin1 in stimulating autophagy was confirmed by examining the increased levels of LC3-II, a marker of autophagic flux, using western blot analysis

(figure 13 B). These data further indicate that induction of autophagy has no impact on the clearance of the poly-GA aggregates in this cell model.

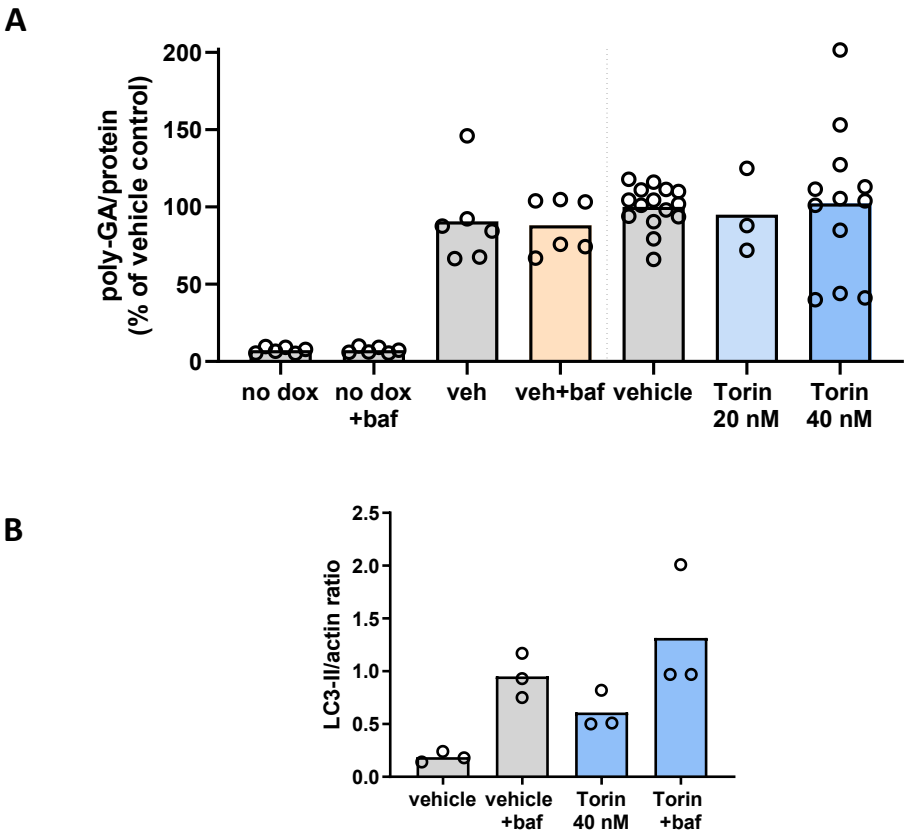

Figure 13. Poly-GA is not rapidly cleared. A) HEK cells induced to express poly-GA with doxycycline for 24 hrs. followed by dox washout and Torin1 treatment for 24 hrs. Some groups were treated with a pulse of bafilomycin A1, 100 nM for 2 hrs at the end of the incubation period in order to confirm autophagy activation. Bafilomycin and Torin groups are not different from vehicle (Kruskal-Wallis non-parametric ANOVA followed by Dunn's test, $p>0.999$). **B)** Samples from a subset of A) were assayed by western blot for LC3-II as a marker of autophagic flux. Increased LC3 values in Torin vs vehicle and Torin+bafilomycin vs vehicle+bafilomycin indicate stimulation of autophagy.

4.1.1.4. Summary of the inducible poly-GA HEK cell model.

We have established a model system of poly-GA induction in HEK cells that rapidly produced poly-GA aggregates presenting some properties of aggresomes. The poly-GA aggregates are often found adjacent to the nucleus and are positive for SQSTM1/p62, two characteristics present in the poly-GA aggregates in ALS patient CNS tissue (O. Hardiman et al., 2017). However, the formation of complex SQSTM1-protein aggregates is not an indication for autophagy *versus* proteasome mechanism of clearance. The further lack of the reduction of poly-GA aggregates abundance or distribution in the conditions where cells are challenged with prototypical modulators of autophagy suggests that, in this model, a therapeutic strategy targeting autophagy may not be the way to impact poly-GA-related pathology. It is also possible that these results may be explained by various experimental conditions, including: i) the model using a non neuronal cell line, ii) the rapid kinetics of the poly-GA aggregate production, iii) the stability of poly-GA in the cell and iv) the 24 hour time point being too early for the clearance mechanisms.

4.1.2. Poly-GA Effects on cell physiology

Context:

Poly-dipeptide repeat proteins have been proposed to interfere directly with nucleocytoplasmic transport by binding in the pore channel. For example, Shi and collaborators found labeled PR20 bound in the nuclear pore channel adjacent to the nucleoporin GP210 in a preparation of *Xenopus* oocyte nuclear envelope after incubation with PR20 (K. Y. Shi et al., 2017). They also detected an inhibition of movement into the nucleus of U2OS cell line using a GFP reporter protein coupled to nuclear import and export sequences.

Objective and plans of the experimental studies:

To determine whether poly-GA could modulate nucleocytoplasmic transport, our HEK-GA161 cell model was transiently transfected with a plasmid coding for a shuttle protein of tdTomato fused to HIV-Rev-NLS and MAPKK-NES. This plasmid can induce to production of a complete protein that was approximately 70 kDa, this large size preclude any passive movement across the nuclear envelope (Figure 14B). This type of fluorescent reporter protein has been previously used for a variety of experiments on nucleocytoplasmic transport (Fu, Fung, Cağatay, Baumhardt, & Chook, 2018; Fukuda, Gotoh, Gotoh, & Nishida, 1996; K. Zhang et al., 2015). In addition, we used an inhibitor of the exportin protein, XPO1 (also known as CRM1) to validate the functionality of this model system. The inhibitor, KPT-335, is a compound developed by Karyopharm, Inc. identified by structurally modeling the interaction between a natural product compound, leptomycin B (LMB) and the nuclear export sequence recognition site of XPO1 (Lapalombella et al., 2012). Interestingly, analogs of this compound have shown neuroprotection in some cellular and animal models of neurological disease (Haines et al., 2015) (Silvestrini et al., 2018), although the exact mechanism(s) by which the inhibition of XP01 could reduce neurodegeneration has not been clearly established.

In this section, we also aimed to characterize the relation between poly-GA and selected nucleoporins based on their known biology related to ALS pathology in mammalian cells including POM21, TPR, Nup153 (see section **3.6.3.2.)**. In addition, we examined using immunofluorescence and proximity ligation assay the relation between poly-GA and nucleoporin in the context of TDP-43 pathology as revealed by TDP-43 cytoplasmic mislocalization and C-term fragmentation.

4.1.2.1. No change in transport at equilibrium

In our HEK-GA161 model we showed that after 48h transfection, the tdTomato fluorescence was detected primarily in the cytoplasm (figure 14A). There was no difference between HEK induced to express poly-GA and uninduced HEK-GA161 (Figure 14C). This suggests that expression of poly-GA does not alter the dynamic equilibrium of the reporter protein while it is being transported into and out of the nucleus. However, it is conceivable that the rate of transport may be changed, so that although the equilibrium amount of shuttle protein is not different, the speed at which the protein arrives at that equilibrium is altered.

4.1.2.2. No change in transport during export block

To address the possibility that poly-GA aggregates in HEK cells can impact the rate of nucleocytoplasmic transport, the cells were incubated with a nuclear dye and Leptomycin B (LMB), an inhibitor of XPO1 export chaperone (Sun et al., 2013).

The accumulation of tdTomato fluorescence in the nucleus was followed over time after LMB treatment. There was no difference in the time course of accumulation in the nucleus between control and poly-GA expressing cells (Figure 14D), implying no interference with nuclear import. Thus, we conclude that, at least in this system, expression of poly-GA alone does not interfere with nuclear import of proteins.

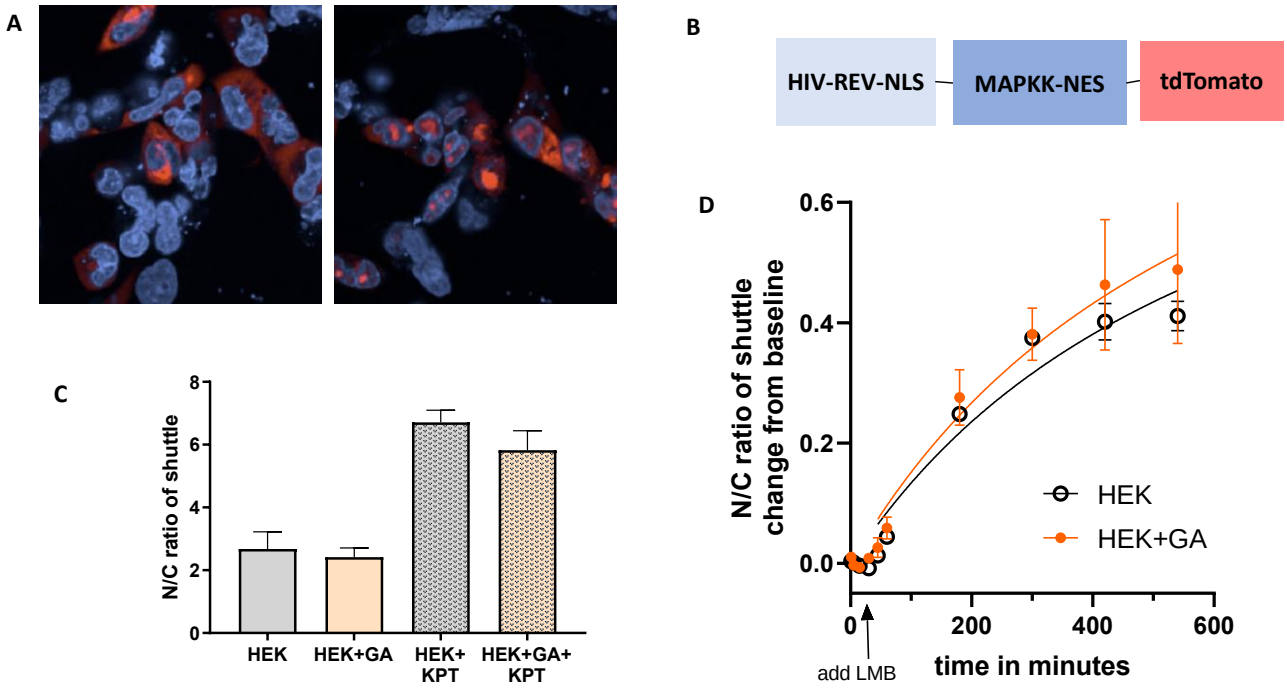

Figure 14. HEK expressing shuttle protein. **A**) HEK immediately after (left) and 7 hrs. after (right) LMB addition. **B)** Diagram of shuttle protein transfected into HEK-GA161. **C)** N/C ratio of shuttle protein 48 hrs. after transfection in HEK cells + expression of poly-GA. KPT=KPT-335, 1 μM. HEK is not different from HEK+GA (ANOVA followed by Šídák's multiple comparisons test, F= 248.7, p= 0.4695). KPT increased the N/C ratio significantly (Šídák's multiple comparisons test, HEK vs. HEK+KPT, p<0.0001, HEK+GA vs HEK+GA+KPT, p<0.0001) **D)** Non-linear best fit of each time course. Y= (Ymax * X)/(Th + X) where Th = time to half maximal ratio. Extra-sum-of-squares F=0.135, p=0.7145 null hypothesis is "Th is the same for both curves."

4.1.3. Poly-GA colocalizes with nucleoporins in HEK-GA161

By immunofluorescent confocal microscopy, we found poly-GA aggregates colocalized with specific nuclear pore proteins in HEK-GA161 cells. These were typically found near but outside the nucleus (Figure 15A, 15B). Colocalization could be detected using multiple poly-GA antibodies including either αGA3, αGA4, or V5 antibodies. Both GA and nucleoporin antibodies for POM21, TPR and Nup153 detected these proteins in aggregates that were in the range of 0.2 to 2 microns in diameter. At the sub-micron level, there were regions of the aggregates immunoreactive for either one but not both nucleoporin and poly-GA antibodies, meaning

extensive but not wholly congruent colocalization. This is further evidence that the overlap detected was specific and represented genuine colocalization, rather than artifactual colocalization due to lack of specificity of secondary antibodies or fluorescence crosstalk. Higher resolution microscopy using STED confirmed colocalization of nucleoporins and poly-GA within its limit of resolution (~ 50 nm) and identified apparent ectopic expression of POM121 outside the nuclear envelope (Figure 15B). In contrast, nucleoporin TPR was not found to be colocalized with poly-GA (figure 15C), despite the fact that TPR and Nup153 are part of the same complex within the nuclear pore.

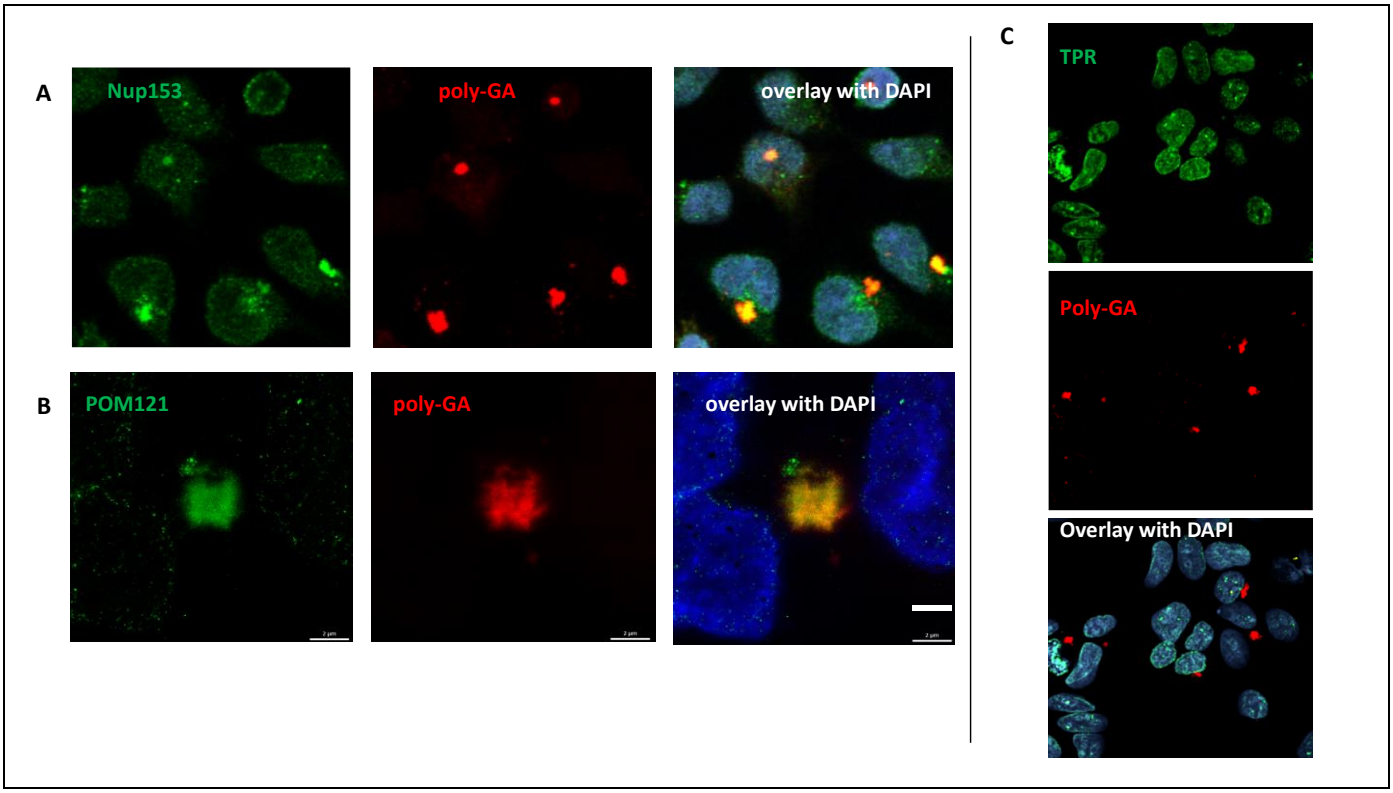

Figure 15. Nucleoporins colocalize with poly-GA in HEK. A) Nucleoporin 153 and poly-GA colocalize in aggregates. **B)** STED images of colocalized, extranuclear POM121 and poly-GA. Scale bar=2 μm **C)** Nucleoporin TPR does not colocalize with poly-GA.

4.1.3.1 Poly-GA colocalizes with TDP-43 C-terminal region in HEK-GA161 by immunofluorescence.

In addition to nucleoporins, we also detected TDP-43 colocalized with poly-GA aggregates (figure 16A). The colocalized TDP-43 typically was labeled with an antibody directed to the C-terminal region, but not other epitopes of TDP-43, possibly reflecting that it is the a cleaved form of TDP-43 protein found more specifically in the cytoplasm that can react with poly-GA (figure 16B). In some cases, the aggregates contained at least three species: TDP-43 C-terminal region, Nup153 and poly-GA (figure 16C).

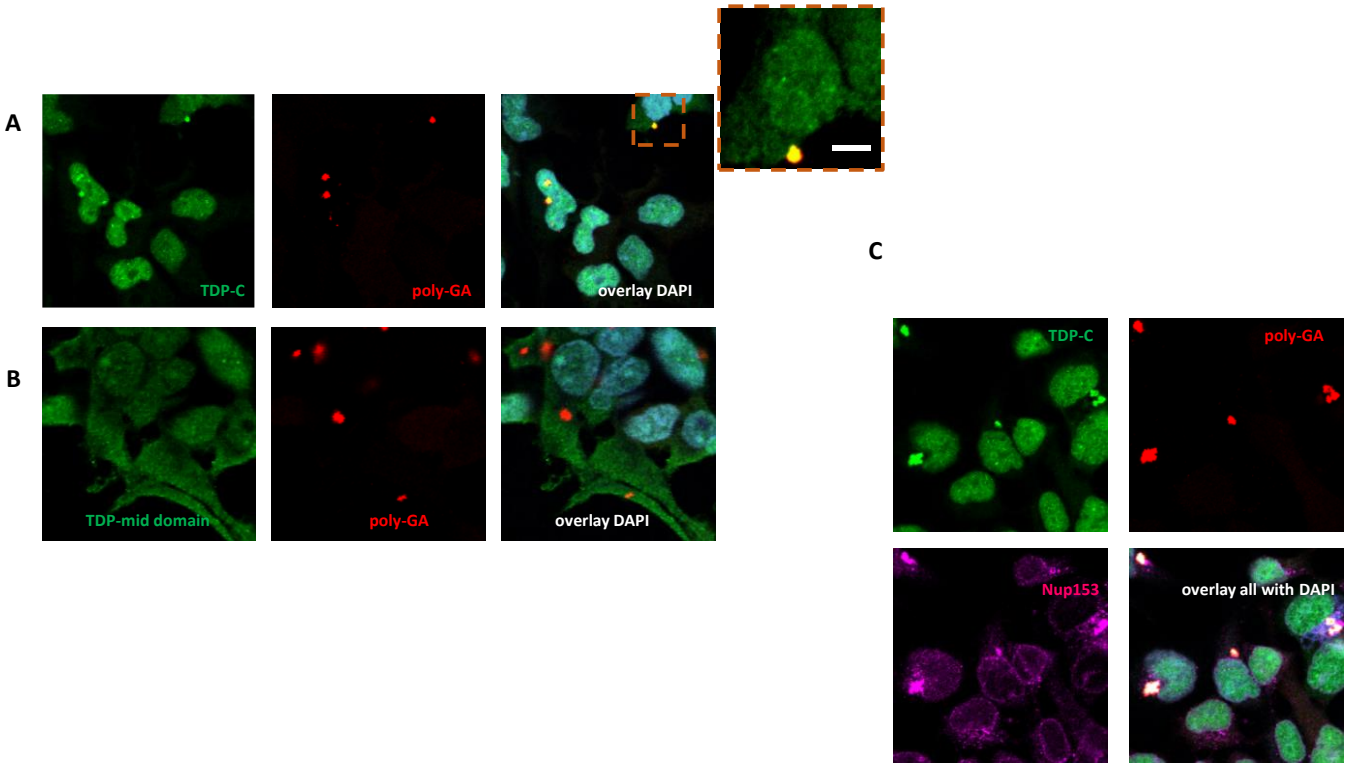

Figure 16. TDP-43 and poly-GA colocalize in aggregates in induced HEK-GA161 cells.

A) Antibody directed against C-terminal of TDP-43 colocalizes with poly-GA. Inset scale bar=5 μm. **B)** Antibody directed against mid-domain of TDP-43 does not colocalize with poly-GA. **C)** In some instances, aggregates contain both TDP-43 and Nup153.

4.1.3.2. Poly-GA colocalizes with Nup98 and TDP-43 C-terminal region in HEK-GA161 by proximity ligation assay

To reinforce our observations, we used a proximity ligation assay that relies on secondary antibodies coupled to DNA oligonucleotides. In the presence of a DNA ligase and polymerase, an amplified fluorescent signal is formed only when the primary antibodies recognize epitopes adjacent to each other (Jarvius et al., 2007). Based on an estimated immunoglobulin size of about 10 nm diameter, the maximum possible distance between two detected epitopes is about 40 nm. Using this method, we found colocalization between poly-GA and Nup98; and poly-GA and the C-terminus of TDP-43 (figure 17).

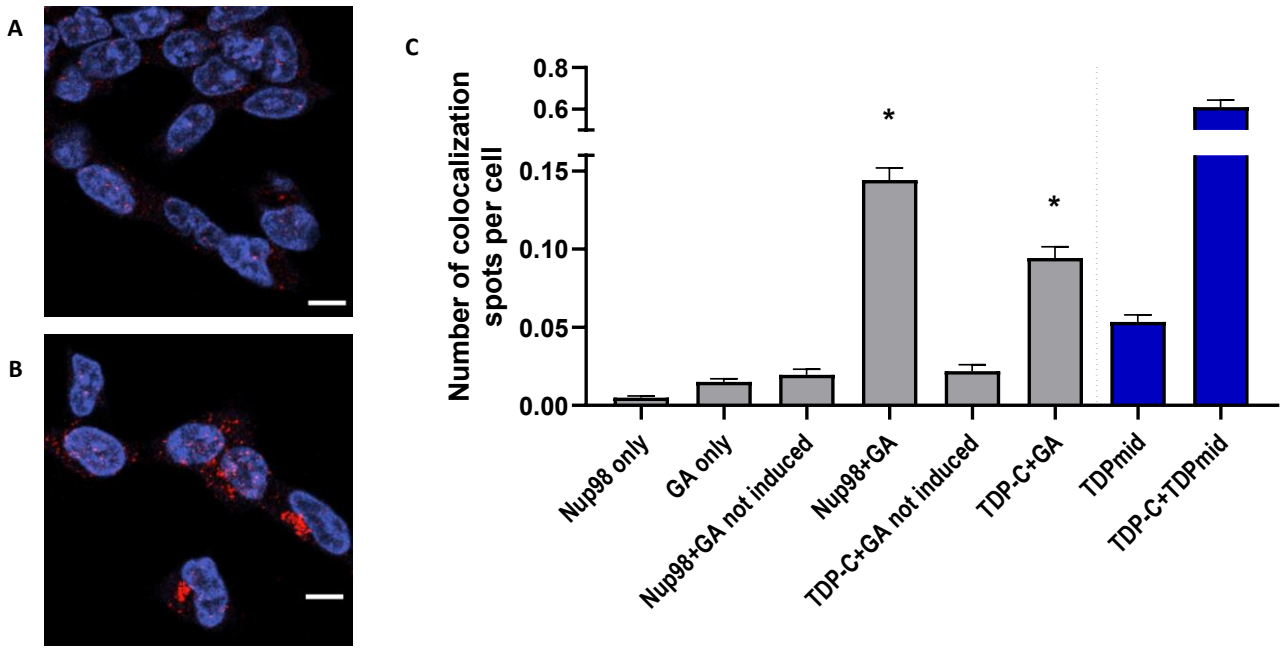

Figure 17. Proximity ligation assay detects colocalization between Nup98 and poly-GA

Proximity ligation assay produced fluorescent spots representing one or more instance of colocalization between the targets of two antibodies. **A)** Nup98 and poly-GA, not induced **B)** Nup98 and poly-GA in induced cells. Scale bars=10 μm. **C)** Quantification of PLA images. Nup98 and poly-GA colocalization signal and TDP-43 C-term and poly-GA colocalization signal were significantly greater than the highest control (both antibodies in non-induced cells), ANOVA F= 240.8 followed by Šídák's multiple comparisons test, $p<0.0001$ (Nup98+poly-GA vs. not induced) and $p=0.0004$ (TDP+poly-GA vs. not induced). Antibodies directed against two epitopes of TDP-43 served as a positive control.

4.1.4. Poly-GA alters TDP-43 expression in HEK-GA161

To study the potential impact of expressing poly-GA in HEK-GA161 on total TDP-43 protein expression and distribution, we used an antibody directed against the mid-domain of TDP-43 that generally does not detect TDP-43 aggregates. We showed that induction of poly-GA increased both cytoplasmic and nuclear TDP-43 fluorescence intensity (figure 18). However, the relative

expression in the two cell compartments and the nuclear/cytoplasmic *ratio* was not significantly different after poly-GA expression. This result may suggest that the poly-GA/TDP-43 interaction could impact the homeostasis of TDP-43 in this cell system potentially by slowing the clearance of TDP43.

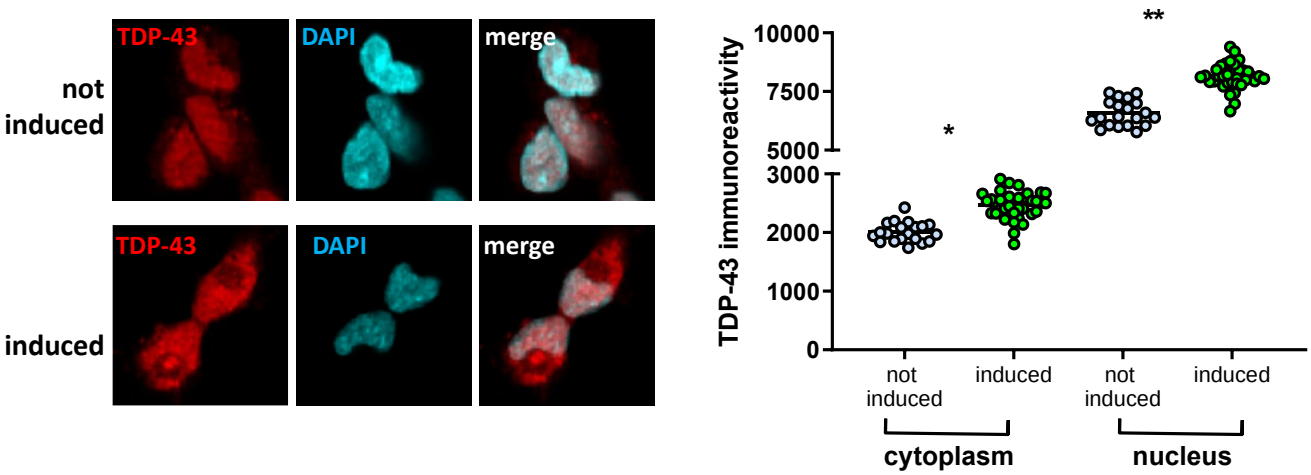

Figure 18. Poly-GA expression increases TDP-43 in nucleus and cytoplasm

HEK-GA161 cells treated for 48 hrs. with doxycycline to induce poly-GA showed greater TDP-43 immunofluorescence in both nucleus and cytoplasm than untreated cells (ANOVA F=198 followed by Šídák's multiple comparisons test, *p=0.0002 (cytoplasm), **p<0.0001 (nucleus).

4.1.5. Poly-GA sequesters nucleoporins away from the nucleus in HEK-GA161

4.1.5.1. Nuclear pore proteins are found outside nuclear membrane

Nuclear pore proteins are mainly restricted to the nuclear pore complex and present in fixed ratios. The association of nucleoporins or TDP-43 with poly-GA aggregates suggests that some of the nuclear proteins may be mislocalized. However, the long-lived nuclear pore proteins are synthesized in the cytoplasm before transport to the nuclear pore, so merely detecting the

extranuclear presence of nuclear proteins may not represent ectopic expression and a potential role for TDP-43 in disturbing the physiological shuttling of these proteins. Therefore, quantitative fluorescence microscopy was used to determine whether the induction of poly-GA in the HEK-GA161 cells changed the distribution of nuclear pore proteins in HEK-GA161. All extranuclear puncta of nucleoporin immunoreactivity in a single z-plane were counted, regardless of whether colocalization with poly-GA was detected, in cultures of wild-type HEK, HEK-GA161 without doxycycline (non-induced), and HEK-GA161 induced to express poly-GA. Expressing poly-GA caused an increase in extranuclear nucleoporins POM121 and Nup153 (Figure 16). Despite Nup98 being colocalized with poly-GA aggregates (figure 17), it was not found outside the nuclear membrane. So, at least in this system, colocalization does not always imply sequestration away from the nuclear membrane.

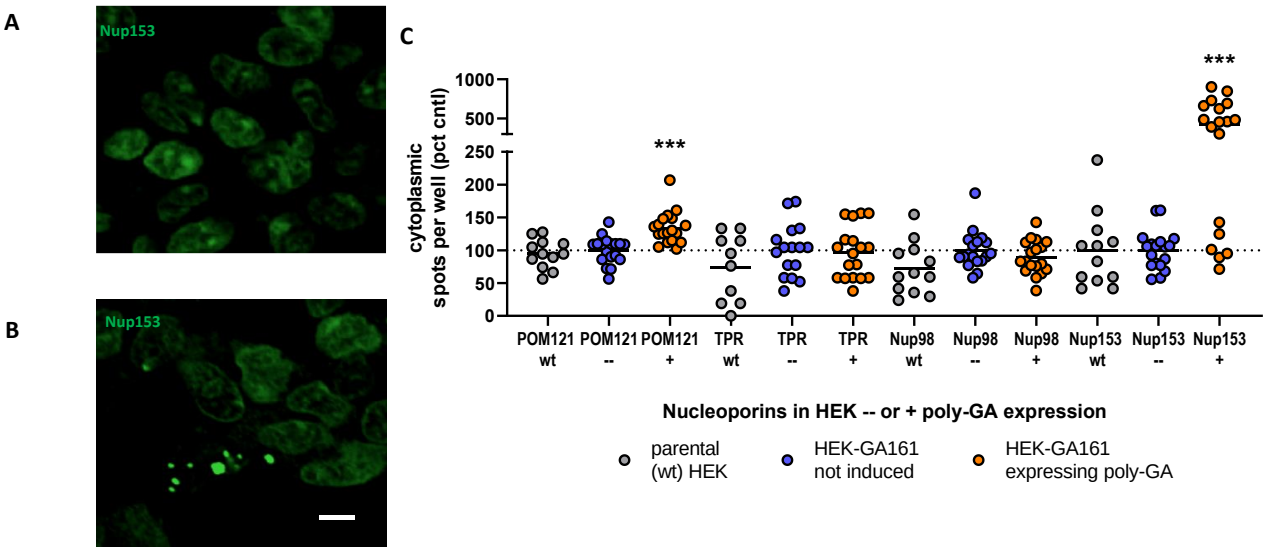

Figure 19. Expression of poly-GA causes appearance of extranuclear nucleoporins. A) Nup153 in HEK-GA161 non-induced. **B)** HEK-GA161 induced. scale bar=10 μm **C)** Cells induced to express poly-GA had a greater number of extranuclear spots of nucleoporins POM121 (ANOVA $F=14.24$ followed by Tukey's, $p<0.0001$) and Nup153 (ANOVA $F=19.68$ followed by Tukey's, $p<0.0001$)

4.1.5.2. Extranuclear poly-GA is not exclusive to stress granules

Oxidative and other types of stress can cause the formation of stress granules, which are also known to impact the distribution of TDP-43 and extranuclear nuclear pore proteins (Patterson, Wood, & Schisa, 2011; K. Zhang et al., 2018). Thus, it is possible that poly-GA aggregates outside of the nucleus could be part of stress granules. Stress granules were visualized with an antibody to G3BP stress granule assembly factor (G3BP). We examined if the extranuclear poly-GA accumulations could be incorporated into such granules. Stress granules were not detected under basal conditions (figure 20A), but with exposure of a known inducer of cell stress, sodium arsenite (500 µM 1 hr.). We found that sodium arsenite (500 µM) for 1 hr. induced G3BP-positive puncta in the HEK-GA161 (figure 20B). In some but not all instances, they colocalized with poly-GA (figure 20D). In absence of quantification, we also cannot conclude here if cell stress induced by sodium arsenite can impact the production and/or cell distribution of the poly-GA aggregates compared to non-activated cells.

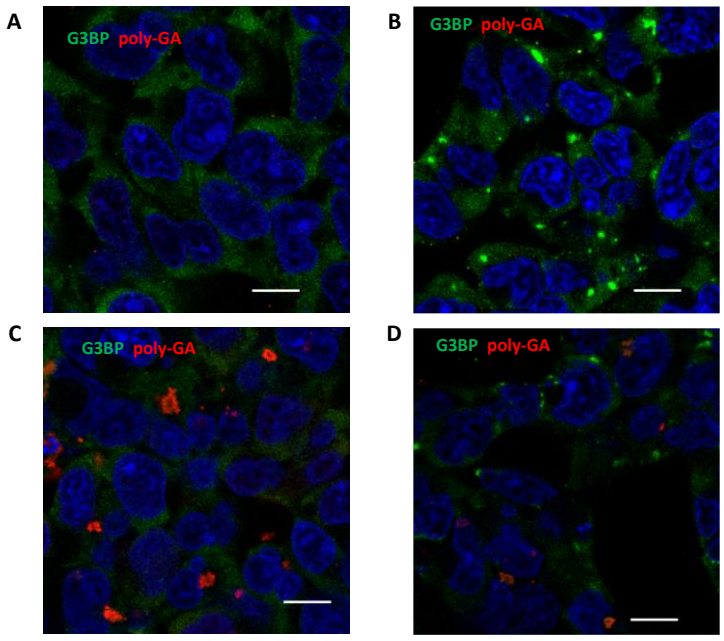

Figure 20. Poly-GA is not highly colocalized with stress granules in HEK. HEK-GA161 were immunolabeled with antibodies against poly-GA (red) and G3BP (green). **A)** No induction no arsenite **B)** no induction**,** sodium arsenite 0.5 mM 1 hr**. C)** induced to express poly-GA, no arsenite **D)** induced to express poly-GA, sodium arsenite 0.5 mM 1 hr. Scale bar=10 μm

4.1.6. Poly-GA protein expression is modulated by Nup153

Because Nup153 was found both to be coaggregated with and redistributed by poly-GA, we wished to explore further the relationship between this nucleoporin and poly-GA expression that is still a matter of debates. Increasing or decreasing nucleoporin expression has been found to modulate both G4C2 toxicity and dipeptide repeat protein toxicity in fly screens (Freibaum et al., 2015). Knockdown of Nup153 specifically was found to potentiate RNA toxicity in a model of G4C2 repeat (58x) (Freibaum et al., 2015), although no poly-GA was reported in that model. In our study, we transfected HEK-GA161 cells after induction with siRNA against Nup153 (OriGene) or a control siRNA against a scrambled nucleotide sequence. We then measured the levels of Nup153 knock-down and poly-GA at 48 hrs. after siRNA treatment (Figure 21). The siRNA

treatment reduced expression of Nup 153 mRNA by 75%, without changing expression of the poly-GA mRNA (Figure 21). The loss of Nup153, however, reduced the poly-GA accumulation in the cells by 40% (Figure 21). These experiments suggest that in this model Nup153 is a significant mediator of the accumulation of poly-GA protein in this cell model.

	mRNA (percent control)		
	XPO1	**poly-GA**	**Nup153**
control siRNA	100.3%	100.6%	100.5%
Nup153 siRNA A	118.7%	124.0%	25.8%
Nup153 siRNA C	108.5%	132.7%	23.5%

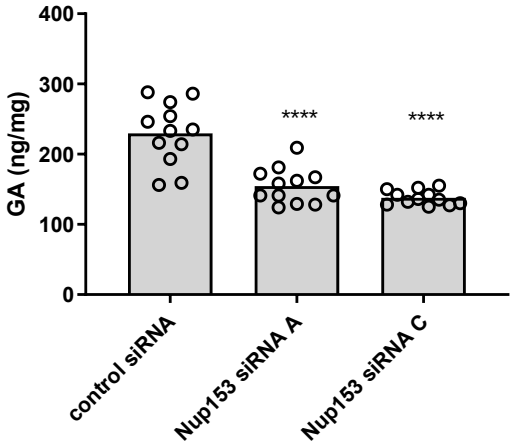

Figure 21. Nup153 knockdown reduces poly-GA. Treatment of HEK-GA161 with an siRNA against Nup153 successfully reduced Nup153 message to 26% or 24% of control, did not decrease XPO1 or poly-GA (transgene) message, but reduced poly-GA protein to 67% (siRNA-A) or 60% (siRNA-C) of control. ANOVA F=31.67 followed by Tukey's test for multiple comparisons, $p<0.0001$

4.1.7. HEK cell model summary.

The HEK cell model allows rapid accumulation of a disease-relevant length of poly-GA strands into aggregates in a cellular context. This model allowed us to study whether poly-GA aggregates functionally blocks the transport of a reporter protein through the nuclear pore, it also helps testing potential poly-GA clearance mechanism. Using this model, we discovered that expression of poly-GA without other intervention subtly alters TDP-43 expression, and sequesters a subset of nuclear pore proteins in the cytoplasm. This is consistent with recent reports of poly-GA forming SQSTM+ inclusions in the nucleus and cytoplasm with little effect on cell survival (Frottin et al., 2021). However, these results differ from Frottin and collaborators as we were not able to

show any impact of poly-GA on the protein and mRNA export system. This model, using non-neuronal cells also does not inform on whether the identified mechanisms associated with this rapid poly-GA accumulation can also be found in neuronal cells, nor on the potential chronic effect of poly-GA expression over many days in culture. To address those questions, we turned to another cellular model system using iPSC MN.

4.2 Poly-GA in an ips-derived motor neuron model.

Because selective degeneration of motor neurons is the essential defining characteristic of ALS, using motor neurons as a model system has been a goal of ALS research. Some previous models aimed at achieving this included the use of a motor neuron-like cell line, a neuroblastoma/spinal cord neuronal hybrid cell line NSC-34 ((Matusica, Fenech, Rogers, & Rush, 2008)) or primary motor neurons from mouse or chick (Duplan et al., 2010; Horwich, Engel, & Chauvin, 1974). After the development of a method to produce differentiated motor neurons from cells harvested from adult or even aged patients (Dimos et al., 2008), iPSC MN became a useful model, in part due to their face validity in understanding human neurological disease (Myszczynska & Ferraiuolo, 2016) (Ichida et al., 2018). Here, we used a growth factor-based approach to create cultures of human motor neurons (Maury et al., 2015).

The aims were to characterize the iPSC MN with respect to endogenous poly-GA production, subcellular localization, and clearance before embarking on experiments to understand any interaction between poly-GA and nucleocytoplasmic transport. For this purpose, we used iPSC MN derived from C9-ALS patient cells. We characterized phenotypic differences associated with C9 ALS patient-derived *versus* healthy donor-derived motor neurons.

4.2.1. Poly-GA is expressed in nucleus and neurites of C9-patient-derived, but not control, ips motor neurons.

We aimed to examine the effects of poly-GA expressed via RAN translation in its endogenous context in neurons. Therefore, we cultured motor neurons derived From a C9-ALS patient (HRE

and an unaffected relative (Coriell Institute lines 9607E and 7189L, respectively). Using an established, growth factor and small molecule-driven differentiation protocol to produce a culture enriched in motor neurons, we prepared cultures that were typically > 90% β-III-tubulin positive neurons. At 34 DIV, more than 99% of the cells with nuclei > 30 μm^2 in area were positive for β-III-tubulin and Islet1/2, a marker of developing motor neurons (Table 4). Approximately 0.21% of the control cells were positive for Ki-67, a marker of dividing cells (Table 4). In the C9 donor cells, more dividing cells were present with 6% positive for Ki-67 even though >99% were positive for Islet1/2 due to physical overlap of dividing cells with cell bodies of neurons (Table 4) during automated counting.

	n(cells) evaluated	**β-III-tubulin +**	**Islet1/2+**	**Ki67 +**
control donor	6171	99.96% ± 0.15%	99.69% ± 0.43%	0.21% ± 0.56%
C9 ALS patient donor	9001	99.95% ± 0.15%	99.36% ± 0.47%	6.53% ± 3.18%

Table 4: Cell type abundance in ips-derived motor neuron cultures.

We used previously described antibodies to poly-GA that recognize only GA sequences greater than ten gly-ala repeats (Nguyen et al., 2020),(M. Jambeau et al., 2022). Both antibodies αGA3 and αGA4 robustly detected expression of poly-GA in the C9 ALS patient-derived motor neurons. A faint signal above background was detected in healthy donor-derived motor neurons that was visible with long exposure (figure 22 A, B). The intensity of poly-GA staining varied among C9 neurons, a property detected by either antibody (figure 22C). Poly-GA staining was predominantly within the nucleus (figure 23A). At 30 DIV, small amounts of cytosolic poly-GA were also detected (figure 23B).

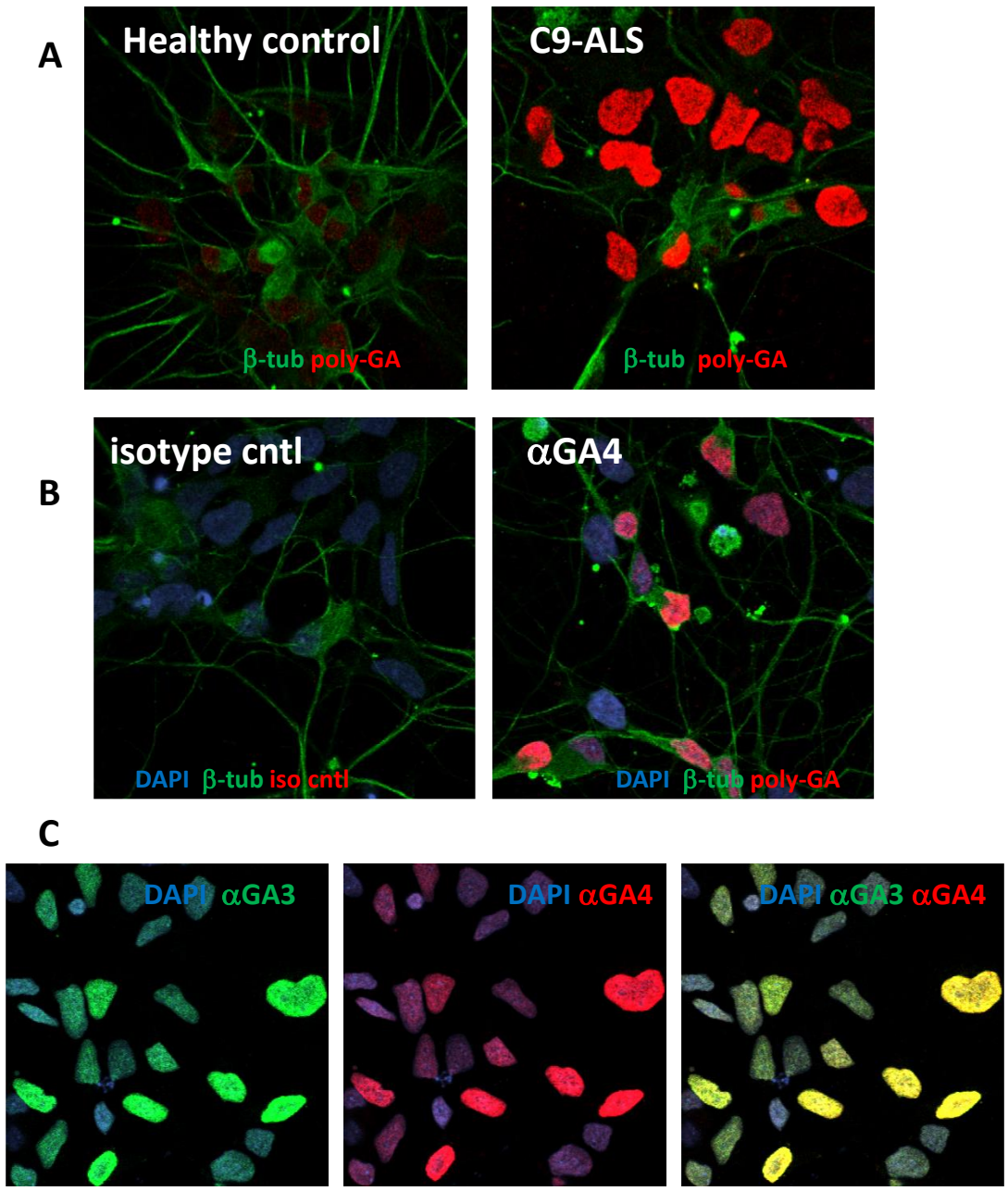

Figure 22. C9 ALS- but not healthy donor-derived motor neurons express poly-GA.

A) Poly-GA immunoreactivity in control (left) or C9 (right) neurons **B)** C9-ALS-derived ips motor neurons labeled with isotype control or αGA4 antibodies. **C)** αGA3 and αGA4 stain nuclei of C9 motor neurons with similar pattern.

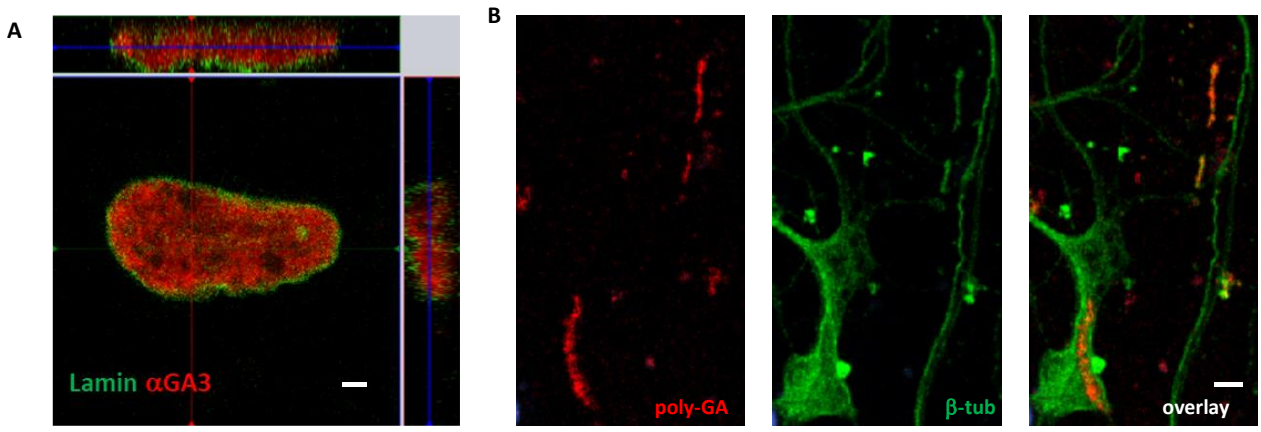

Figure 23. C9 patient-derived motor neurons express poly-GA in nucleus and cytoplasm. A) Orthogonal projection view of poly-GA within the nuclear membrane. Scale bar=2 μm. **B)** poly-GA staining in neurites as detected by αGA3. Scale bar=5 μm.

Poly-GA at the ultrastructural level confirmed the immunofluorescent result. Using αGA4, we detected some immunoreactivity in nuclei of healthy donor-derived ips motor neurons (Figure 24A), but more in the patient-derived neurons (Figure 24B). At higher magnification, poly-GA could be detected close to the nuclear envelope and near the inner nuclear membrane region near nuclear pores

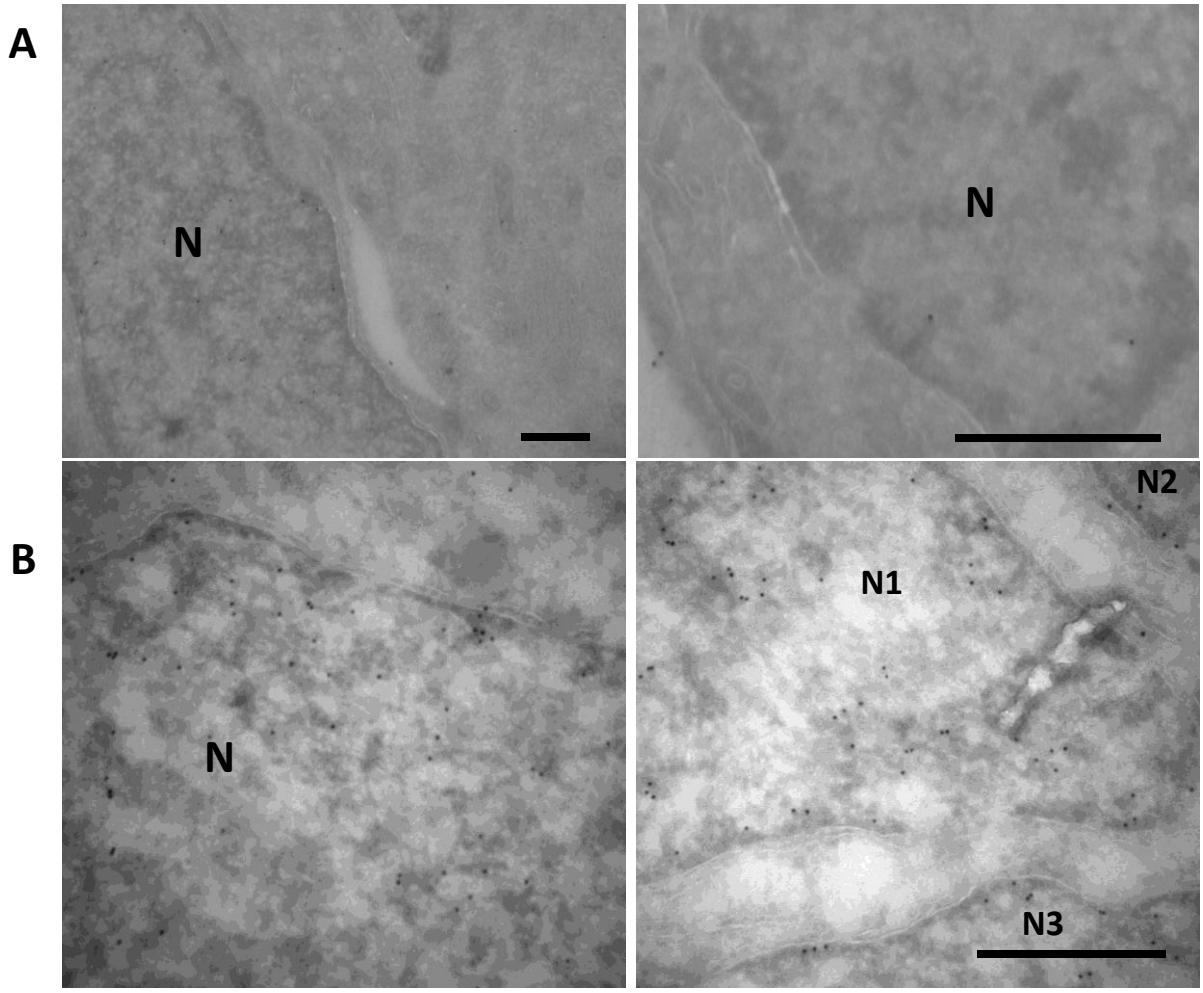

Figure 24. Poly-GA labeling in ips-derived motor neurons.

Background labeling in the nuclei of 30 DIV healthy control ips motor neurons (**10A**, top) and in nuclei of C9 patient-derived ips motor neurons (**10B**, bottom). Poly-GA antibody is labeled with 10 nm gold beads. Scale bars=500 nm. N=nucleus. Three nuclei are visible in B, right panel.

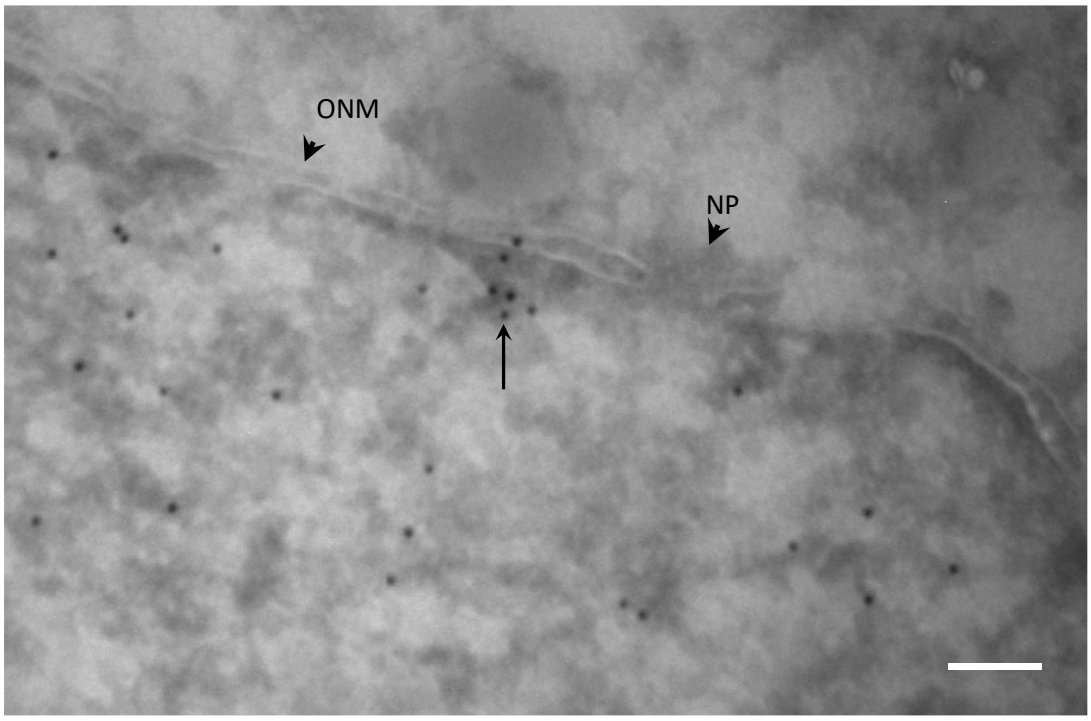

Figure 25. Higher magnification view of immuno-EM for poly-GA in C9 ips MN, 30 DIV. In a higher magnification view of figure 24B (above) poly-GA labeling is visible in the nucleus, especially near the inner nuclear membrane. A cluster of poly-GA labeling (arrow) exists near a nuclear pore. Arrowhead ONM=outer nuclear membrane, arrowhead NP=nuclear pore, visible as a gap in the nuclear membrane. Scale bar=100 nm.

4.2.2. Poly-GA is not rapidly cleared from ips-derived motor neurons.

As with the HEK-GA161, we wanted to understand how, if at all, the cultured motor neurons dispose of poly-GA as it accumulates over time. Therefore, we tested both the autophagic and proteasomal routes of clearance. Treatment of patient-derived motor neurons with Torin1 for 48 hours had no effect on the amount of poly-GA found in the cell lysates (figure 26). We then tested the alternate mechanism of clearance *via* the proteasome. Treating motor neurons derived from a C9 patient with a proteasome inhibitor, MG-132, or a putative proteasome activator, chlorpromazine (Jones, Njomen, Sjogren, Dexheimer, & Tepe, 2017), also had no effect on the amount of poly-GA recovered in the cell lysate (Figure 26.)

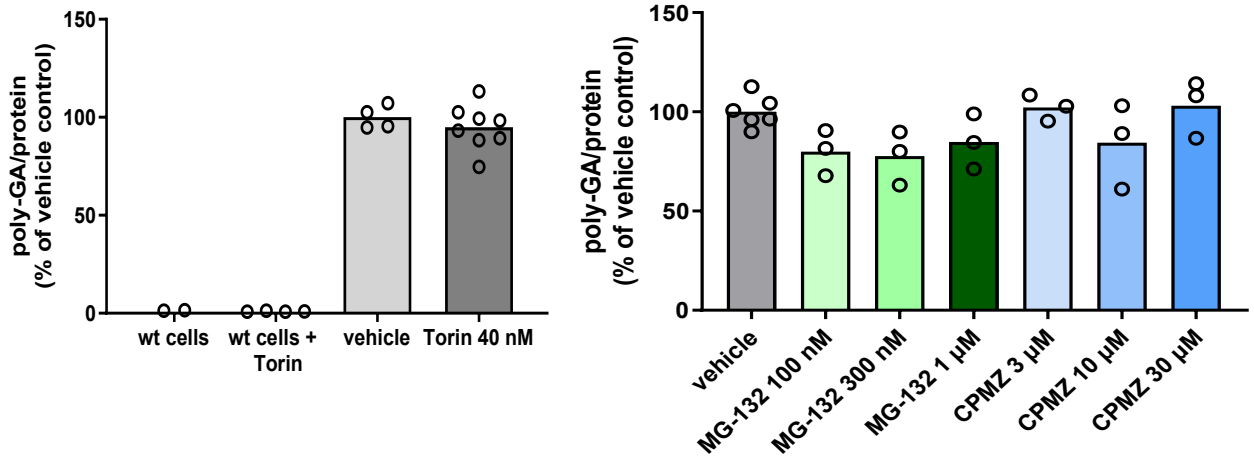

Figure 26. Poly-GA is not rapidly cleared from C9 patient-derived motor neurons. A) ips-derived motor neurons (27 DIV) were treated with Torin1 for 48 hrs. Torin-treated cells were not significantly different from vehicle control (Welch's t=2.681, p=0.0788. Each point represents one well, assayed for poly-GA in duplicate. **B)** No evidence for clearance of poly-GA by proteasome activity. Motor neurons (35 DIV) were treated with MG-132 or chlorpromazine (CPMZ), a proteasome activator, for 48 hrs. No group was significantly different from control (ANOVA, F=2.52, p=0.0627).

4.2.3. Poly-GA is not exclusive to stress granules in ips-derived motor neurons.

Stress granules are RNA granules that develop in a cell in response to a variety of stressors, including oxidative and osmotic stress. Stress granules are formed in the cytoplasm and consist of RNA and protein that coalesce around mRNA stalled in translation initiation (Protter & Parker, 2016). Stress granules contain TDP-43, including C-terminal phosphorylated TDP-43, and have been speculated to be a seed around which TDP-43 inclusions might form, or that the processes that lead to stress granule formation also produce pathological forms of TDP-43 (Colombrita et al., 2009). Formation of stress granules is also known to impair nucleocytoplasmic transport (K. Zhang et al., 2018). Stress granule associated proteins G3BP and eIF3η have been found in C9

repeat-expressing mice (J. Chew et al., 2019). Many nucleoporins contain intrinsically disordered regions that makes them prone to liquid-liquid phase separation involved with the formation of several kinds of membrane-less organelles like stress granules (Taylor, Brown, & Cleveland, 2016). In our study, we wished to determine whether poly-GA endogenously expressed by the C9 iPSC MN was localized exclusively to stress granules, as possible explanation for poly-GA sequestration of the intrinsically disordered proteins such as nucleoporins.

Stress granules were not detected under basal conditions, but with exposure to sodium arsenite (500 µM 1 hr.), we found G3BP-positive puncta in the ips motor neurons (figure 27A,B). In some but not all instances, they colocalized with poly-GA (figure 27). Untreated cells did not have large G3BP positive puncta, but poly-GA in the nucleus and in extranuclear spots was still present (figure 27), confirming the existence of extranuclear aggregates of poly-GA in the absence of evoked stress granules.

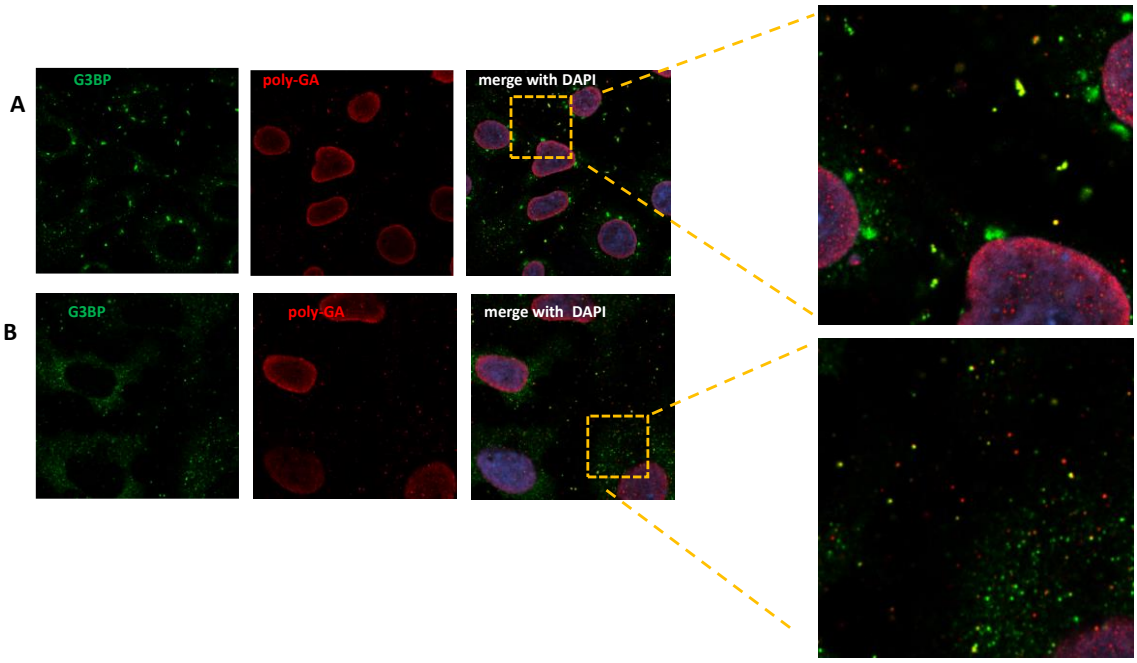

Figure 27. Extranuclear poly-GA does not depend upon stress granule formation. A) 500 µM sodium arsenite, 1hr., produced G3BP+ stress granules in C9 patient-derived ips motor neurons. **B)** cultures not treated with arsenite.

4.2.4. Summary of C9 patient-derived ips motor neuron characterization

The C9 patient-derived motor neurons do not differ in appearance from the healthy donor-derived motor neurons, but they express poly-GA both in the nucleus and in neurites. As with the HEK-GA161, it is unclear what, if any, mechanism clears the poly-GA as modulators of the proteasome and autophagy had little effect on the amount of poly-GA present. Also like the HEK-GA161, poly-GA is present in evoked stress granules as detected by colocalization between G3BP1 and poly-GA, but it is not clear whether increased cell stress impact the formation of poly-GA.

Using this characterized model, we then sought to understand the relationship among poly-GA, nucleoporins, and TDP-43 in the C9 patient-derived motor neurons.

4.3 Findings in the characterized ips-derived motor neurons

4.3.1. TDP-43 in ips-derived motor neurons

Because TDP-43 mislocalization is a nearly universal characteristic of ALS pathology, we sought to determine whether the C9 patient-derived motor neurons showed this characteristic. TDP-43 immunoreactivity was assessed in the ips-derived motor neuron cultures. We did not detect a substantial shift of TDP-43 away from the nucleus into the cytoplasm (figure 28A). However, both immunofluorescence and immuno-EM using antibodies directed to either the mid-domain or the C-terminal of TDP-43 revealed TDP-43 more heterogeneously distributed within the nucleus of C9 than healthy donor motor neurons (Figure 28B, C).

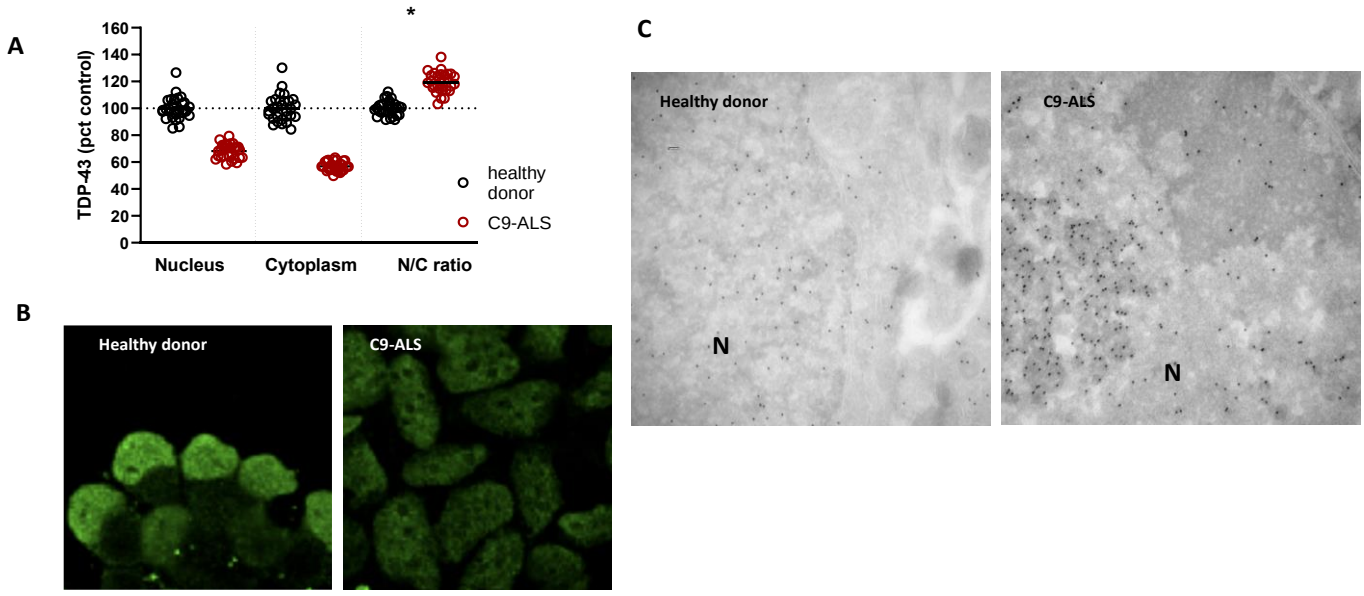

Figure 28. TDP-43 N/C ratio is slightly increased in C9 ALS patient-derived motor neurons A) Both nuclear and cytoplasmic intensity of TDP-43 immunoreactivity are decreased in C9 motor neurons, but the N/C ratio is slightly increased**. ***Mann-Whitney U-test of N/C ratio, $p<0.0001$ **B)** TDP-43 immunofluorescence (mid-domain antibody) in ips-derived motor neurons **C)** Immuno-EM detection of TDP-43 (C-term antibody) reveals clumping in C9 ALS motor neurons.

4.3.2. CHMP7 is not relocalized to the nucleus in C9 patient-derived motor neurons

Research on nuclear pore proteins in ips-derived motor neurons has found a selective loss of a subset of nucleoporins (Coyne et al., 2020), with POM121 the first nucleoporin lost. Cells maintain the nuclear membrane integrity via the ESCRT pathway, and a relocalization of one of the ESCRT proteins, called Charged Multivesicular Body Protein 7 (CHMP7), has been proposed to be the cause of nucleoporin loss in ALS (Coyne et al., 2021). Specifically, a recent study reported an accumulation of CHMP7 in nuclei isolated from C9 and sALS ips-derived motor neurons (Coyne et al., 2021). Therefore, we examined whether nuclear CHMP7 was increased in our C9 patient-derived motor neurons. We saw no evidence of increased CHMP7 in the nucleus of ips motor neurons derived from C9 ALS patient (figure 29), while CHMP7 in the cytoplasm was only slightly reduced. We did not detect a substantial loss in POM121. In fact, we saw greater POM121 in the neuronal population identified as poly-GA positive (figure 29) compared to neurons poly-GA negative.

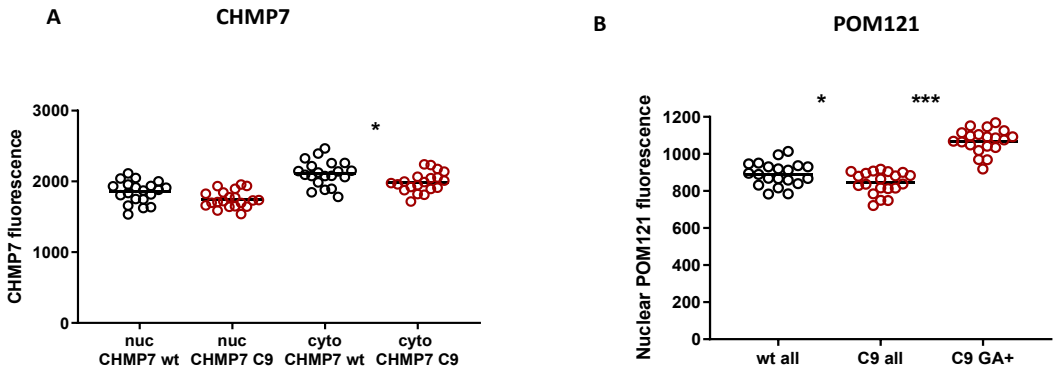

Figure 29. CHMP7 is not increased and POM121 is not lost from the nucleus of C9-derived ips motor neurons. A) Cytoplasmic intensity of CHMP7 immunofluorescence is slightly decreased in C9 neurons. ANOVA, F=22.7, Šídák's multiple comparisons test (nucleus) p=0.0635, *(cytoplasm) p=0.0217 **B)** Nuclear POM121 is slightly decreased in C9 neurons overall, but increased in GA+ C9 neurons. ANOVA, F=72.01 followed by Dunnett's test *"wt all" vs. "C9 all" p= 0.0372, ***"wt all" vs. "C9 GA+" p<0.0001

4.3.3. Nup153 and POM121 expression are correlated with poly-GA expression in C9-derived ips motor neurons

These results indicated that as previously described for the HEK-GA161 cells model, the ips motor neurons derived from a C9 expansion carrier did not show obvious toxicity under basal conditions. However, unlike the HEK-GA161 cells, poly-GA did not accumulate in aggresome-like deposits within or outside the nucleus. Instead, we found that poly-GA was primarily found within the nucleus (figures 22,23). Because nucleoporins POM121 and Nup153 were mislocalized in HEK during poly-GA expression, we examined these nucleoporins in the motor neuron culture. Nuclear Nup153 expression with similar in C9 ALS and control iPSC MNs, and POM121 was only slightly decreased in the C9 cells (Figure 30). However, because poly-GA was very heterogeneously expressed among the C9 ALS MN cells, the results were analyzed differentiating poly-GA positive versus poly-GA negative expressing neuronal population. Both POM121 and Nup153 abundance were increased in cells expressing more poly-GA (r-squared values of 0.686 (POM121) and 0.726 (Nup153), figure 30B). When non-poly-GA+ cells (<2000 fluorescence units in nucleus) are omitted from the analysis, the correlation is even stronger (0.809 for POM121; 0.781 for Nup153). By contrast, neurons from healthy donor cultures did not show a strong correlation between background GA-like fluorescence, suggesting that the correlation is not an artifact.

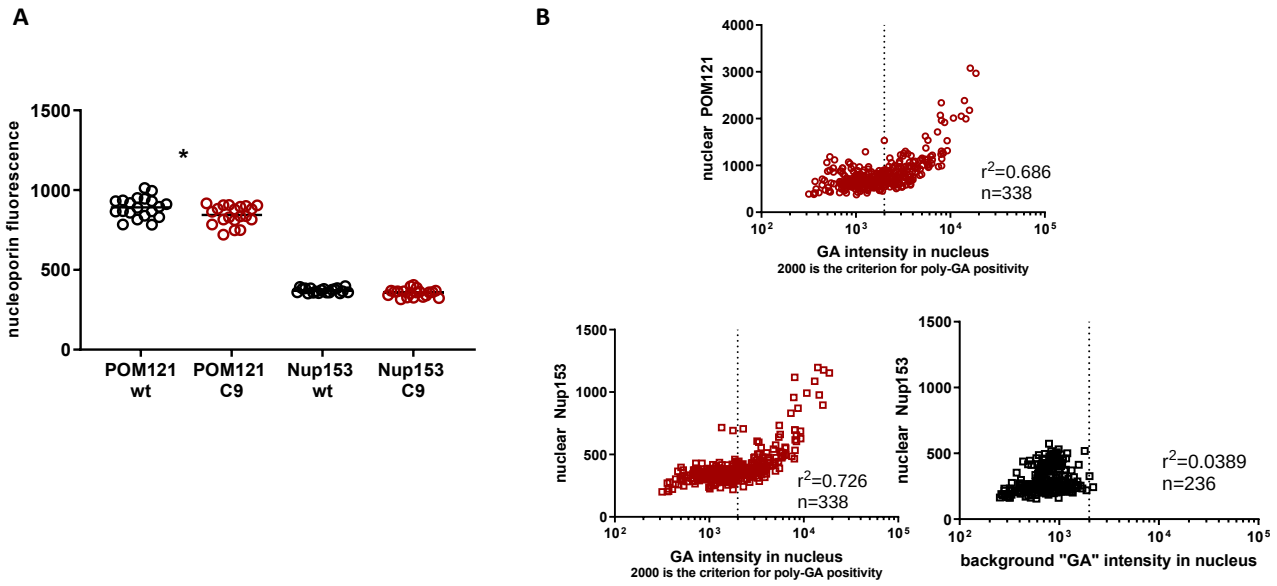

Figure 30. POM121 and Nup153 are positively correlated with poly-GA in C9-derived ips motor neurons. A) POM121 is slightly decreased overall in the nucleus of C9 as compared with healthy donor cells and Nup153 is unchanged. One point=mean of one well. ANOVA F=816, Šídák's multiple comparisons test: (POM121) p=0.0032 (Nup153) p>0.05. **B)** Cells expressing more poly-GA also express more POM121 and Nup153, r-squared values 0.686 (POM121) and 0.726 (Nup153), in contrast to healthy donor cells, where the background fluorescence in the poly-GA channel is poorly correlated with nucleoporin expression. One point=one cell.

4.3.4. C9-derived ips neurons have disrupted nuclear membranes

As we were able to detect poly-GA within the nucleus of the C9 patient-derived motor neurons, we searched for possible structural consequences of this expression. By conventional EM, we found aberrant nuclear membranes in C9, but not healthy donor-derived motor neurons (figure 31). In addition to disorganized nuclear membranes, we found small, circular structures resembling published images of nuclear pores from cells overexpressing Nup153 (Bastos, Lin, Enarson, & Burke, 1996) (figure 31B). Nuclear membrane disruptions could be caused by any phenotype associated with the C9-derived motor neurons, whether due to a dipeptide repeat protein, a different consequence of C9 expansion, or something specific to the patient donor but unrelated to the C9 expansion. However, not only did we observe disrupted nuclear membranes and putative ectopic nuclear pores (figure 32B), we detected poly-GA located within the nuclear envelope; that is, between the inner and outer nuclear membrane, suggesting a possible direct physical disruption of the nuclear membrane by poly-GA aggregation (figure 32A).

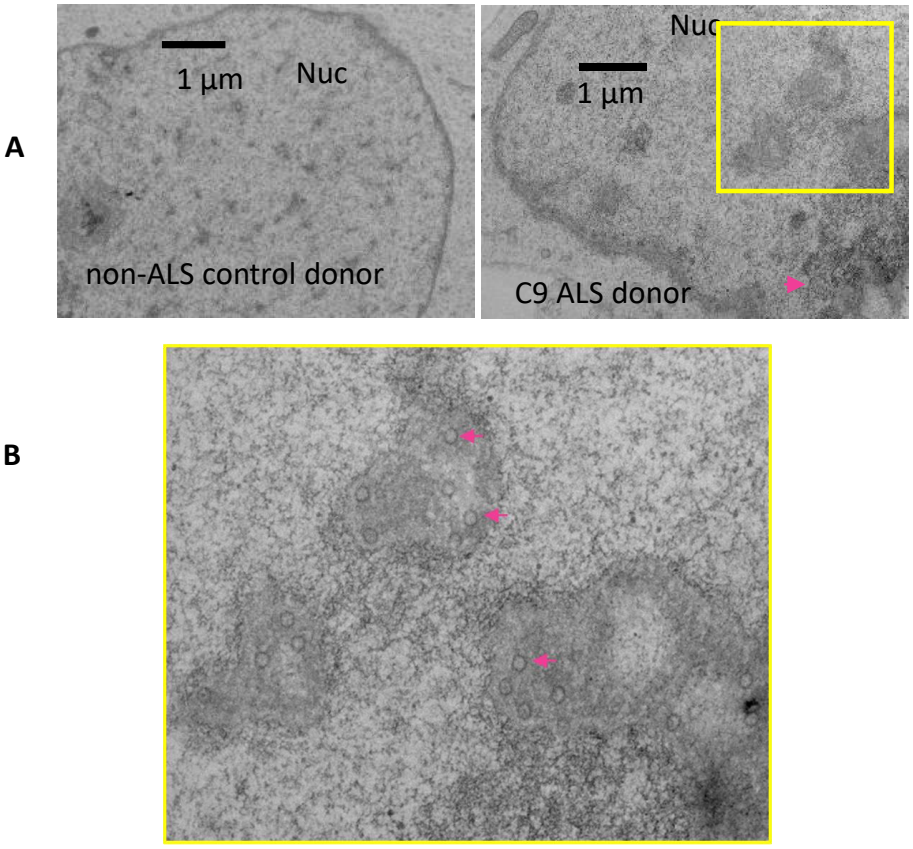

Figure 31. C9 ALS patient-derived motor neurons have disrupted nuclear membranes. Conventional EM of ips motor neurons (30 DIV) reveals altered nuclear membrane morphology. **A)** Example of typical nuclei in cross section in healthy- vs. patient-derived ips neurons. Note atypical density and loss of membrane integrity (arrowhead). **B)** Enlarged area from A. Larger whorls suggest an indentation in the nuclear membrane in the z-dimension. Small, circular, membrane-enclosed structures suggest nuclear pores viewed in cross section (arrows).

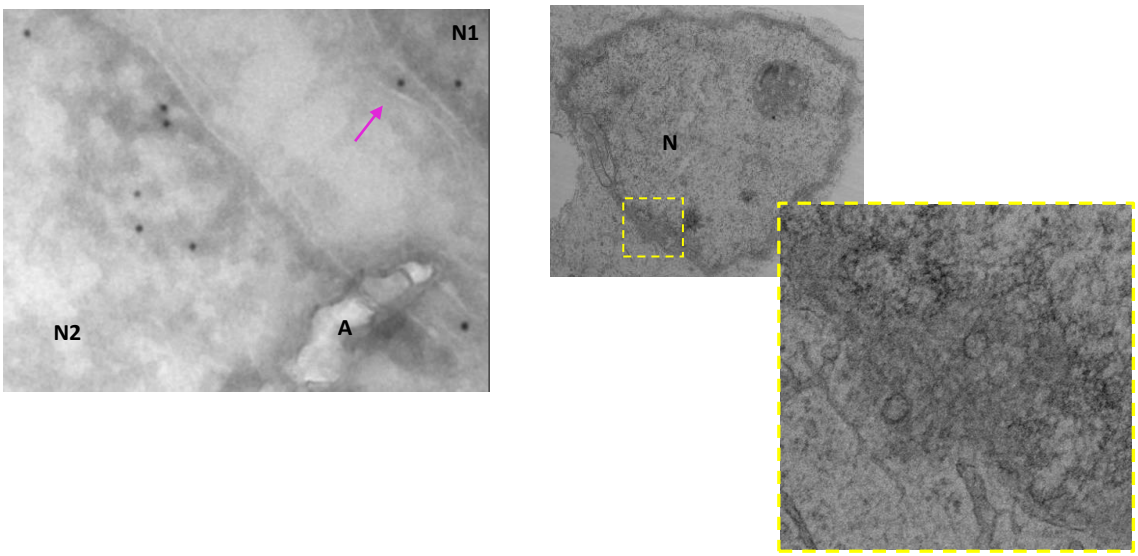

Figure 32 (left) Immuno-EM labeling of poly-GA (black dots) near nuclear membrane in C9 patient-derived motor neurons N=nucleus A=artifact in sample **Arrow indicates poly-GA apparently within the nuclear envelope**. (right) conventional EM showing disrupted nuclear membrane and possible ectopic nuclear pores in C9 patient-derived motor neuron.

4.3.5. C9-derived ips motor neurons show increased vulnerability to puromycin

We used the protein translation inhibitor, puromycin, as a toxic insult to the ips-derived motor neurons. Puromycin has been reported to activate a set of genes similar to those upregulated in the cortex of C9 ALS-FTD patients (Klim, Pintacuda, Nash, Guerra San Juan, & Eggan, 2021). After treatment with puromycin, 7 μM 48 hrs., cells were stained with Calcein AM/ethidium homodimer to label both live and dead cells, a sensitive measure of cell death that avoids artifacts from washing away dead cells during fixation. Puromycin killed 18.8% of the cells in the healthy donor cultures and 56.8% in the C9 ALS patient-derived cells (figure 21A).

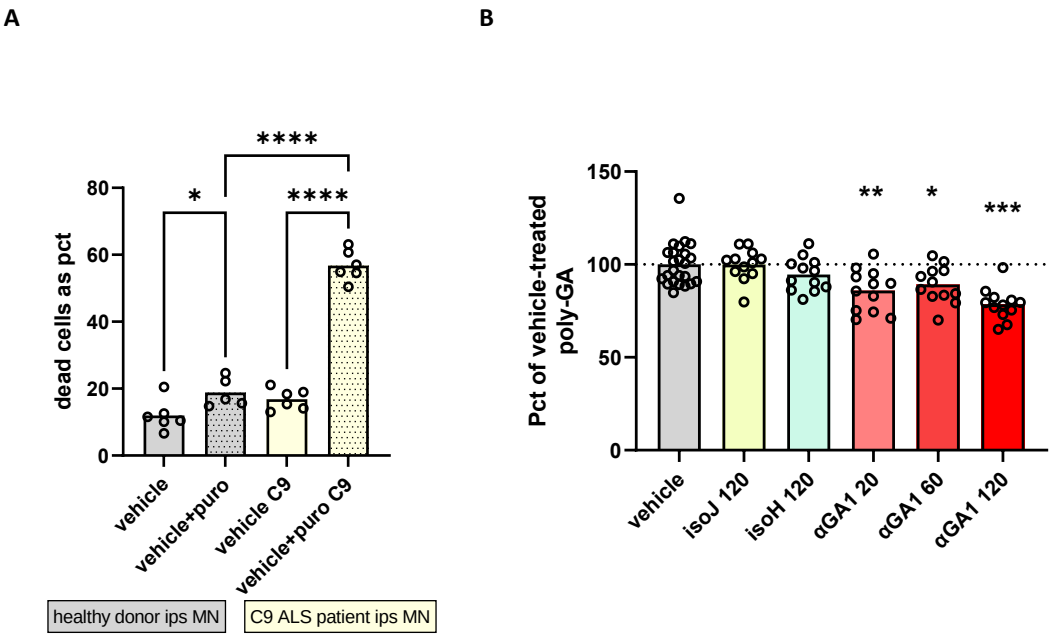

Figure 33. A) Patient-derived ips motor neurons are more sensitive than control neurons to puromycin. Treatment with puromycin, 7 mM, 48 hrs, killed 18.8 (+4.4)% of healthy but 56.8% (+4.6) of C9 ALS patient-derived motor neurons (ANOVA, F=143.2, followed by Šídák's multiple comparisons test, *healthy vehicle vs healthy vehicle+puromycin, p=0.0434; **** C9 vehicle vs C9 vehicle+puromycin, p<0.0001; **** healthy vehicle+puromycin vs C9 vehicle+puromycin, p<0.0001).

B) αGA1 reduces poly-GA in C9-patient-derived ips motor neurons. Motor neurons were treated for 12 days beginning at DIV 30 with antibodies αGA1 and isotype control added every two days. The 120 nM αGA1 treatment reduced poly-GA by 26% (±8.56%) vs. vehicle (ANOVA, F=6.950, followed by Šídák's multiple comparisons test, **20 nM p=0.0013, *60 nM p=0.0238, ***120 nM p<0.0001)

4.3.6. Treating C9-derived ips motor neurons with antibody reduces poly-GA but does not protect against puromycin

Because scavenging of poly-GA with an antibody provided neuroprotection in mice expressing a repeat expansion in C9orf72 (Nguyen et al., 2020), the possible protective effect in the C9-patient-derived ips motor neuron culture was investigated. We treated motor neurons for 12

days beginning at DIV 30 with antibodies added every two days, using human αGA1 from Nguyen et al. and isotype control antibodies. We evaluated the number of dead cells as a percent of total and the poly-GA content of the cells in the same wells. The αGA1 treatment led to a reduction in poly-GA, whereas the isotype control antibodies did not (figure 21B). The highest concentration of αGA1, 120 nM, reduced the amount of poly-GA by 26% (±8.56%). Nevertheless, the antibody treatment did not protect the cells as measured by percent cell death (Figure 21C). Similarly, the average intensity of staining for cleaved caspase, a marker of activation of apoptosis, was also unchanged by antibody treatment (figure 36).

Thus, we conclude that removing at least 24% of poly-GA from the C9 ALS patient-derived motor neuron cultures does not provide protection against puromycin insult.

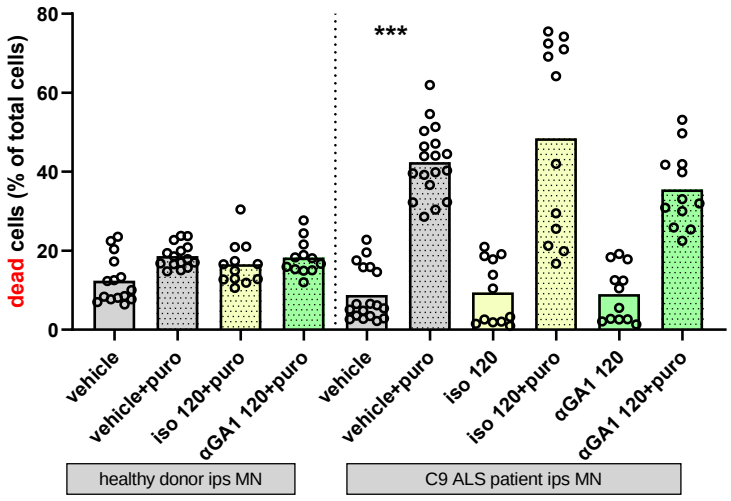

Figure 34. αGA1 does not protect C9 ALS patient-derived motor neurons from puromycin-induced cell death. The same motor neurons as in figure 33 were treated for 12 days beginning at DIV 30 with antibodies αGA1 and isotype control added every two days. Puromycin increased the number of dead C9 cells from 8.8 ±6.8% to 42.4 ±8.8% of total cells per well. Nonparametric analysis was used because of the substantial scatter in the data. (Kruskal-Wallis statistic=51.2 followed by Dunn's multiple comparisons test, vehicle vs. vehicle+puro $p<0.001$; vehicle+puro vs. iso 120+puro $p>0.999$; vehicle+puro vs. αGA1 120+puro $p>0.999$; iso 120+puro vs. αGA1 120+puro $p>0.999$)

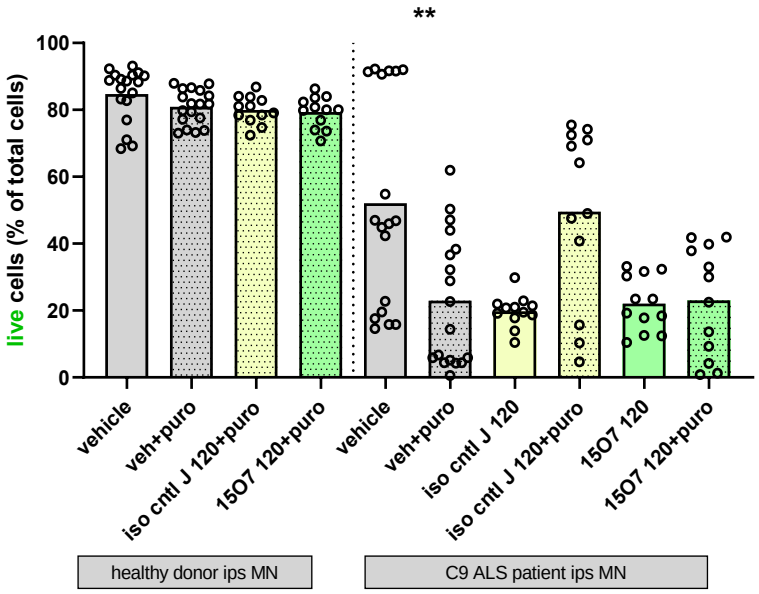

Figure 35. αGA1 does not protect live C9 ALS patient-derived motor neurons from puromycin

The same motor neurons as in figures 34 and 33 were treated for 12 days beginning at DIV 30 with antibodies αGA1 and isotype control added every two days. Puromycin reduced the number of live C9 cells from 52.1±31% to 23.0±20% of total cells per well. Nonparametric analysis was used because of the substantial scatter in the data. (Kruskal-Wallis statistic=16.19 followed by Dunn's multiple comparisons test, **vehicle vs. vehicle+puro p=0.0082; *vehicle+puro vs. iso 120+puro p=0.0280; vehicle+puro vs. αGA1 120+puro p>0.999; *iso 120+puro vs. αGA1 120+puro p>0.0392. Although αGA1+puro was marginally significantly different from iso J+puro, in light of the dead cell results and the fact that the iso control differed significant from vehicle, this was not considered to be compelling evidence of protection.

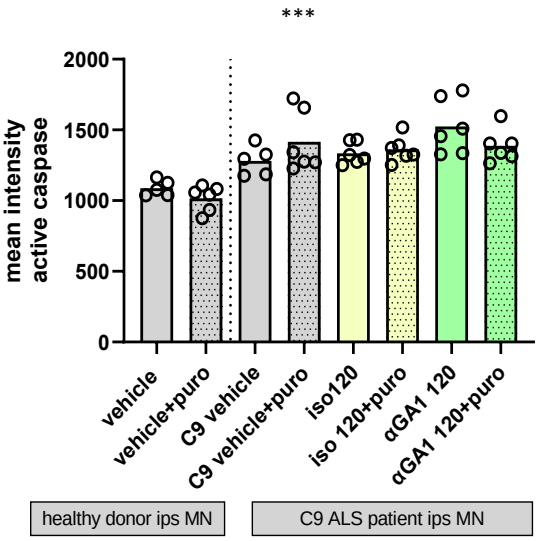

Figure 36. αGA1 does not protect C9 ALS patient-derived motor neurons from puromycin.

Motor neurons were treated for 12 days beginning at DIV 30 with antibodies αGA1 and isotype control added every two days. Cleaved caspase staining was greater in the C9 than in healthy control donor neurons treated with puromycin, but none of the antibody treatments was different from C9 vehicle + puromycin. (ANOVA, F=9.570, ***vehicle+puro vs. C9 vehicle+puro, p<0.0001; C9 vehicle+puro vs. iso 120+puro p=0.9657; C9 vehicle+puro vs. αGA1 120+puro p=0.9978; iso 120+puro vs. αGA1 120+puro p=0.9991)

5. Discussion

5.1. Summary of major findings

In our models of C9 patient-derived motor neurons and poly GA-expressing HEK cells, we detected a distribution of poly-GA accumulation at the nuclear membrane that was associated with the appearance of disrupted nuclear membranes. In the case of HEK-GA161, we showed that the poly-GA aggregated into SQSTM1/P62-positive, aggresome-like bodies. We confirmed colocalization of poly-GA with TDP-43 (C-terminal) and nucleoporins using a proximity ligation assay (PLA). We identified mislocalized nucleoporins aggregated with poly-GA, including POM121, which has been identified as the earliest nucleoporin lost in C9 ips-derived motor neurons (Coyne et al., 2020). However, we saw in our ips MN model no evidence for loss of POM121 coupled with an increase in nuclear CHMP7 as previously described by (Coyne et al., 2021). In C9 ips-derived motor neurons and HEK-GA161, we showed that the poly-GA aggregates were not due purely to stress granule formation. We detected at the ultrastructural level apparently disrupted nuclear membranes and possibly ectopic nuclear pores. We then validated a model of neurodegeneration in C9 ALS patient-derived motor neurons by modulating protein homeostasis using puromycin. Using this model, we showed that the treatment with a specific antibody targeting poly-GA (αGA1) effectively reduced the poly-GA content of the cells by 30% but this treatment had no impact on neurodegeneration.

Although the ips-derived motor neurons model could more closely reflect than HEK cell line the neurons of the human nervous system, they remain immature neurons, unlike the aged neurons of the aging adult human. It is possible that the HEK cell system, with its quick accumulation of poly-GA into SQSTM-positive aggregates, may represent a rapid route to the type of SQSTM1-positive inclusions seen in patient tissue at autopsy (Vatsavayai et al., 2019). It is also possible that the C9-derived ips motor neuron cultures represent a stage similar to a disease prodromal state in human, with DPR accumulating in or near the nuclear membrane, but not yet aggregated.

We identified sequestration of nuclear pore proteins by poly-GA. Sequestration of Nups has been reported by others (Freibaum et al., 2015; Y. J. Zhang et al., 2016), but not in the context of poly-GA only expression. *In vivo*, identified POM121 in accumulations of poly-GA in the brains of

poly-GA50-expressing mice(Y. J. Zhang et al., 2016). We extended that by finding that poly-GA expression resulted in ectopic accumulation of POM121, Nup153 and TDP-43. We did not find a substantial loss of POM121 as has been reported by others (Coyne et al., 2020). The disparate result could be due purely to technical factors, because Coyne and colleagues first isolated nuclei from the cells, then imaged immunofluorescence using structured illumination microscopy, two techniques not applied here. Nevertheless, it is intriguing that both POM121 and Nup153 were positively correlated with poly-GA expression in our C9 ips-derived motor neuron cultures. Because there was no substantial loss of these nucleoporins throughout the cell, it is possible that the ectopic nucleoporin expression seen in HEK cells could be due to increased synthesis or slower turnover of nucleoporins, rather than relocalization of the same pool of existing protein. It cannot be ruled out that in the C9 motor neurons, increased GA expression is associated with additional expression of nucleoporins. This could be tested in future experiments by biochemically quantifying the total amount of nuclear and cytoplasmic nucleoporins, or by examining the difference when protein synthesis is inhibited.

5.2. Parallels with disease pathology

To what extent do the model cell systems reveal changes similar to those found in patient tissue post-mortem? Nuclear pore changes have been detected in patient tissue. For example, a loss of POM121 has been reported in C9orf72 patient motor cortex, both in isolated nuclei extracted from cortex and in paraffin-embedded thin sections of motor cortex (Coyne et al., 2020). After the loss of POM121, the authors detected decreased expression of an additional cohort of six nucleoporins, including TPR and Nup50. In this study, they did not, however, see such a change with Nup153. Increases, rather than decreases, of nucleoporins are typically not detected in ALS tissue. However, cytoplasmic upregulation of RanGAP1, GP210 and NUP50 have been found in sALS lumbar motor neurons (Shang et al., 2017). In addition to these expression changes, colocalization of Nup205 and TDP-43 were also detected. Despite lacking extensive intrinsically disordered domains that are proposed to be a mechanism of TDP-43 interaction, Nup205 was also found to interact with TDP-43 insoluble fraction in an in vitro system (Chou et al., 2018). (Chou et al., 2018)

5.3. Nuclear membrane structure

At the microstructure level, several groups have reported apparently malformed nuclear membranes in neurons in patient tissue. Kinoshita et al. found irregular nuclear membranes in anterior horn cells of sALS patients but not control cases (Kinoshita et al., 2009). Distorted nuclear membranes have been reported in Alzheimer's disease (Napoletano et al., 2021) where they were associated with PIN1 dysfunction. Distorted nuclear membranes and cytoplasmic mislocalization of FG Nups were also reported in Alzheimer's disease by (Eftekharzadeh et al., 2018), where Nup98 was found with tau protein. The presence of nuclear membrane pathology in ips-derived neurons remains controversial. Paonessa et al. reported misfolded membranes in tau-associated FTD and ips neurons(Paonessa et al., 2019). Increased nuclear membrane distortion in (G4C2)-149 mice has been reported (J. Chew et al., 2019) , but others have not seen membrane changes in ips neurons specific to ALS (Coyne & Rothstein, 2021), but rather to aging in general. Therefore, it remains possible that nuclear membrane distortion occurs, but only in specific circumstances. Detecting such changes alone in the absence of another marker must be done in a very well-controlled fashion with a large cohort of age-matched tissue.

5.4. Poly-GA persistence

The endogenous clearance mechanism(s), if they exist, have not been determined for DPR. (Nguyen et al., 2020) also found no change in poly-GA in their HEK cell system when treated with autophagy blocker 3-MA or protease inhibitor MG-132. On the other hand, Guo and colleagues (Guo et al., 2018), found engagement with the proteasome by poly-GA; resulting in stalling of the proteasome, and others (Yamakawa et al., 2014) found poly-GA inhibited proteasome activity. It is also unclear how cells deal with a long polypeptide lacking any of the amino acids with the reactive side chains lysine, cysteine, serine, or threonine. Relatively short, 15-repeat peptides of poly-GA have been shown to form β-pleated sheet structures that aggregate into amyloid fibrils (Chang et al., 2016), which are toxic and can be transmitted from cell to cell. Degradation of the fibrils was not investigated. In fact, sequence similarity searching detects the protein FIBH, fibroin heavy chain, as the most similar, validated protein (UniProt.org/blast). FIBH is a silk protein, which has repeated sequences of GAGAGS (Chang et al., 2016), hinting at the properties of such sequences.

We observed poly-GA aggregates adjacent to the nuclear membrane, similar to those described by (Lee et al., 2017) in a similar context, and a striking interaction of the poly-GA aggregates with nucleoporins outside the nuclear membrane. The C-terminal region of TDP-43 has been found to interact with nucleoporins via their FG-rich regions (Chou et al., 2018). These regions are important for the barrier-forming properties of the pore, but may also be responsible for pathological interactions with other hydrophobic proteins in disease. Several attempts to use poly-GA as a bait protein for co-immunoprecipitation experiments failed in our lab. However, very recently, the protein interactome of poly GA, GR and PR was investigated using a proximity labeling technique (F. Liu et al., 2022). They found the interactomes of GR and PR were quite similar, and both distinct from poly-GA. The arginine containing DPR were more associated with nuclear pore proteins, and poly-GA with proteasome components. Poly-GA did, however, associate with RANBP1 (F. Liu et al., 2022). Poly-GA has been found to sequester a variety of proteins, including HR23 (RAD23 homolog) (Y. J. Zhang et al., 2016), Unc-119 (May et al., 2014) and others. It has been reported to impair importin-α function (Khosravi et al., 2017), which may reduce TDP-43 import. Many of the same groups also find toxicity of poly-GA, but what properties are responsible for the toxicity in cell models and which may be relevant for motor neuron death are unclear. Recent reports have found that poly-GA in fibrillar form differs from the oligomeric form in how they are taken up and transmitted from cell to cell (Marchi et al., 2022).

5.5. Interaction with TDP-43

In nearly all cases of ALS except for those caused by mutations in SOD1 or FUS, TDP-43 pathology is present. Instead of diffuse staining throughout the nucleoplasm, aggregates of TDP-43 immunoreactivity are found in the cytoplasm or as fiber-like wisps in the cytoplasm. Accompanying these are nuclei that appear relatively depleted of TDP-43 (I. R. A. Mackenzie et al., 2007). The loss of TDP-43 could be due to impaired import, excessive export, or to the appearance of a cytosolic sink for TDP-43, removing it from the cell's pool of TDP-43 under regulation. The latter mechanism is supported by findings of TDP-43 or fragments of TDP-43 found in liquid-liquid phase separated structures, whether stress granules (P. Zhang et al., 2019) or other structures (Gasset-Rosa et al., 2019).

By immunofluorescence, we detected TDP-43 C-terminal in the cytoplasm of HEK in aggregates with poly-GA and nucleoporins. This may reflect the formation of either stress granules that later capture nucleoporins, or aggregates of poly-GA and nucleoporins that later serve as a sink for cytoplasmic TDP-43. Either could serve as a possible starting point for TDP-43 extranuclear aggregation. It is not known whether the TDP-43 identified here as interacting with poly-GA is a C-terminal fragment or the complete protein. The C-terminal region, which contains the intrinsically disordered domain, of TDP-43 is known to be prone to aggregation and can form droplet-like accumulations both as a component of stress granules or in a stress granule-independent fashion (Chen & Cohen, 2019). Further work is needed to understand whether this is due to a cleavage event before accumulation in the aggregates. In any case, the existence of poly-GA protein in the cytosol is likely either to initiate or to aggravate the accumulation of TDP-43 away from the nucleus. The sequestration away from the nucleus may result in an initial increase in TDP-43 synthesis as the cell responds to less TDP-43 moving into and out of the nucleus. This could account for the apparent increase in total TDP-43 seen in the HEK on induction of poly-GA (Figure 15). We did not find a net decrease in the TDP-43 nuclear to cytoplasmic ratio in ips-derived motor neuron cultures, but we did see evidence of possible clumping or aggregation of TDP-43 within C9-derived nuclei.

5.6. Role of Nup153

Genetic screens have identified certain nucleoporins as regulators of either G4C2 or dpr toxicity. For example, Freibaum and colleagues (Freibaum et al., 2015), using a genetic screen in *Drosophila* expressing G4C2, identified knockdown of the following nucleoporins provided a protective effect against the neurodegeneration elicited by expression of the hexanucleotide repeats (human ortholog names): Nup107, Nup160, and Nup98. All three of these nucleoporins are pore-forming members with FG sequences. Reduction of ALYREF, a protein coupling RNA transcription to export, also provided protection. Knockdown of Nup50, Nup153, or XPO1, on the other hand, enhanced the degeneration (Freibaum et al., 2015). Protective or pro-degenerative effects of Nups have been detected against both expression of the hexanucleotide repeat and against dpr production in the absence of potentially toxic G4C2 RNA. Nup50 and Nup153 are members of the nuclear basket and are essential for the binding and transit of mRNA

to the cytosol. NES-containing *proteins*, in contrast, require binding to XPO1 which chaperones them through the hydrophobic central pore.

In the present work, we found knockdown of Nup153 reduced the amount of poly-GA found in the HEK-GA161. There was no effect on the mRNA (Figure 21), which would have suggested an artifactual suppression of the transgene. Instead, without affecting message, knockdown of Nup153 diminished the amount of poly-GA protein through an unknown mechanism. Although Nup153 plays a role in nuclear export, it is also essential for the reassembly of the nuclear pore complex after cell division (LaJoie et al., 2022). In the dividing HEK-GA161, knockdown of Nup153 for 48 hours may result in cells with incompletely assembled nuclear pores, reducing overall cell health and reducing the ability to express the large amount of poly-GA detected in the cells. In fact, recent experiments on nuclear pore function avoid the use of RNA knockdown to silence Nup153 for this reason (Li, Aksenova, et al., 2021).

It is also possible that reducing the amount of Nup153 leads to less poly-GA/nucleoporin aggregation, leaving more poly-GA in a non-aggregated state, and therefore more accessible to some form of degradation. Finally, it is known that overexpression of Nup153 alone causes Nup153 to accumulate at the inner nuclear membrane, rather than throughout the nucleus as occurs with other nuclear proteins including other nucleoporins (Bastos et al., 1996). The insertion into the membrane is driven by the amino-terminal portion of the protein, in contrast to the carboxy terminal which is critical to mRNA binding and translocation. In addition, the overexpression of Nup153 alone causes elongated nuclear membranes and the appearance of Nup153 in complex with lamins (Bastos et al., 1996). This results in ectopic nuclear pores as seen by EM (Bastos et al., 1996). Combining this information with our observation of a possible ectopic nuclear pores and the positive correlation between poly-GA and Nup153 in the ips-derived motor neurons suggests that poly-GA at the nuclear membrane may itself drive Nup153 expression, subsequently leading to formation of aberrant pores or pore-like structures. Biochemically assessing whether there is an induction of Nup153 or a redistribution of existing Nup153 will clarify whether there is indeed increased expression of the nucleoporin in the presence of poly-GA. Assessing this possible relationship is a promising area for additional research.

5.7. Effect of antibody treatment

We found an approximately 25% reduction in RIPA-extractable poly-GA after 12 days treatment with 120 nM of αGA1. This is similar to the 31% reduction found by Nguyen et al. after 13 days of treatment with the same antibody in their ips motor neurons, although they did not show a protection against a neurotoxic insult in that system (Nguyen et al., 2020). It is not clear why there was no protection in our model. It is possible that the poly-GA reduction was insufficient and that a higher antibody concentration or longer treatment time would provide some protection. There are alternative explanations, however. Puromycin halts protein synthesis by causing premature termination of the nascent polypeptide chain by acting as an analog of the 3'-terminal end of the aminoacyl-tRNA. This produces many small, puromycylated polypeptides, which are usually targeted for degradation (Aviner, 2020). One possibility is that the peptides overwhelm a proteolytic system already compromised by poly-GA. Another, similar, possibility is that the C9 genotype already means that the cells have a compromised system of protein degradation, making them more susceptible to puromycin independent of poly-GA. In fact, the partial haploinsufficiency of C9 and its role in autophagy make this a promising hypothesis.

In summary, both cell models provide information on the mechanisms by which the dipeptide repeat protein, poly-GA, disrupts cellular processes. This work confirms the effect of exogenously applied poly-GA antibody reducing poly-GA in cell culture, but does not capture the therapeutic effect suggested by the *in vivo* experiments in (Nguyen et al., 2020). The results also suggest that there may be a role for Nup153 in the generation of nuclear pore pathology in C9 ALS-FTD that deserves further research. The goals of this work included the characterization and validation of the HEK-GA161 model as a system to understand certain elements of the effect of poly-GA. Despite being a non-neuronal cell line, the HEK-GA161 produced poly-GA inclusions physically resembling those found in patient neurons post-mortem (compare figures 4, 11, and 12). It was used successfully to test the hypothesis that poly-GA can directly block the nuclear pore. In addition, it provided evidence that poly-GA alone, in the absence of repeat RNA or ALS genotype,

can bind and sequester nuclear pore proteins away from the nuclear membrane. It remains a useful and valid system for exploring the biochemistry of poly-GA.

On the other hand, the HEK cell system does not provide information about neuron-specific processing of poly-GA. The patient-derived stem cell system provides such a model. There, I found robust poly-GA expression that was found primarily in the nucleus and, to a lesser extent, in neurites. These cells also showed an unanticipated positive correlation between poly-GA expression and at least two nucleoporins. The ultrastructure of these cells confirmed a speculated existence of poly-GA within the nuclear envelope itself (figures 10, 25, and 32). EM and immuno-EM also showed the existence of disrupted nuclear membranes and possibly ectopic nuclear pores or pore-like structures. Because Nup153 is already known to regulate the formation of pores (Bastos et al., 1996), the role of Nup153 and GA in promoting the formation of these mislocated pores is a promising area for further research. These results also prompt questions of why the poly-GA is found in the nucleus of the motor neurons and whether movement of poly-GA or other DPRs from the nucleus to aggregates in cytosol and nucleus is part of the disease process.

Finally, this system allowed an exploration of the utility of poly-GA antibodies as a therapeutic approach. As previously shown by Nguyen and colleagues, chronic administration of the poly-GA antibody reduced RIPA-soluble GA found in the cultures. However, that provided little protection against a puromycin insult. There are many possible reasons for this. Poly-GA may, in fact, not be relevant in the context of protein synthesis inhibition in C9 ALS genotype cells. Other possibilities include insufficient reduction of poly-GA or the great variability across wells and experiments. Notably, this was much greater in the patient-derived than the healthy donor-derived ips motor neurons. Additionally, challenges other than puromycin may better reveal protective effects of antibody treatment. This cell system, which includes other aspects of C9-ALS such as haploinsufficiency of C9orf72 protein(s), RNA foci, and DPRs other than poly-GA, remains a highly valuable model system for developing possible therapies.

6. Perspectives

This work highlights a role of poly-GA in disrupting the structure of the nuclear membrane. Previous work identified several pathways by which the C9 expansion mutation interferes with nucleocytoplasmic transport (Y. J. Zhang et al., 2016), (Jovicic et al., 2015), (Fallini, Khalil, Smith, & Rossoll, 2020). The present works adds to our body of knowledge in several ways. We described an *in vitro* system in which poly-GA alone specifically binds nucleoporins, sequesters them outside of the nuclear envelope, and alters TDP-43 expression. Evidence at the ultrastructural level suggests a direct interaction between poly-GA and the nuclear envelope in both the cell line model and in ips-derived motor neurons. Evidence of ectopic nuclear pores is particularly striking. Previous models have considered a variety of ways in which repeat expansion-derived RNA or proteins might interfere with nucleocytoplasmic transport by sequestering a needed factor or blocking transport. One possibility suggested by the present data is that something in the C9 patient-derived motor neurons actually induces the formation of ectopic or non-functioning nuclear pores or pore-like assemblies. These could interfere with transport in a number of ways, including binding of the ectopic pores to endogenous nucleoporins, reducing their availability to functional pores. Because this was detected in the ips motor neurons in the context of the C9 expansion genotype, it cannot be attributed solely to poly-GA, but could be the result of any of the phenotypic changes that these neurons display. This suggests future experiments to explore the factors leading to the ectopic pore formation.

Another fact highlighted by the present experiments is the substantial difference in appearance between the aggregated poly-GA found in the HEK cells in SQSTM/P62-positive inclusions and the more dispersed poly-GA found in the C9 patient-derived motor neurons. Although the cell types are very different, they could be modeling different stages of poly-GA accumulation in the human nervous system. The motor neurons still represent an immature stage of neuronal development whereas the HEK-GA161, despite being non-neuronal, may process the poly-GA in a way that more closely resembles the adult stage.

Several of the dipeptide repeat proteins form amyloids in the CNS. The fact that neither modulators of the proteasome nor of autophagy had an effect on poly-GA, at least in the short

term, highlights the difficulty of clearing this highly unusual protein. Wild-type C9 protein interacts with Rab GTPases, including those involved in the initiation of autophagy (Sellier et al., 2016; Sullivan et al., 2016). Thus, in the case of C9 ALS, the survival of neurons may be challenged on several fronts: the reduction of a protein essential for proper endosomal trafficking and autophagy; and the build-up of toxic proteins in the form of the DPRs, causing a double stress to cellular proteostasis. This is another promising area of research in understanding C9 ALS.

7. Methods

7.1. Generation of HEK cell line

HEK cells harboring lacZ-Zeocin fusion gene and tet repressor (Thermofisher Flp-In T-Rex) were transfected with the expression plasmid shown in Figure 5, including V5-tagged, codon optimized sequence encoding poly-GA161 after a CMV promoter. Clones were selected based on robust expression of the transgene with no detectable constitutive expression.

7.2. Maintenance of cultures

HEK cells were maintained at 37 °C with 5% CO2 in Dulbecco's Modified Medium (ThermoFisher 11965-092) supplemented with 10% tet-approved fetal calf serum (Takara Bio 631106), glutaMax (ThermoFisher), antibiotic/antimycotic (Invitrogen 15240-062), Hygromycin B (GIBCO 10687010), and Blasticidin (GIBCO A11139-03). All HEK were used between passages 4 to 30.

7.3. iPSC-derived neuronal differentiation

Lymphoblastoid cell lines from ALS-affected (ND09607E) or ALS-unaffected (ND70189) were obtained from Coriell, Inc. and reprogrammed using episomal reprogramming. iPSCs were cultured in mTesr1+ Media (Stem Cell Technologies 05826, 05827) on ESC-qualified Matrigel (Corning 354277), bulk passaged using ReLeSR (Stem Cell Technologies 05872) and grown until 80-90% confluency. iPSCs were treated with 0.5 mM EDTA (ThermoFisher 15575020), detached using a cell scraper and grown as embryoid body (EB) suspension for 14 days in the presence of small molecules as previously described in Maury et al. 2015 (Maury et al., 2015). Briefly, EBs were grown in the presence of 5 μM Y-27632 (R and D Systems 1254-50MG) on differentiation day 1, 40 μM SB431542 (SIGMA 301836418) and 3 μM CHIR99021 (Tocris Biosciences 252197-06-9) on differentiation days 1-3, 0.2 μM LDN193189 (StemCell Technology 72142) on differentiation days 1-5, 1 μM Retinoic Acid (SIGMA R2625-50MG) and 0.5 μM Smoothened Agonist (Millipore 566660) on differentiation days 2-12, and 10 μM DAPT (SIGMA D5942- 25 mg) on differentiation days 8-14. At day 14, EBs were enzymatically dissociated with Papain/DNase (Worthington Biochemical LK003176, LK003170) and plated in Neurobasal medium (ThermoFisher 21103049) containing N2 supplement (ThermoFisher 17502048), B27 supplement (ThermoFisher 17504044), Knock-out serum (ThermoFisher 10828010), Y27632 (R and D Systems

1254/50), 10 ng/mL BDNF (Tocris 248-BDB-01M), 10 ng/mL GDNF (R and D Systems 212-GD-01M), 10 ng/mL CNTF (R and D Systems 257-NT-050), 10 μM DAPT (Sigma 208255805). 48 hours after plating, the medium was replaced iPSC-MN feed medium (Neurobasal medium containing N2 supplement, B27 supplement, 10 ng/mL BDNF, 10 ng/mL GDNF, 10 ng/mL CNTF). Media was replaced with 50% conditioned medium 1-2 times weekly.

7.4. Immunofluorescence

Cells were processed for immunofluorescence by washing in PBS followed by fixation with paraformaldehyde (4%)/sucrose (4%) in TBS for 15 min at room temperature, followed by permeabilization in 0.1% Triton X-100 in TBS. Cells were blocked in blocking buffer before adding antibodies diluted in blocking buffer. Blocking buffer consisted of 1% BSA (Sigma A6003) 5% goat serum (Abcam 7481) and 0.3M glycine in TBS. Secondary antibodies were anti-species-specific Ig as appropriate, coupled to AlexaFluor labels. Highly cross-adsorbed antibodies were used whenever possible.

7.5. Confocal imaging

Images were collected using either a Zeiss 710 or 980 laser scanning confocal microscope equipped with a Zeiss AxioCam 503 camera and processed with Zen software. In some instances, confocal images were acquired and processed using Zeiss' "Airyscan" hardware and software, an enhancement to ordinary confocal imaging.

7.6. High-content imaging

Cultures were imaged in 96-well Cell Carrier Ultra plates using Perkin-Elmer Opera Phenix system operating in confocal mode with a 40x NA 1.1 water-immersion objective. Fluorescence at adjacent wavelengths was collected sequentially.

7.7. STED imaging

STED images were collected using an Abberior STEDYCON device with a Zeiss Axio Observer Z1 microscope body equipped with a 100x oil-immersion objective. Images were processed using Abberior's proprietary software and ImageJ.

7.8. Proximity Ligation Assay (PLA)

Cells were processed as for immunofluorescence, followed by proximity ligation according to the manufacturer's instructions. Briefly, samples were incubated with PLA secondary antibody probes then treated with ligase at 37 degrees, followed by amplification for 100 minutes at 37 degrees before counterstaining with DAPI. Cells were imaged in a high-content imaging system for spot counting of fluorescent reaction product at Texas Red wavelengths. Images of PLA shown in this work are single z-planes.

7.9. Poly-GA ELISA

Poly-GA was measured in RIPA lysates of cells using a sandwich ELISA with Meso-Scale Discovery (MSD) electrochemiluminescent detection as described in (Melanie Jambeau et al., 2022). Samples were treated with heat, SDS and reducing agent to denature any treatment antibody that might be present.

7.10. siRNA

Nucleoporin 153 was suppressed using Origene 27-mer oligonucleotide duplexes, catalog number SR322948. The siRNA sequences were: (A) rArArGrGrUrCrArCrArUrUrGrGrUrGrUrGrUrArCrUrCAA and (C) rGrCrGrCrUrArArArCrUrUrUrCrUrGrArUrArGrArGrGAA. Duplexes were prepared in sterile buffer and mixed with Origene "siTran" transfection reagent before being added to cells at a final concentration of 2 nM. Culture medium was changed 5 hr after transfection.

7.11. Electron microscopy

For immunocytochemistry: Cell samples were fixed in a mixture of 2% PFA and 0.125% glutaraldehyde in a 0.1M phosphate buffer pH7.4 and processed for ultracryomicrotomy as described in (Slot & Geuze, 2007). Ultrathin cryosections were prepared with an ultracryomicrotome Ultracut FCS (Leica) and immunogold labeled with anti- Poly-GA or anti-TDP43 antibodies followed by protein A conjugated to 10 nm gold particles (Cell Microscopy Center, Department of Cell Biology, Utrecht University). Sections were analyzed on a Tecnai Spirit G2 electron microscope (FEI, Eindhoven, The Netherlands) and digital acquisitions were made with a 4k CCD camera (Quemesa, Olympus, Münster, Germany)

For conventional EM: Cell samples were fixed in 2.5% glutaraldehyde in a 0.1M cacodylate buffer, post fixed with 1% osmium tetroxide supplemented with 1.5% potassium ferrocyanide, dehydrated in in ethanol and embedded in Epon resin. Thin sectioned samples of 60-70nm were post stained with 4% aqueous uranyl acetate for 10 minutes and lead citrate for 1 minute as described (Hurbain, Romao, Bergam, Heiligenstein, & Raposo, 2017).

Electron micrographs were acquired on a Tecnai Spirit G2 electron microscope (FEI, Eindhoven, The Netherlands) equipped with a 4k CCD camera (Quemesa, Olympus, Münster, Germany)

7.12. Antibodies used

Target protein	Clone	Vendor	Product #	Dilution	
CHMP7		Protein Tech	16424-1-AP	1:100	
COX-IV	3E11	Cell Signaling	4850	1:250	
cleaved Caspase-3		Cell Signaling	9661	1:400	
G3BP		Abcam	ab181149	1:200	
HDAC6		Cell Signaling	7558S	1:200	
Lamin A/C		Active Motif	39288	1:1000-1:250	
LC3B		Abcam	ab48394	1:5000	
b-III-tubulin		Abcam	ab107216	1:400	
Nup 153	QE5	Abcam	ab24700	1:200	
Nup 98	C39A3	Cell Signaling	2598S	1:500	
poly-GA	αGA1	Nguyen et al., 2020			
poly-GA	αGA3	Nguyen et al., 2020			
poly-GA	αGA4	Nguyen et al., 2020			
POM121		Protein Tech	15645-1-AP	1:400	
SQSTM		Abcam	ab109012	1 ug/mL	
TDP-43 (mid)		Abnova	H00023435	1:1000	
TDP-43 (C-term)		Protein Tech	12892	1:500	
TDP-43 (N-term)		Protein Tech	10782-2-AP	1:500	
TPR		Abcam	ab84516	1:200	
vimentin		Abcam	ab24525	1:1000	

7.13. Statistical analysis

Quantitative results were analyzed statistically with GraphPad Prism software using t-test or ANOVA when appropriate, followed by Šídák's multiple comparisons test for selected group comparisons. In instances when one control group was compared against all others, Dunnett's test was used (Motulsky, 2022). When ANOVA was not appropriate, the nonparametric Kruskal-Wallis test followed by Dunn's multiple comparisons test was used.

8. Acknowledgements

I acknowledge the PICT-IBiSA , Institut Curie, Paris, France, member of the France-BioImaging national-research-infrastructure.
This work was supported by the French National Research Agency through the "Investments for the Future" program (France-BioImaging, ANR-10-INSB-04) and by the CelTisPhyBio Labex (N°ANR-10-LBX-0038) part of the IDEX PSL (N°ANR-10-IDEX-0001-02 PSL).

I would like to thank the Biogen/PSL doctoral program for the opportunity to do this work.

I would like to thank Dr. Chris Henderson and the Biogen/PSL doctoral program steering committee for their organization and support. I thank Yuriko Hirohata and Jessie Shi for their organizational support of the program.

I sincerely thank my PSL advisor at the Curie Institute, Dr. Graça Raposo, for daring to accept an unknown student from a U.S. biotechnology company and for all of her guidance and support during this project.

I thank each of my Biogen advisors (in chronological order!) Dr. Alex McCampbell, Dr. Mark Kankel, and Dr. Sophie Parmentier Batteur.

I am truly indebted to Dr. Maryse Romao for all her training, advice, and hard work in everything related to electron microscopy. I am equally grateful to the Biogen experts in stem cell technology, Dr. Paige Cundiff and Sean Dwyer.

All science is collaborative, so there are many contributors to this work. I would like to thank in particular Biogen colleagues Drs. Param Murugan, Brian Grabiner, Yuanzheng Gu, and Bing Li.

I am very grateful for the advice and help of Dr. Mia Rushe of Biogen.

Special Acknowledgement

I would especially like to thank all the patients, family members, and healthy individuals who so graciously donated samples to brain and tissue banks, entrusting to future researchers the materials needed to help discover treatments for diseases of the nervous system.

9. References

Abe, K., Aoki, M., Tsuji, S., Itoyama, Y., Sobue, G., Togo, M., Hamada, C., Tanaka, M., Akimoto, M., Nakamura, K., Takahashi, F., Kondo, K., Yoshino, H., Abe, K., Aoki, M., Tsuji, S., Itoyama, Y., Sobue, G., Togo, M., Hamada, C., Sasaki, H., Yabe, I., Doi, S., Warita, H., Imai, T., Ito, H., Fukuchi, M., Osumi, E., Wada, M., Nakano, I., Morita, M., Ogata, K., Maruki, Y., Ito, K., Kano, O., Yamazaki, M., Takahashi, Y., Ishiura, H., Ogino, M., Koike, R., Ishida, C., Uchiyama, T., Mizoguchi, K., Obi, T., Watanabe, H., Atsuta, N., Aiba, I., Taniguchi, A., Sawada, H., Hazama, T., Fujimura, H., Kusaka, H., Kunieda, T., Kikuchi, H., Matsuo, H., Ueyama, H., Uekawa, K., Tanaka, M., Akimoto, M., Ueda, M., Murakami, A., Sumii, R., Kudou, T., Nakamura, K., Morimoto, K., Yoneoka, T., Hirai, M., Sasaki, K., Terai, H., Natori, T., Matsui, H., Kotani, K., Yoshida, K., Iwasaki, T., Takahashi, F., Kondo, K., & Yoshino, H. (2017). Safety and efficacy of edaravone in well defined patients with amyotrophic lateral sclerosis: a randomised, double-blind, placebo-controlled trial. *The Lancet Neurology, 16*(7), 505-512. doi:10.1016/s1474-4422(17)30115-1

Abe, K., Itoyama, Y., Sobue, G., Tsuji, S., Aoki, M., Doyu, M., Hamada, C., Kondo, K., Yoneoka, T., Akimoto, M., Yoshino, H., & Edaravone, A. L. S. S. G. (2014). Confirmatory double-blind, parallel-group, placebo-controlled study of efficacy and safety of edaravone (MCI-186) in amyotrophic lateral sclerosis patients. *Amyotroph Lateral Scler Frontotemporal Degener, 15*(7-8), 610-617. doi:10.3109/21678421.2014.959024

Afzelius, B. A. (1955). The ultrastructure of the nuclear membrane of the sea urchin oocyte as studied with the electron microscope. *Experimental Cell Research, 8*, 11. doi: 10.1016/0014-4827(55)90051-3

Al-Chalabi, A., Fang, F., Hanby, M. F., Leigh, P. N., Shaw, C. E., Ye, W., & Rijsdijk, F. (2010). An estimate of amyotrophic lateral sclerosis heritability using twin data. *J Neurol Neurosurg Psychiatry, 81*(12), 1324-1326. doi:10.1136/jnnp.2010.207464

Aramburu, I. V., & Lemke, E. A. (2017). Floppy but not sloppy: Interaction mechanism of FG-nucleoporins and nuclear transport receptors. *Semin Cell Dev Biol, 68*, 34-41. doi:10.1016/j.semcdb.2017.06.026

Archbold, H. C., Jackson, K. L., Arora, A., Weskamp, K., Tank, E. M., Li, X., Miguez, R., Dayton, R. D., Tamir, S., Klein, R. L., & Barmada, S. J. (2018). TDP43 nuclear export and neurodegeneration in models of amyotrophic lateral sclerosis and frontotemporal dementia. *Sci Rep, 8*(1), 4606. doi:10.1038/s41598-018-22858-w

Aviner, R. (2020). The science of puromycin: From studies of ribosome function to applications in biotechnology. *Comput Struct Biotechnol J, 18*, 1074-1083. doi:10.1016/j.csbj.2020.04.014

Azimi, M., & Mofrad, M. R. (2013). Higher nucleoporin-Importinβ affinity at the nuclear basket increases nucleocytoplasmic import. *PLoS One, 8*(11), e81741. doi:10.1371/journal.pone.0081741

Banack, S. A., Dunlop, R. A., Stommel, E. W., Mehta, P., & Cox, P. A. (2022). miRNA extracted from extracellular vesicles is a robust biomarker of amyotrophic lateral sclerosis. *J Neurol Sci, 442*, 120396. doi:10.1016/j.jns.2022.120396

Bang, J., Spina, S., & Miller, B. L. (2015). Frontotemporal dementia. *The Lancet, 386*(10004), 1672-1682. doi:https://doi.org/10.1016/S0140-6736(15)00461-4

Bastos, R., Lin, A., Enarson, M., & Burke, B. (1996). Targeting and function in mRNA export of nuclear pore complex protein Nup153. *Journal of Cell Biology, 134*(5), 1141-1156.

Beswick, E., Fawcett, T., Hassan, Z., Forbes, D., Dakin, R., Newton, J., Abrahams, S., Carson, A., Chandran, S., Perry, D., & Pal, S. (2022). A systematic review of digital technology to evaluate motor function and disease progression in motor neuron disease. *J Neurol*, 1-15. doi:10.1007/s00415-022-11312-7

Boeynaems, S., Bogaert, E., Michiels, E., Gijselinck, I., Sieben, A., Jovičić, A., De Baets, G., Scheveneels, W., Steyaert, J., Cuijt, I., Verstrepen, K. J., Callaerts, P., Rousseau, F., Schymkowitz, J., Cruts, M., Van Broeckhoven, C., Van Damme, P., Gitler, A. D., Robberecht, W., & Van Den Bosch, L. (2016). Drosophila screen connects nuclear transport genes to DPR pathology in c9ALS/FTD. *Sci Rep, 6*, 20877. doi:10.1038/srep20877

Burberry, A., Suzuki, N., Wang, J. Y., Moccia, R., Mordes, D. A., Stewart, M. H., Suzuki-Uematsu, S., Ghosh, S., Singh, A., Merkle, F. T., Koszka, K., Li, Q. Z., Zon, L., Rossi, D. J., Trowbridge, J. J., Notarangelo, L. D., & Eggan, K. (2016). Loss-of-function mutations in the C9ORF72 mouse ortholog cause fatal autoimmune disease. *Sci Transl Med, 8*(347), 347ra393. doi:10.1126/scitranslmed.aaf6038

Carvalho, T. (2022). Biomarker data prove critical for ALS drug evaluation at FDA. *Nat Med*. doi:10.1038/d41591-022-00098-w

Chang, Y. J., Jeng, U. S., Chiang, Y. L., Hwang, I. S., & Chen, Y. R. (2016). The Glycine-Alanine Dipeptide Repeat from C9orf72 Hexanucleotide Expansions Forms Toxic Amyloids Possessing Cell-to-Cell Transmission Properties. *J Biol Chem, 291*(10), 4903-4911. doi:10.1074/jbc.M115.694273

Chen, Y., & Cohen, T. J. (2019). Aggregation of the nucleic acid-binding protein TDP-43 occurs via distinct routes that are coordinated with stress granule formation. *J Biol Chem, 294*(10), 3696-3706. doi:10.1074/jbc.RA118.006351

Chew, J., Cook, C., Gendron, T. F., Jansen-West, K., Del Rosso, G., Daughrity, L. M., Castanedes-Casey, M., Kurti, A., Stankowski, J. N., Disney, M. D., Rothstein, J. D., Dickson, D. W., Fryer, J. D., Zhang, Y. J., & Petrucelli, L. (2019). Aberrant deposition of stress granule-resident proteins linked to C9orf72-associated TDP-43 proteinopathy. *Mol Neurodegener, 14*(1), 9. doi:10.1186/s13024-019-0310-z

Chew, J., Tania F. Gendron, Mercedes Prudencio, Hiroki Sasaguri, Yong-Jie Zhang,, Monica Castanedes-Casey, C. W. L., Karen Jansen-West, Aishe Kurti, Melissa E., Murray, K. F. B., Peter O. Bauer, Ena C. Whitelaw, Linda Rousseau, Jeannette, N. Stankowski, C. S., Lillian M. Daughrity, Emilie A. Perkerson, Pamela, Desaro, A. J., Karen Overstreet, Dieter Edbauer, Rosa Rademakers, Kevin B., & Boylan, D. W. D., John D. Fryer, Leonard Petrucelli. (2015). C9ORF72 repeat expansions in mice cause TDP-43 pathology, neuronal loss, and behavioral deficits. *Science, 348*(6239).

Chiò, A., Logroscino, G., Hardiman, O., Swingler, R., Mitchell, D., Beghi, E., & Traynor, B. G. (2009). Prognostic factors in ALS: A critical review. *Amyotroph Lateral Scler, 10*(5-6), 310-323. doi:10.3109/17482960802566824

Chou, C. C., Zhang, Y., Umoh, M. E., Vaughan, S. W., Lorenzini, I., Liu, F., Sayegh, M., Donlin-Asp, P. G., Chen, Y. H., Duong, D. M., Seyfried, N. T., Powers, M. A., Kukar, T., Hales, C. M., Gearing, M., Cairns, N. J., Boylan, K. B., Dickson, D. W., Rademakers, R., Zhang, Y. J., Petrucelli, L., Sattler, R., Zarnescu, D. C., Glass, J. D., & Rossoll, W. (2018). TDP-43 pathology disrupts nuclear pore complexes and nucleocytoplasmic transport in ALS/FTD. *Nat Neurosci, 21*(2), 228-239. doi:10.1038/s41593-017-0047-3

Colombrita, C., Zennaro, E., Fallini, C., Weber, M., Sommacal, A., Buratti, E., Silani, V., & Ratti, A. (2009). TDP-43 is recruited to stress granules in conditions of oxidative insult. *J Neurochem, 111*(4), 1051-1061. doi:10.1111/j.1471-4159.2009.06383.x

Cooper-Knock, J., Higginbottom, A., Connor-Robson, N., Bayatti, N., Bury, J. J., Kirby, J., Ninkina, N., Buchman, V. L., & Shaw, P. J. (2013). C9ORF72 transcription in a frontotemporal dementia case with two expanded alleles. *Neurology, 81*(19), 1719-1721. doi:10.1212/01.wnl.0000435295.41974.2e

Corbier, C., & Sellier, C. (2017). C9ORF72 is a GDP/GTP exchange factor for Rab8 and Rab39 and regulates autophagy. *Small GTPases, 8*(3), 181-186. doi:10.1080/21541248.2016.1212688

Couratier, P., Corcia, P., Lautrette, G., Nicol, M., Preux, P. M., & Marin, B. (2016). [Epidemiology of amyotrophic lateral sclerosis]. *La Revue du practicien, 66*(5), 556-558.

Coyne, A. N., Baskerville, V., Zaepfel, B. L., Dickson, D. W., Rigo, F., Bennett, F., Lusk, C. P., & Rothstein, J. D. (2021). Nuclear accumulation of CHMP7 initiates nuclear pore complex injury and subsequent TDP-43 dysfunction in sporadic and familial ALS. *Sci Transl Med, 13*(604). doi:10.1126/scitranslmed.abe1923

Coyne, A. N., & Rothstein, J. D. (2021). Nuclear lamina invaginations are not a pathological feature of C9orf72 ALS/FTD. *Acta Neuropathol Commun, 9*(1), 45. doi:10.1186/s40478-021-01150-5

Coyne, A. N., Zaepfel, B. L., Hayes, L., Fitchman, B., Salzberg, Y., Luo, E. C., Bowen, K., Trost, H., Aigner, S., Rigo, F., Yeo, G. W., Harel, A., Svendsen, C. N., Sareen, D., & Rothstein, J. D. (2020). G4C2 Repeat RNA Initiates a POM121-Mediated Reduction in Specific Nucleoporins in C9orf72 ALS/FTD. *Neuron, 107*(6), 1124-1140 e1111. doi:10.1016/j.neuron.2020.06.027

DeJesus-Hernandez, M., Mackenzie, I. R., Boeve, B. F., Boxer, A. L., Baker, M., Rutherford, N. J., Nicholson, A. M., Finch, N. A., Flynn, H., Adamson, J., Kouri, N., Wojtas, A., Sengdy, P., Hsiung, G. Y., Karydas, A., Seeley, W. W., Josephs, K. A., Coppola, G., Geschwind, D. H., Wszolek, Z. K., Feldman, H., Knopman, D. S., Petersen, R. C., Miller, B. L., Dickson, D. W., Boylan, K. B., Graff-Radford, N. R., & Rademakers, R. (2011). Expanded GGGGCC hexanucleotide repeat in noncoding region of C9ORF72 causes chromosome 9p-linked FTD and ALS. *Neuron, 72*(2), 245-256. doi:10.1016/j.neuron.2011.09.011

Denning, D. P., Patel, S. S., Uversky, V., Fink, A. L., & Rexach, M. (2003). Disorder in the nuclear pore complex: the FG repeat regions of nucleoporins are natively unfolded. *Proc Natl Acad Sci U S A*(0027-8424 (Print)). doi:https://doi.org/10.1073/pnas.0437902100

Dimos, J. T., Rodolfa, K. T., Niakan, K. K., Weisenthal, L. M., Mitsumoto, H., Chung, W., Croft, G. F., Saphier, G., Leibel, R., Goland, R., Wichterle, H., Henderson, C. E., & Eggan, K. (2008). Induced pluripotent stem cells generated from patients with ALS can be differentiated into motor neurons. *Science, 321*(5893), 1218-1221. doi:10.1126/science.1158799

Doble, A. (1996). The pharmacology and mechanism of action of riluzole. *Neurology, 47*(6 Suppl 4), S233-241. doi:10.1212/wnl.47.6_suppl_4.233s

Dong, W., Ma, Y., Guan, F., Zhang, X., Chen, W., Zhang, L., & Zhang, L. (2021). Ablation of C9orf72 together with excitotoxicity induces ALS in rats. *Febs j, 288*(5), 1712-1723. doi:10.1111/febs.15501

Dong, X., Biswas, A., Süel, K. E., Jackson, L. K., Martinez, R., Gu, H., & Chook, Y. M. (2009). Structural basis for leucine-rich nuclear export signal recognition by CRM1. *Nature, 458*(7242), 1136-1141. doi:10.1038/nature07975

Dormann, D., Rodde, R., Edbauer, D., Bentmann, E., Fischer, I., Hruscha, A., Than, M. E., Mackenzie, I. R., Capell, A., Schmid, B., Neumann, M., & Haass, C. (2010). ALS-associated fused in sarcoma (FUS) mutations disrupt Transportin-mediated nuclear import. *Embo j, 29*(16), 2841-2857. doi:10.1038/emboj.2010.143

Duan, L., Zaepfel, B. L., Aksenova, V., Dasso, M., Rothstein, J. D., Kalab, P., & Hayes, L. R. (2022). Nuclear RNA binding regulates TDP-43 nuclear localization and passive nuclear export. *Cell Rep, 40*(3). doi:10.1016/j.celrep.2022.111106

Duplan, L., Bernard, N., Casseron, W., Dudley, K., Thouvenot, E., Honnorat, J., Rogemond, V., De Bovis, B., Aebischer, P., Marin, P., Raoul, C., Henderson, C. E., & Pettmann, B. (2010). Collapsin response mediator protein 4a (CRMP4a) is upregulated in motoneurons of mutant SOD1 mice and can trigger motoneuron axonal degeneration and cell death. *J Neurosci, 30*(2), 785-796. doi:10.1523/jneurosci.5411-09.2010

Ederle, H., Funk, C., Abou-Ajram, C., Hutten, S., Funk, E. B. E., Kehlenbach, R. H., Bailer, S. M., & Dormann, D. (2018). Nuclear egress of TDP-43 and FUS occurs independently of Exportin-1/CRM1. *Sci Rep, 8*(1), 7084. doi:10.1038/s41598-018-25007-5

Eftekharzadeh, B., Daigle, J. G., Kapinos, L. E., Coyne, A., Schiantarelli, J., Carlomagno, Y., Cook, C., Miller, S. J., Dujardin, S., Amaral, A. S., Grima, J. C., Bennett, R. E., Tepper, K., DeTure, M., Vanderburg, C. R., Corjuc, B. T., DeVos, S. L., Gonzalez, J. A., Chew, J., Vidensky, S., Gage, F. H., Mertens, J., Troncoso, J., Mandelkow, E., Salvatella, X., Lim, R. Y. H., Petrucelli, L., Wegmann, S., Rothstein, J. D., & Hyman, B. T. (2018). Tau Protein Disrupts Nucleocytoplasmic Transport in Alzheimer's Disease. *Neuron, 99*(5), 925-940 e927. doi:10.1016/j.neuron.2018.07.039

Elamin, M., Bede, P., Montuschi, A., Pender, N., Chio, A., & Hardiman, O. (2015). Predicting prognosis in amyotrophic lateral sclerosis: a simple algorithm. *Journal of Neurology*(1432-1459 (Electronic)). doi:10.1007/s00415-015-7731-6

Fagan, T. (2022). FDA Approves ALS Drug on Phase 2 Data. *Alzforum.org*.

Fallini, C., Khalil, B., Smith, C. L., & Rossoll, W. (2020). Traffic jam at the nuclear pore: All roads lead to nucleocytoplasmic transport defects in ALS/FTD. *Neurobiol Dis, 140*, 104835. doi:10.1016/j.nbd.2020.104835

Fratta, P., Poulter, M., Lashley, T., Rohrer, J. D., Polke, J. M., Beck, J., Ryan, N., Hensman, D., Mizielinska, S., Waite, A. J., Lai, M.-C., Gendron, T. F., Petrucelli, L., Fisher, E. M. C., Revesz, T., Warren, J. D., Collinge, J., Isaacs, A. M., & Mead, S. (2013). Homozygosity for the C9orf72 GGGGCC repeat expansion in frontotemporal dementia. *Acta Neuropathol, 126*(3), 401-409. doi:10.1007/s00401-013-1147-0

Freibaum, B. D., Lu, Y., Lopez-Gonzalez, R., Kim, N. C., Almeida, S., Lee, K. H., Badders, N., Valentine, M., Miller, B. L., Wong, P. C., Petrucelli, L., Kim, H. J., Gao, F. B., & Taylor, J. P. (2015). GGGGCC repeat expansion in C9orf72 compromises nucleocytoplasmic transport. *Nature, 525*(7567), 129-133. doi:10.1038/nature14974

Freibaum, B. D., & Taylor, J. P. (2017). The Role of Dipeptide Repeats in C9ORF72-Related ALS-FTD. *Front Mol Neurosci, 10*, 35. doi:10.3389/fnmol.2017.00035

Frottin, F., Perez-Berlanga, M., Hartl, F. U., & Hipp, M. S. (2021). Multiple pathways of toxicity induced by C9orf72 dipeptide repeat aggregates and G4C2 RNA in a cellular model. *Elife, 10*. doi:10.7554/eLife.62718

Fu, S. C., Fung, H. Y. J., Cağatay, T., Baumhardt, J., & Chook, Y. M. (2018). Correlation of CRM1-NES affinity with nuclear export activity. *Mol Biol Cell, 29*(17), 2037-2044. doi:10.1091/mbc.E18-02-0096

Fukuda, M., Gotoh, I., Gotoh, Y., & Nishida, E. (1996). Cytoplasmic Localization of Mitogen-activated Protein Kinase Kinase Directed by Its NH2-terminal, Leucine-rich Short Amino Acid Sequence, Which Acts as a Nuclear Export Signal. *journal of Biological chemistry, 271*(33).

Fung, H. Y., Fu, S. C., & Chook, Y. M. (2017). Nuclear export receptor CRM1 recognizes diverse conformations in nuclear export signals. *Elife, 6*. doi:10.7554/eLife.23961

Gasset-Rosa, F., Lu, S., Yu, H., Chen, C., Melamed, Z., Guo, L., Shorter, J., Da Cruz, S., & Cleveland, D. W. (2019). Cytoplasmic TDP-43 De-mixing Independent of Stress Granules Drives Inhibition of Nuclear Import, Loss of Nuclear TDP-43, and Cell Death. *Neuron, 102*(2), 339-357 e337. doi:10.1016/j.neuron.2019.02.038

Gill, A. L., Wang, M. Z., Levine, B., Premasiri, A., & Vieira, F. G. (2019). Primary Neurons and Differentiated NSC-34 Cells Are More Susceptible to Arginine-Rich ALS Dipeptide Repeat Protein-Associated Toxicity than Non-Differentiated NSC-34 and CHO Cells. *Int J Mol Sci, 20*(24). doi:10.3390/ijms20246238

Grad, L. I., Rouleau, G. A., Ravits, J., & Cashman, N. R. (2017). Clinical Spectrum of Amyotrophic Lateral Sclerosis (ALS). *Cold Spring Harb Perspect Med, 7*(8). doi:10.1101/cshperspect.a024117

Guo, Q., Lehmer, C., Martinez-Sanchez, A., Rudack, T., Beck, F., Hartmann, H., Perez-Berlanga, M., Frottin, F., Hipp, M. S., Hartl, F. U., Edbauer, D., Baumeister, W., & Fernandez-Busnadiego, R. (2018). In Situ Structure of Neuronal C9orf72 Poly-GA Aggregates Reveals Proteasome Recruitment. *Cell, 172*(4), 696-705 e612. doi:10.1016/j.cell.2017.12.030

Haines, J. D., Herbin, O., de la Hera, B., Vidaurre, O. G., Moy, G. A., Sun, Q., Fung, H. Y., Albrecht, S., Alexandropoulos, K., McCauley, D., Chook, Y. M., Kuhlmann, T., Kidd, G. J., Shacham, S., & Casaccia, P. (2015). Nuclear export inhibitors avert progression in preclinical models of inflammatory demyelination. *Nat Neurosci, 18*(4), 511-520. doi:10.1038/nn.3953

Hardiman, O., Al-Chalabi, A., Chio, A., Corr, E. M., Logroscino, G., Robberecht, W., Shaw, P. J., Simmons, Z., & van den Berg, L. H. (2017). Amyotrophic lateral sclerosis. *Nat Rev Dis Primers, 3*, 17071. doi:10.1038/nrdp.2017.71

Hardiman, O., & van den Berg, L. H. (2017). Edaravone: a new treatment for ALS on the horizon? *The Lancet Neurology, 16*(7), 490-491. doi:10.1016/s1474-4422(17)30163-1

Harms, M. B., Cady, J., Zaidman, C., Cooper, P., Bali, T., Allred, P., Cruchaga, C., Baughn, M., Libby, R. T., Pestronk, A., Goate, A., Ravits, J., & Baloh, R. H. (2013). Lack of C9ORF72 coding mutations supports a gain of function for repeat expansions in amyotrophic lateral sclerosis. *Neurobiol Aging, 34*(9), 2234.e2213-2239. doi:10.1016/j.neurobiolaging.2013.03.006

Harrison, R. G. (2009). Recombinant Protein Solubility Prediction. Retrieved from https://biotech.ou.edu/

Hartono, Hazawa, M., Lim, K. S., Dewi, F. R. P., Kobayashi, A., & Wong, R. W. (2019). Nucleoporin Nup58 localizes to centrosomes and mid-bodies during mitosis. *Cell Division, 14*(1), 7. doi:10.1186/s13008-019-0050-z

Horwich, M. S., Engel, W. K., & Chauvin, P. B. (1974). Amyotrophic lateral sclerosis sera applied to cultured motor neurons. *Arch Neurol, 30*(4), 332-333. doi:10.1001/archneur.1974.00490340060015

Hurbain, I., Romao, M., Bergam, P., Heiligenstein, X., & Raposo, G. (2017). Analyzing Lysosome-Related Organelles by Electron Microscopy. *Methods Mol Biol, 1594*, 43-71. doi:10.1007/978-1-4939-6934-0_4

Ichida, J. K., Staats, K. A., Davis-Dusenbery, B. N., Clement, K., Galloway, K. E., Babos, K. N., Shi, Y., Son, E. Y., Kiskinis, E., Atwater, N., Gu, H., Gnirke, A., Meissner, A., & Eggan, K. (2018). Comparative genomic analysis of embryonic, lineage-converted and stem cell-derived motor neurons. *Development, 145*(22). doi:10.1242/dev.168617

Jambeau, M., Meyer, K. D., Hruska-Plochan, M., Tabet, R., Lee, C.-Z., Ray-Soni, A., Aguilar, C., Savage, K., Mishra, N., Cavegn, N., Borter, P., Lin, C.-C., Jansen-West, K., Jiang, J., Freyermuth, F., Li, N., De Rossi, P., Pérez-Berlanga, M., Jiang, X., Daughrity, L. M., Pereira, J., Narayanan, S., Gu, Y., Dhokai, S., Dalkilic-Liddle, I., Maniecka, Z., Weber, J., Workman, M., McAlonis-Downes, M., Berezovski, E., Zhang, Y.-J., Berry, J., Wainger, B. J., Kankel, M. W., Rushe, M., Hock, C., Nitsch, R. M., Cleveland, D. W., Petrucelli, L., Gendron, T., Montrasio, F., Grimm, J., Polymenidou, M., & Lagier-Tourenne, C. (2022). *biorxiv*. doi:10.1101/2022.01.13.475329

Jambeau, M., Meyer, K. D., Hruska-Plochan, M., Tabet, R., Lee, C. Z., Ray-Soni, A., Aguilar, C., Savage, K., Mishra, N., Cavegn, N., Borter, P., Lin, C. C., Jansen-West, K. R., Jiang, J., Freyermuth, F., Li, N., De Rossi, P., Pérez-Berlanga, M., Jiang, X., Daughrity, L. M., Pereira, J., Narayanan, S., Gu, Y., Dhokai, S., Dalkilic-Liddle, I., Maniecka, Z., Weber, J., Workman, M., McAlonis-Downes, M., Berezovski, E., Zhang, Y. J., Berry, J., Wainger, B. J., Kankel, M. W., Rushe, M., Hock, C., Nitsch, R. M., Cleveland, D. W., Petrucelli, L., Gendron, T. F., Montrasio, F., Grimm, J., Polymenidou, M., & Lagier-Tourenne, C. (2022). Comprehensive evaluation of human-derived anti-poly-GA antibodies in cellular and animal models of C9orf72 disease. *Proc Natl Acad Sci U S A, 119*(49), e2123487119. doi:10.1073/pnas.2123487119

Jaronen, M., Goldsteins, G., & Koistinaho, J. (2014). ER stress and unfolded protein response in amyotrophic lateral sclerosis-a controversial role of protein disulphide isomerase. *Front Cell Neurosci, 8*, 402. doi:10.3389/fncel.2014.00402

Jarvius, M., Paulsson, J., Weibrecht, I., Leuchowius, K. J., Andersson, A. C., Wählby, C., Gullberg, M., Botling, J., Sjöblom, T., Markova, B., Ostman, A., Landegren, U., & Söderberg, O. (2007). In situ detection of phosphorylated platelet-derived growth factor receptor beta using a generalized proximity ligation method. *Mol Cell Proteomics, 6*(9), 1500-1509. doi:10.1074/mcp.M700166-MCP200

Jones, C. L., Njomen, E., Sjogren, B., Dexheimer, T. S., & Tepe, J. J. (2017). Small Molecule Enhancement of 20S Proteasome Activity Targets Intrinsically Disordered Proteins. *ACS Chem Biol, 12*(9), 2240-2247. doi:10.1021/acschembio.7b00489

Jovicic, A., Mertens, J., Boeynaems, S., Bogaert, E., Chai, N., Yamada, S. B., Paul, J. W., 3rd, Sun, S., Herdy, J. R., Bieri, G., Kramer, N. J., Gage, F. H., Van Den Bosch, L., Robberecht, W., & Gitler, A. D. (2015). Modifiers of C9orf72 dipeptide repeat toxicity connect nucleocytoplasmic transport defects to FTD/ALS. *Nat Neurosci, 18*(9), 1226-1229. doi:10.1038/nn.4085

Kabachinski, G., & Schwartz, T. U. (2015). The nuclear pore complex--structure and function at a glance. *J Cell Sci, 128*(3), 423-429. doi:10.1242/jcs.083246

Kalderon, D., Roberts, B. L., Richardson, W. D., & Smith, A. E. (1984). A short amino acid sequence able to specify nuclear location. *Cell, 39*(0092-8674 (Print)), 499-509.

Kaneb, H. M., Folkmann, A. W., Belzil, V. V., Jao, L.-E., Leblond, C. S., Girard, S. L., Daoud, H., Noreau, A., Rochefort, D., Hince, P., Szuto, A., Levert, A., Vidal, S., André-Guimont, C., Camu, W., Bouchard, J.-P., Dupré, N., Rouleau, G. A., Wente, S. R., & Dion, P. A. (2015). Deleterious mutations in the essential mRNA metabolism factor, hGle1, in amyotrophic lateral sclerosis. *Hum Mol Genet, 24*(5), 1363-1373. doi:10.1093/hmg/ddu545

Kankel, M. W., Sen, A., Lu, L., Theodorou, M., Dimlich, D. N., McCampbell, A., Henderson, C. E., Shneider, N. A., & Artavanis-Tsakonas, S. (2020). Amyotrophic Lateral Sclerosis Modifiers in Drosophila Reveal the Phospholipase D Pathway as a Potential Therapeutic Target. *Genetics, 215*(3), 747-766. doi:10.1534/genetics.119.302985

Kaur, B., Bhat, A., Chakraborty, R., Adlakha, K., Sengupta, S., Roy, S., & Chakraborty, K. (2018). Proteomic profile of 4-PBA treated human neuronal cells during ER stress. *Mol Omics, 14*(1), 53-63. doi:10.1039/c7mo00114b

Keating, S. S., San Gil, R., Swanson, M. E. V., Scotter, E. L., & Walker, A. K. (2022). TDP-43 pathology: From noxious assembly to therapeutic removal. *Prog Neurobiol, 211*, 102229. doi:10.1016/j.pneurobio.2022.102229

Khalaf, K., Tornese, P., Cocco, A., & Albanese, A. (2022). Tauroursodeoxycholic acid: a potential therapeutic tool in neurodegenerative diseases. *Translational Neurodegeneration, 11*(1), 33. doi:10.1186/s40035-022-00307-z

Khosravi, B., Hartmann, H., May, S., Mohl, C., Ederle, H., Michaelsen, M., Schludi, M. H., Dormann, D., & Edbauer, D. (2017). Cytoplasmic poly-GA aggregates impair nuclear import of TDP-43 in C9orf72 ALS/FTLD. *Hum Mol Genet, 26*(4), 790-800. doi:10.1093/hmg/ddw432

Khosravi, B., LaClair, K. D., Riemenschneider, H., Zhou, Q., Frottin, F., Mareljic, N., Czuppa, M., Farny, D., Hartmann, H., Michaelsen, M., Arzberger, T., Hartl, F. U., Hipp, M. S., & Edbauer, D. (2020). Cell-to-cell transmission of C9orf72 poly-(Gly-Ala) triggers key features of ALS/FTD. *Embo j*, e102811. doi:10.15252/embj.2019102811

Kim, S. J., Fernandez-Martinez, J., Nudelman, I., Shi, Y., Zhang, W., Raveh, B., Herricks, T., Slaughter, B. D., Hogan, J. A., Upla, P., Chemmama, I. E., Pellarin, R., Echeverria, I., Shivaraju, M., Chaudhury, A. S., Wang, J., Williams, R., Unruh, J. R., Greenberg, C. H., Jacobs, E. Y., Yu, Z., de la Cruz, M. J., Mironska, R., Stokes, D. L., Aitchison, J. D., Jarrold, M. F., Gerton, J. L., Ludtke, S. J., Akey, C. W., Chait, B. T., Sali, A., & Rout, M. P. (2018). Integrative structure and functional anatomy of a nuclear pore complex. *Nature, 555*(7697), 475-482. doi:10.1038/nature26003

Kinoshita, Y., Ito, H., Hirano, A., Fujita, K., Wate, R., Nakamura, M., Kaneko, S., Nakano, S., & Kusaka, H. (2009). Nuclear Contour Irregularity and Abnormal Transporter Protein Distribution in Anterior Horn Cells in Amyotrophic Lateral Sclerosis. *Journal of Neuropathology & Experimental Neurology, 68*(11), 1184-1192. doi:10.1097/NEN.0b013e3181bc3bec %J Journal of Neuropathology & Experimental Neurology

Klim, J. R., Pintacuda, G., Nash, L. A., Guerra San Juan, I., & Eggan, K. (2021). Connecting TDP-43 Pathology with Neuropathy. *Trends Neurosci, 44*(6), 424-440. doi:10.1016/j.tins.2021.02.008

Kopito, R. R. (2000). Aggresomes, inclusion bodies and protein aggregation. *Trends Cell Biol, 10*(12), 524-530. doi:10.1016/s0962-8924(00)01852-3

Koppers, M., Blokhuis, A. M., Westeneng, H. J., Terpstra, M. L., Zundel, C. A., Vieira de Sá, R., Schellevis, R. D., Waite, A. J., Blake, D. J., Veldink, J. H., van den Berg, L. H., & Pasterkamp, R. J. C9orf72 ablation in mice does not cause motor neuron degeneration or motor deficits. (1531-8249 (Electronic)).

Kuersten, S., Ohno, M., & Mattaj, I. W. (2001). Nucleocytoplasmic transport: Ran beta beyond. *Trends Cell Biol, 11*(12). doi:https://doi.org/10.1016/S0962-8924(01)02144-4

Kutay, U., Bischoff, F. R., Kostka, S., Kraft, R., & Görlich, D. (1997). Export of importin alpha from the nucleus is mediated by a specific nuclear transport factor. *Cell, 90*(6), 1061-1071. doi:10.1016/s0092-8674(00)80372-4

Kwiatkowski, T. J., Jr., Bosco, D. A., Leclerc, A. L., Tamrazian, E., Vanderburg, C. R., Russ, C., Davis, A., Gilchrist, J., Kasarskis, E. J., Munsat, T., Valdmanis, P., Rouleau, G. A., Hosler, B. A., Cortelli, P., de Jong, P. J., Yoshinaga, Y., Haines, J. L., Pericak-Vance, M. A., Yan, J., Ticozzi, N., Siddique, T., McKenna-Yasek, D., Sapp, P. C., Horvitz, H. R., Landers, J. E., & Brown, R. H., Jr. (2009). Mutations in the FUS/TLS gene on chromosome 16 cause familial amyotrophic lateral sclerosis. *Science, 323*(5918), 1205-1208. doi:10.1126/science.1166066

Kwon, I., & Xian, S. (2014). Poly-dipeptides encoded by the C9orf72 repeats bind nucleoli, impede RNA biogenesis, and kill cells. *Science, 345*(6201).

LaClair, K. D., Zhou, Q., Michaelsen, M., Wefers, B., Brill, M. S., Janjic, A., Rathkolb, B., Farny, D., Cygan, M., de Angelis, M. H., Wurst, W., Neumann, M., Enard, W., Misgeld, T., Arzberger, T., & Edbauer, D. (2020). Congenic expression of poly-GA but not poly-PR in mice triggers selective neuron loss and interferon responses found in C9orf72 ALS. *Acta Neuropathol, 140*(2), 121-142. doi:10.1007/s00401-020-02176-0

LaJoie, D., Turkmen, A. M., Mackay, D. R., Jensen, C. C., Aksenova, V., Niwa, M., Dasso, M., & Ullman, K. S. (2022). A Role for Nup153 in Nuclear Assembly Reveals Differential Requirements for Targeting of Nuclear Envelope Constituents. *Mol Biol Cell*, mbcE22050189. doi:10.1091/mbc.E22-05-0189

Lapalombella, R., Sun, Q., Williams, K., Tangeman, L., Jha, S., Zhong, Y., Goettl, V., Mahoney, E., Berglund, C., Gupta, S., Farmer, A., Mani, R., Johnson, A. J., Lucas, D., Mo, X., Daelemans, D., Sandanayaka, V., Shechter, S., McCauley, D., Shacham, S., Kauffman, M., Chook, Y. M., & Byrd, J. C. (2012). Selective inhibitors of nuclear export show that CRM1/XPO1 is a target in chronic lymphocytic leukemia. *Blood, 120*(23), 4621-4634. doi:10.1182/blood-2012-05-429506

Lee, Y. B., Baskaran, P., Gomez-Deza, J., Chen, H. J., Nishimura, A. L., Smith, B. N., Troakes, C., Adachi, Y., Stepto, A., Petrucelli, L., Gallo, J. M., Hirth, F., Rogelj, B., Guthrie, S., & Shaw, C. E. (2017). C9orf72 poly GA RAN-translated protein plays a key role in amyotrophic lateral sclerosis via aggregation and toxicity. *Hum Mol Genet, 26*(24), 4765-4777. doi:10.1093/hmg/ddx350

Lee, Y. B., Chen, H. J., Peres, J. N., Gomez-Deza, J., Attig, J., Stalekar, M., Troakes, C., Nishimura, A. L., Scotter, E. L., Vance, C., Adachi, Y., Sardone, V., Miller, J. W., Smith, B. N., Gallo, J. M., Ule, J., Hirth, F., Rogelj, B., Houart, C., & Shaw, C. E. (2013). Hexanucleotide repeats in ALS/FTD form length-dependent RNA foci, sequester RNA binding proteins, and are neurotoxic. *Cell Rep, 5*(5), 1178-1186. doi:10.1016/j.celrep.2013.10.049

Li, Y., Aksenova, V., Tingey, M., Yu, J., Ma, P., Arnaoutov, A., Chen, S., Dasso, M., & Yang, W. (2021). Distinct roles of nuclear basket proteins in directing the passage of mRNA through the nuclear pore. *Proc Natl Acad Sci U S A, 118*(37). doi:10.1073/pnas.2015621118

Li, Y., Sun, B., Wang, Z., He, Z., Yang, F., Wang, H., Cui, F., Chen, Z., Ling, L., Wang, C., & Huang, X. (2021). Mutation Screening of the GLE1 Gene in a Large Chinese Cohort of Amyotrophic Lateral Sclerosis Patients. *Frontiers in Neuroscience*(1662-4548 (Print)).

Liu, F., Morderer, D., Wren, M. C., Vettleson-Trutza, S. A., Wang, Y., Rabichow, B. E., Salemi, M. R., Phinney, B. S., Oskarsson, B., Dickson, D. W., & Rossoll, W. (2022). Proximity proteomics of C9orf72 dipeptide repeat proteins identifies molecular chaperones as modifiers of poly-GA aggregation. *Acta Neuropathol Commun, 10*(1), 22. doi:10.1186/s40478-022-01322-x

Liu, Y., Pattamatta, A., Zu, T., Reid, T., Bardhi, O., Borchelt, D. R., Yachnis, A. T., & Ranum, L. P. (2016). C9orf72 BAC Mouse Model with Motor Deficits and Neurodegenerative Features of ALS/FTD. *Neuron, 90*(3), 521-534. doi:10.1016/j.neuron.2016.04.005

Lu, W. Z., Lin, H. A., Hou, S. K., Lee, C. F., Bai, C. H., & Lin, S. F. (2022). Split-hand index for amyotrophic lateral sclerosis diagnosis: A frequentist and Bayesian meta-analysis. *Clin Neurophysiol, 143*, 56-66. doi:10.1016/j.clinph.2022.08.020

Mackenzie, I. R., Arzberger, T., Kremmer, E., Troost, D., Lorenzl, S., Mori, K., Weng, S.-M., Haass, C., Kretzschmar, H. A., Edbauer, D., & Neumann, M. (2013). Dipeptide repeat protein pathology in C9ORF72 mutation cases: clinico-pathological correlations. *Acta Neuropathol, 126*(6), 859-879. doi:10.1007/s00401-013-1181-y

Mackenzie, I. R., Frick, P., Grasser, F. A., Gendron, T. F., Petrucelli, L., Cashman, N. R., Edbauer, D., Kremmer, E., Prudlo, J., Troost, D., & Neumann, M. (2015). Quantitative analysis and clinico-pathological correlations of different dipeptide repeat protein pathologies in C9ORF72 mutation carriers. *Acta Neuropathol, 130*(6), 845-861. doi:10.1007/s00401-015-1476-2

Mackenzie, I. R. A., Bigio, E. H., Ince, P. G., Geser, F., Neumann, M., Cairns, N. J., Kwong, L. K., Forman, M. S., Ravits, J., Stewart, H., Eisen, A., McClusky, L., Kretzschmar, H. A., Monoranu, C. M., Highley, J. R., Kirby, J., Siddique, T., Shaw, P. J., Lee, V. M.-Y., & Trojanowski, J. Q. (2007). Pathological TDP-43 distinguishes sporadic amyotrophic lateral sclerosis from amyotrophic lateral sclerosis with SOD1 mutations. *61*(5), 427-434. doi:https://doi.org/10.1002/ana.21147

Marchi, P. M., Marrone, L., Brasseur, L., Coens, A., Webster, C. P., Bousset, L., Destro, M., Smith, E. F., Walther, C. G., Alfred, V., Marroccella, R., Graves, E. J., Robinson, D., Shaw, A. C., Wan, L. M., Grierson, A. J., Ebbens, S. J., De Vos, K. J., Hautbergue, G. M., Ferraiuolo, L., Melki, R., & Azzouz, M. (2022). C9ORF72-derived poly-GA DPRs undergo endocytic uptake in iAstrocytes and spread to motor neurons. *Life Sci Alliance, 5*(9). doi:10.26508/lsa.202101276

Matusica, D., Fenech, M. P., Rogers, M. L., & Rush, R. A. (2008). Characterization and use of the NSC-34 cell line for study of neurotrophin receptor trafficking. *J Neurosci Res, 86*(3), 553-565. doi:10.1002/jnr.21507

Maury, Y., Come, J., Piskorowski, R. A., Salah-Mohellibi, N., Chevaleyre, V., Peschanski, M., Martinat, C., & Nedelec, S. (2015). Combinatorial analysis of developmental cues efficiently converts human pluripotent stem cells into multiple neuronal subtypes. *Nat Biotechnol, 33*(1), 89-96. doi:10.1038/nbt.3049

May, S., Hornburg, D., Schludi, M. H., Arzberger, T., Rentzsch, K., Schwenk, B. M., Grasser, F. A., Mori, K., Kremmer, E., Banzhaf-Strathmann, J., Mann, M., Meissner, F., & Edbauer, D. (2014). C9orf72 FTLD/ALS-associated Gly-Ala dipeptide repeat proteins cause neuronal toxicity and Unc119 sequestration. *Acta Neuropathol, 128*(4), 485-503. doi:10.1007/s00401-014-1329-4

McEachin, Z. T., Gendron, T. F., Raj, N., Garcia-Murias, M., Banerjee, A., Purcell, R. H., Ward, P. J., Todd, T. W., Merritt-Garza, M. E., Jansen-West, K., Hales, C. M., Garcia-Sobrino, T., Quintans, B., Holler, C. J., Taylor, G., San Millan, B., Teijeira, S., Yamashita, T., Ohkubo, R., Boulis, N. M., Xu, C., Wen, Z., Streichenberger, N., Neuro, C. E. B. N. N., Fogel, B. L., Kukar, T., Abe, K., Dickson, D. W., Arias, M., Glass, J. D., Jiang, J., Tansey, M. G., Sobrido, M. J., Petrucelli, L., Rossoll, W., & Bassell, G. J. (2020). Chimeric Peptide Species Contribute to Divergent Dipeptide Repeat Pathology in c9ALS/FTD and SCA36. *Neuron*. doi:10.1016/j.neuron.2020.04.011

McEachin, Z. T., Parameswaran, J., Raj, N., Bassell, G. J., & Jiang, J. (2020). RNA-mediated toxicity in C9orf72 ALS and FTD. *Neurobiol Dis, 145*, 105055. doi:10.1016/j.nbd.2020.105055

Mehta, A. R., Walters, R., Waldron, F. M., Pal, S., Selvaraj, B. T., Macleod, M. R., Hardingham, G. E., Chandran, S., & Gregory, J. M. (2019). Targeting mitochondrial dysfunction in amyotrophic lateral sclerosis: a systematic review and meta-analysis. *Brain Commun, 1*(1), fcz009. doi:10.1093/braincomms/fcz009

Melamed, Z., Lopez-Erauskin, J., Baughn, M. W., Zhang, O., Drenner, K., Sun, Y., Freyermuth, F., McMahon, M. A., Beccari, M. S., Artates, J. W., Ohkubo, T., Rodriguez, M., Lin, N., Wu, D., Bennett, C. F., Rigo, F., Da Cruz, S., Ravits, J., Lagier-Tourenne, C., & Cleveland, D. W. (2019). Premature polyadenylation-mediated loss of stathmin-2 is a hallmark of TDP-43-dependent neurodegeneration. *Nat Neurosci, 22*(2), 180-190. doi:10.1038/s41593-018-0293-z

Miller, J. W., Urbinati, C. R., Teng-Umnuay, P., Stenberg, M. G., Byrne, B. J., Thornton, C. A., & Swanson, M. S. (2000). Recruitment of human muscleblind proteins to (CUG)(n) expansions associated with myotonic dystrophy. *Embo j, 19*(17), 4439-4448. doi:10.1093/emboj/19.17.4439

Miller, R. G., Mitchell, J. D., & Moore, D. H. (2012). Riluzole for amyotrophic lateral sclerosis (ALS)/motor neuron disease (MND). *Cochrane Database Syst Rev, 2012*(3), Cd001447. doi:10.1002/14651858.CD001447.pub3

Miller, T. M., Cudkowicz, M. E., Genge, A., Shaw, P. J., Sobue, G., Bucelli, R. C., Chiò, A., Van Damme, P., Ludolph, A. C., Glass, J. D., Andrews, J. A., Babu, S., Benatar, M., McDermott, C. J., Cochrane, T., Chary, S., Chew, S., Zhu, H., Wu, F., Nestorov, I., Graham, D., Sun, P., McNeill, M., Fanning, L., Ferguson, T. A., & Fradette, S. (2022). Trial of Antisense Oligonucleotide Tofersen for SOD1 ALS. *N Engl J Med, 387*(12), 1099-1110. doi:10.1056/NEJMoa2204705

Mizielinska, S., Grönke, S., & Niccoli, T. (2014). C9orf72 repeat expansions cause neurodegeneration in Drosophila through arginine-rich proteins. *Science, 345*(6201).

Mizielinska, S., Lashley, T., Norona, F. E., Clayton, E. L., Ridler, C. E., Fratta, P., & Isaacs, A. M. (2013). C9orf72 frontotemporal lobar degeneration is characterised by frequent neuronal sense and antisense RNA foci. *Acta Neuropathol, 126*(6), 845-857. doi:10.1007/s00401-013-1200-z

Moens, T. G., Mizielinska, S., Niccoli, T., Mitchell, J. S., Thoeng, A., Ridler, C. E., Grönke, S., Esser, J., Heslegrave, A., Zetterberg, H., Partridge, L., & Isaacs, A. M. (2018). Sense and antisense RNA are not toxic in Drosophila models of C9orf72-associated ALS/FTD. *Acta Neuropathol, 135*(3), 445-457. doi:10.1007/s00401-017-1798-3

Mohr, D., Frey, S., Fischer, T., Güttler, T., & Görlich, D. (2009). Characterisation of the passive permeability barrier of nuclear pore complexes. *28*(17), 2541-2553. doi:https://doi.org/10.1038/emboj.2009.200

Mori, K., Arzberger, T., Grässer, F. A., Gijselinck, I., May, S., Rentzsch, K., Weng, S.-M., Schludi, M. H., van der Zee, J., Cruts, M., Van Broeckhoven, C., Kremmer, E., Kretzschmar, H. A., Haass, C., & Edbauer, D. (2013). Bidirectional transcripts of the expanded C9orf72 hexanucleotide repeat are translated into aggregating dipeptide repeat proteins. *Acta Neuropathol, 126*(6), 881-893. doi:10.1007/s00401-013-1189-3

Motulsky, H. J. (2022). Multiplicity adjusted P values. *GraphPad Statistics Guide.* Retrieved from https://www.graphpad.com/guides/prism/latest/statistics/stat_multiplicity_adjusted_p_values.htm

Musiwaro, P., Smith, M., Manifava, M., Walker, S. A., & Ktistakis, N. T. (2013). Characteristics and requirements of basal autophagy in HEK 293 cells. *Autophagy, 9*(9), 1407-1417. doi:10.4161/auto.25455

Myszczynska, M., & Ferraiuolo, L. (2016). New In Vitro Models to Study Amyotrophic Lateral Sclerosis. *Brain Pathol, 26*(2), 258-265. doi:10.1111/bpa.12353

Nagoshi, N., Nakashima, H., & Fehlings, M. G. (2015). Riluzole as a neuroprotective drug for spinal cord injury: from bench to bedside. *Molecules, 20*(5), 7775-7789. doi:10.3390/molecules20057775

Napoletano, F., Ferrari Bravo, G., Voto, I. A. P., Santin, A., Celora, L., Campaner, E., Dezi, C., Bertossi, A., Valentino, E., Santorsola, M., Rustighi, A., Fajner, V., Maspero, E., Ansaloni, F., Cancila, V., Valenti, C. F., Santo, M., Artimagnella, O. B., Finaurini, S., Gioia, U., Polo, S., Sanges, R., Tripodo, C., Mallamaci, A., Gustincich, S., d'Adda di Fagagna, F., Mantovani, F., Specchia, V., & Del Sal, G. (2021). The prolyl-isomerase PIN1 is essential for nuclear Lamin-B structure and function and protects heterochromatin under mechanical stress. *Cell Rep, 36*(11), 109694. doi:10.1016/j.celrep.2021.109694

Nguyen, L., Montrasio, F., Pattamatta, A., Tusi, S. K., Bardhi, O., Meyer, K. D., Hayes, L., Nakamura, K., Banez-Coronel, M., Coyne, A., Guo, S., Laboissonniere, L. A., Gu, Y., Narayanan, S., Smith, B., Nitsch, R. M., Kankel, M. W., Rushe, M., Rothstein, J., Zu, T., Grimm, J., & Ranum, L. P. W. (2020). Antibody Therapy Targeting RAN Proteins Rescues C9 ALS/FTD Phenotypes in C9orf72 Mouse Model. *Neuron, 105*(4), 645-662 e611. doi:10.1016/j.neuron.2019.11.007

Nishimura, A. L., Zupunski, V., Troakes, C., Kathe, C., Fratta, P., Howell, M., Gallo, J. M., Hortobágyi, T., Shaw, C. E., & Rogelj, B. (2010). Nuclear import impairment causes cytoplasmic trans-activation response DNA-binding protein accumulation and is associated with frontotemporal lobar degeneration. *Brain, 133*(Pt 6), 1763-1771. doi:10.1093/brain/awq111

O'Rourke, J. G., Bogdanik, L., Yáñez, A., Lall, D., Wolf, A. J., Muhammad, A. K. M. G., Ho, R., Carmona, S., Vit, J. P., Zarrow, J., Kim, K. J., Bell, S., Harms, M. B., Miller, T. M., Dangler, C. A., Underhill, D. M., Goodridge, H. S., Lutz, C. M., & Baloh, R. H. (2016). C9orf72 is required for proper macrophage and microglial function in mice. *Science, 351*(6279), 1324-1329. doi:10.1126/science.aaf1064

Paganoni, S., Hendrix, S., Dickson, S. P., Knowlton, N., Berry, J. D., Elliott, M. A., Maiser, S., Karam, C., Caress, J. B., Owegi, M. A., Quick, A., Wymer, J., Goutman, S. A., Heitzman, D., Heiman-Patterson, T. D., Jackson, C., Quinn, C., Rothstein, J. D., Kasarskis, E. J., Katz, J., Jenkins, L., Ladha, S. S., Miller, T. M., Scelsa, S. N., Vu, T. H., Fournier, C., Johnson, K. M., Swenson, A., Goyal, N., Pattee, G. L., Babu, S., Chase, M., Dagostino, D., Hall, M., Kittle, G., Eydinov, M., Ostrow, J., Pothier, L., Randall, R., Shefner, J. M., Sherman, A. V., Tustison, E., Vigneswaran, P., Yu, H., Cohen, J., Klee, J., Tanzi, R., Gilbert, W., Yeramian, P., & Cudkowicz, M. (2022). Effect of sodium phenylbutyrate/taurursodiol on tracheostomy/ventilation-free survival and hospitalisation in amyotrophic lateral sclerosis: long-term results from the CENTAUR trial. *Journal of Neurology, Neurosurgery & Psychiatry, 93*(8), 871. doi:10.1136/jnnp-2022-329024

Paganoni, S., Macklin, E. A., Hendrix, S., Berry, J. D., Elliott, M. A., Maiser, S., Karam, C., Caress, J. B., Owegi, M. A., Quick, A., Wymer, J., Goutman, S. A., Heitzman, D., Heiman-Patterson, T., Jackson, C. E., Quinn, C., Rothstein, J. D., Kasarskis, E. J., Katz, J., Jenkins, L., Ladha, S., Miller, T. M., Scelsa, S. N., Vu, T. H., Fournier, C. N., Glass, J. D., Johnson, K. M., Swenson, A., Goyal, N. A., Pattee, G. L., Andres, P. L., Babu, S., Chase, M., Dagostino, D., Dickson, S. P., Ellison, N., Hall, M., Hendrix, K., Kittle, G., McGovern, M., Ostrow, J., Pothier, L., Randall, R., Shefner, J. M., Sherman, A. V., Tustison, E., Vigneswaran, P., Walker, J., Yu, H., Chan, J., Wittes, J., Cohen, J., Klee, J., Leslie, K., Tanzi, R. E., Gilbert, W., Yeramian, P. D., Schoenfeld, D., & Cudkowicz, M. E. (2020). Trial of Sodium Phenylbutyrate-Taurursodiol for Amyotrophic Lateral Sclerosis. *N Engl J Med, 383*(10), 919-930. doi:10.1056/NEJMoa1916945

Pang, W., & Hu, F. (2021). Cellular and physiological functions of C9ORF72 and implications for ALS/FTD. *J Neurochem, 157*(3), 334-350. doi:10.1111/jnc.15255

Paonessa, F., Evans, L. D., Solanki, R., Larrieu, D., Wray, S., Hardy, J., Jackson, S. P., & Livesey, F. J. (2019). Microtubules Deform the Nuclear Membrane and Disrupt Nucleocytoplasmic Transport in Tau-Mediated Frontotemporal Dementia. *Cell Rep, 26*(3), 582-593 e585. doi:10.1016/j.celrep.2018.12.085

Patterson, J. R., Wood, M. P., & Schisa, J. A. (2011). Assembly of RNP granules in stressed and aging oocytes requires nucleoporins and is coordinated with nuclear membrane blebbing. *Dev Biol, 353*(2), 173-185. doi:10.1016/j.ydbio.2011.02.028

Pinarbasi, E. S., Cagatay, T., Fung, H. Y. J., Li, Y. C., Chook, Y. M., & Thomas, P. J. (2018). Active nuclear import and passive nuclear export are the primary determinants of TDP-43 localization. *Sci Rep, 8*(1), 7083. doi:10.1038/s41598-018-25008-4

Protter, D. S. W., & Parker, R. (2016). Principles and Properties of Stress Granules. *Trends Cell Biol, 26*(9), 668-679. doi:10.1016/j.tcb.2016.05.004

Rajesh, K. G., Sasaguri, S., Suzuki, R., & Maeda, H. (2003). Antioxidant MCI-186 inhibits mitochondrial permeability transition pore and upregulates Bcl-2 expression. *american journal of physiology. Heart and circulatory physiology*(0363-6135 (Print)). doi:10.1152/ajpheart.00143.2003

Reddy, K., Zamiri, B., Stanley, S. Y. R., Macgregor, R. B., Jr., & Pearson, C. E. (2013). The disease-associated r(GGGGCC)n repeat from the C9orf72 gene forms tract length-dependent uni- and multimolecular RNA G-quadruplex structures. *J Biol Chem, 288*(14), 9860-9866. doi:10.1074/jbc.C113.452532

Renton, A. E., Chiò, A., & Traynor, B. J. (2014). State of play in amyotrophic lateral sclerosis genetics. *Nat Neurosci, 17*(1), 17-23. doi:10.1038/nn.3584

Renton, A. E., Majounie, E., Waite, A., Simon-Sanchez, J., Rollinson, S., Gibbs, J. R., Schymick, J. C., Laaksovirta, H., van Swieten, J. C., Myllykangas, L., Kalimo, H., Paetau, A., Abramzon, Y., Remes, A. M., Kaganovich, A., Scholz, S. W., Duckworth, J., Ding, J., Harmer, D. W., Hernandez, D. G., Johnson, J. O., Mok, K., Ryten, M., Trabzuni, D., Guerreiro, R. J., Orrell, R. W., Neal, J., Murray, A., Pearson, J., Jansen, I. E., Sondervan, D., Seelaar, H., Blake, D., Young, K., Halliwell, N., Callister, J. B., Toulson, G., Richardson, A., Gerhard, A., Snowden, J., Mann, D., Neary, D., Nalls, M. A., Peuralinna, T., Jansson, L., Isoviita, V. M., Kaivorinne, A. L., Holtta-Vuori, M., Ikonen, E., Sulkava, R., Benatar, M., Wuu, J., Chio, A., Restagno, G., Borghero, G., Sabatelli, M., Consortium, I., Heckerman, D., Rogaeva, E., Zinman, L., Rothstein, J. D., Sendtner, M., Drepper, C., Eichler, E. E., Alkan, C., Abdullaev, Z., Pack, S. D., Dutra, A., Pak, E., Hardy, J., Singleton, A., Williams, N. M., Heutink, P., Pickering-Brown, S., Morris, H. R., Tienari, P. J., & Traynor, B. J. (2011). A hexanucleotide repeat expansion in C9ORF72 is the cause of chromosome 9p21-linked ALS-FTD. *Neuron, 72*(2), 257-268. doi:10.1016/j.neuron.2011.09.010

Rizzu, P., Blauwendraat, C., Heetveld, S., Lynes, E. M., Castillo-Lizardo, M., Dhingra, A., Pyz, E., Hobert, M., Synofzik, M., Simón-Sánchez, J., Francescatto, M., & Heutink, P. (2016). C9orf72 is differentially expressed in the central nervous system and myeloid cells and consistently reduced in C9orf72, MAPT and GRN mutation carriers. *Acta Neuropathol Commun, 4*(1), 37. doi:10.1186/s40478-016-0306-7

Rodrigues, C. M., Solá, S., Sharpe, J. C., Moura, J. J., & Steer, C. J. (2003). Tauroursodeoxycholic acid prevents Bax-induced membrane perturbation and cytochrome C release in isolated mitochondria. *Biochemistry, 42*(10), 3070-3080. doi:10.1021/bi026979d

Rosen, D. R., Siddique, T., Patterson, D., Figlewicz, D. A., Sapp, P., Hentati, A., Donaldson, D., Goto, J., O'Regan, J. P., Deng, H. X., & et al. (1993). Mutations in Cu/Zn superoxide dismutase gene are associated with familial amyotrophic lateral sclerosis. *Nature, 362*(6415), 59-62. doi:10.1038/362059a0

Ryan, M., Heverin, M., McLaughlin, R. L., & Hardiman, O. (2019). Lifetime Risk and Heritability of Amyotrophic Lateral Sclerosis. *JAMA Neurol, 76*(11), 1367-1374. doi:10.1001/jamaneurol.2019.2044

Saberi, S., Stauffer, J. E., Jiang, J., Garcia, S. D., Taylor, A. E., Schulte, D., Ohkubo, T., Schloffman, C. L., Maldonado, M., Baughn, M., Rodriguez, M. J., Pizzo, D., Cleveland, D., & Ravits, J. (2018). Sense-encoded poly-GR dipeptide repeat proteins correlate to neurodegeneration and uniquely co-localize with TDP-43 in dendrites of repeat-expanded C9orf72 amyotrophic lateral sclerosis. *Acta Neuropathol, 135*(3), 459-474. doi:10.1007/s00401-017-1793-8

Safran, M., Rosen, N., Twik, M., BarShir, R., Stein, T. I., Dahary, D., Fishilevich, S., & Lancet, D. (2021). The GeneCards Suite. In I. Abugessaisa & T. Kasukawa (Eds.), *Practical Guide to Life Science Databases* (pp. 27-56). Singapore: Springer Nature Singapore.

Santos, T., Salgado, G. F., Cabrita, E. J., & Cruz, C. (2022). Nucleolin: a binding partner of G-quadruplex structures. *Trends Cell Biol, 32*(7), 561-564. doi:10.1016/j.tcb.2022.03.003

Schludi, M. H., Becker, L., Garrett, L., Gendron, T. F., Zhou, Q., Schreiber, F., Popper, B., Dimou, L., Strom, T. M., Winkelmann, J., von Thaden, A., Rentzsch, K., May, S., Michaelsen, M., Schwenk, B. M., Tan, J., Schoser, B., Dieterich, M., Petrucelli, L., Holter, S. M., Wurst, W., Fuchs, H., Gailus-Durner, V., de Angelis, M. H., Klopstock, T., Arzberger, T., & Edbauer, D. (2017). Spinal poly-GA inclusions in a C9orf72 mouse model

trigger motor deficits and inflammation without neuron loss. *Acta Neuropathol, 134*(2), 241-254. doi:10.1007/s00401-017-1711-0

Schludi, M. H., May, S., Grasser, F. A., Rentzsch, K., Kremmer, E., Kupper, C., Klopstock, T., German Consortium for Frontotemporal Lobar, D., Bavarian Brain Banking, A., Arzberger, T., & Edbauer, D. (2015). Distribution of dipeptide repeat proteins in cellular models and C9orf72 mutation cases suggests link to transcriptional silencing. *Acta Neuropathol, 130*(4), 537-555. doi:10.1007/s00401-015-1450-z

Schwartz, T. U. (2022). Solving the nuclear pore puzzle. *Science, 376*(6598), 1158-1159. doi:10.1126/science.abq4792

Sellier, C., Campanari, M. L., Julie Corbier, C., Gaucherot, A., Kolb-Cheynel, I., Oulad-Abdelghani, M., Ruffenach, F., Page, A., Ciura, S., Kabashi, E., & Charlet-Berguerand, N. (2016). Loss of C9ORF72 impairs autophagy and synergizes with polyQ Ataxin-2 to induce motor neuron dysfunction and cell death. *Embo j, 35*(12), 1276-1297. doi:10.15252/embj.201593350

Shang, J., Yamashita, T., Nakano, Y., Morihara, R., Li, X., Feng, T., Liu, X., Huang, Y., Fukui, Y., Hishikawa, N., Ohta, Y., & Abe, K. (2017). Aberrant distributions of nuclear pore complex proteins in ALS mice and ALS patients. *Neuroscience, 350*, 158-168. doi:https://doi.org/10.1016/j.neuroscience.2017.03.024

Shi, K. Y., Mori, E., Nizami, Z. F., Lin, Y., Kato, M., Xiang, S., Wu, L. C., Ding, M., Yu, Y., Gall, J. G., & McKnight, S. L. (2017). Toxic PRn poly-dipeptides encoded by the C9orf72 repeat expansion block nuclear import and export. *Proceedings of the National Academy of Sciences, 114*(7). doi:10.1073/pnas.1620293114

Shi, Y., Lin, S., Staats, K. A., Li, Y., Chang, W. H., Hung, S. T., Hendricks, E., Linares, G. R., Wang, Y., Son, E. Y., Wen, X., Kisler, K., Wilkinson, B., Menendez, L., Sugawara, T., Woolwine, P., Huang, M., Cowan, M. J., Ge, B., Koutsodendris, N., Sandor, K. P., Komberg, J., Vangoor, V. R., Senthilkumar, K., Hennes, V., Seah, C., Nelson, A. R., Cheng, T. Y., Lee, S. J., August, P. R., Chen, J. A., Wisniewski, N., Hanson-Smith, V., Belgard, T. G., Zhang, A., Coba, M., Grunseich, C., Ward, M. E., van den Berg, L. H., Pasterkamp, R. J., Trotti, D., Zlokovic, B. V., & Ichida, J. K. (2018). Haploinsufficiency leads to neurodegeneration in C9ORF72 ALS/FTD human induced motor neurons. *Nat Med, 24*(3), 313-325. doi:10.1038/nm.4490

Silvestrini, M. J., Johnson, J. R., Kumar, A. V., Thakurta, T. G., Blais, K., Neill, Z. A., Marion, S. W., St Amand, V., Reenan, R. A., & Lapierre, L. R. (2018). Nuclear Export Inhibition Enhances HLH-30/TFEB Activity, Autophagy, and Lifespan. *Cell Rep, 23*(7), 1915-1921. doi:10.1016/j.celrep.2018.04.063

Slot, J. W., & Geuze, H. J. (2007). Cryosectioning and immunolabeling. *Nature Protocols, 2*(10), 2480-2491. doi:10.1038/nprot.2007.365

Smeyers, J., Banchi, E. G., & Latouche, M. (2021). C9ORF72: What It Is, What It Does, and Why It Matters. *Front Cell Neurosci, 15*, 661447. doi:10.3389/fncel.2021.661447

Solomon, D. A., Stepto, A., Au, W. H., Adachi, Y., Diaper, D. C., Hall, R., Rekhi, A., Boudi, A., Tziortzouda, P., Lee, Y. B., Smith, B., Bridi, J. C., Spinelli, G., Dearlove, J., Humphrey, D. M., Gallo, J. M., Troakes, C., Fanto, M., Soller, M., Rogelj, B., Parsons, R. B., Shaw, C. E., Hortobagyi, T., & Hirth, F. (2018). A feedback loop between dipeptide-repeat protein, TDP-43 and karyopherin-alpha mediates C9orf72-related neurodegeneration. *Brain, 141*(10), 2908-2924. doi:10.1093/brain/awy241

Stanley, G. J., Akpinar, B., Shen, Q., Fisher, P. A.-O. X., Lusk, C. A.-O., Lin, C. A.-O., & Hoogenboom, B. A.-O. Quantification of Biomolecular Dynamics Inside Real and Synthetic Nuclear Pore Complexes Using Time-Resolved Atomic Force Microscopy. (1936-086X (Electronic)).

Starr, A., & Sattler, R. (2018). Synaptic dysfunction and altered excitability in C9ORF72 ALS/FTD. *Brain Res, 1693*(Pt A), 98-108. doi:10.1016/j.brainres.2018.02.011

Suaud, L., Miller, K., Panichelli, A. E., Randell, R. L., Marando, C. M., & Rubenstein, R. C. (2011). 4-Phenylbutyrate stimulates Hsp70 expression through the Elp2 component of elongator and STAT-3 in cystic fibrosis epithelial cells. *J Biol Chem, 286*(52), 45083-45092. doi:10.1074/jbc.M111.293282

Sullivan, P. M., Zhou, X., Robins, A. M., Paushter, D. H., Kim, D., Smolka, M. B., & Hu, F. (2016). The ALS/FTLD associated protein C9orf72 associates with SMCR8 and WDR41 to regulate the autophagy-lysosome pathway. *Acta Neuropathol Commun, 4*(1), 51. doi:10.1186/s40478-016-0324-5

Sun, Q., Carrasco, Y. P., Hu, Y., Guo, X., Mirzaei, H., Macmillan, J., & Chook, Y. M. (2013). Nuclear export inhibition through covalent conjugation and hydrolysis of Leptomycin B by CRM1. *Proc Natl Acad Sci U S A, 110*(4), 1303-1308. doi:10.1073/pnas.1217203110

Swinnen, B., Bento-Abreu, A., Gendron, T. F., Boeynaems, S., Bogaert, E., Nuyts, R., Timmers, M., Scheveneels, W., Hersmus, N., Wang, J., Mizielinska, S., Isaacs, A. M., Petrucelli, L., Lemmens, R., Van Damme, P., Van Den Bosch, L., & Robberecht, W. (2018). A zebrafish model for C9orf72 ALS reveals RNA toxicity as a pathogenic mechanism. *Acta Neuropathol, 135*(3), 427-443. doi:10.1007/s00401-017-1796-5

Tang, D., Sheng, J., Xu, L., Yan, C., & Qi, S. (2020). The C9orf72-SMCR8-WDR41 complex is a GAP for small GTPases. *Autophagy, 16*(8), 1542-1543. doi:10.1080/15548627.2020.1779473

Taylor, J. P., Brown, R. H., Jr., & Cleveland, D. W. (2016). Decoding ALS: from genes to mechanism. *Nature, 539*(7628), 197-206. doi:10.1038/nature20413

Thams, S., Lowry, E. R., Larraufie, M. H., Spiller, K. J., Li, H., Williams, D. J., Hoang, P., Jiang, E., Williams, L. A., Sandoe, J., Eggan, K., Lieberam, I., Kanning, K. C., Stockwell, B. R., Henderson, C. E., & Wichterle, H. (2019). A Stem Cell-Based Screening Platform Identifies Compounds that Desensitize Motor Neurons to Endoplasmic Reticulum Stress. *Mol Ther, 27*(1), 87-101. doi:10.1016/j.ymthe.2018.10.010

Trabjerg, B. B., Garton, F. C., van Rheenen, W., Fang, F., Henderson, R. D., Mortensen, P. B., Agerbo, E., & Wray, N. R. (2020). ALS in Danish Registries. *Heritability and links to psychiatric and cardiovascular disorders, 6*(2), e398. doi:10.1212/NXG.0000000000000398 %J Neurology Genetics

Tran, H., Almeida, S., Moore, J., Gendron, Tania F., Chalasani, U., Lu, Y., Du, X., Nickerson, Jeffrey A., Petrucelli, L., Weng, Z., & Gao, F.-B. (2015). Differential Toxicity of Nuclear RNA Foci versus Dipeptide Repeat Proteins in a Drosophila Model of C9ORF72 FTD/ALS. *Neuron, 87*(6), 1207-1214. doi:10.1016/j.neuron.2015.09.015

Traxinger, K., Kelly, C., Johnson, B. A., Lyles, R. H., & Glass, J. D. (2013). Prognosis and epidemiology of amyotrophic lateral sclerosis: Analysis of a clinic population, 1997-2011. *Neurology. Clinical practice, 3*(4), 313-320. doi:10.1212/CPJ.0b013e3182a1b8ab

Turnbull, J. (2018). Is edaravone harmful? (A placebo is not a control). *Amyotroph Lateral Scler Frontotemporal Degener*(2167-9223 (Electronic)). doi:10.1080/21678421.2018.1517179

Uhlén, M., Fagerberg, L., Hallström, B. M., Lindskog, C., Oksvold, P., Mardinoglu, A., Sivertsson, Å., Kampf, C., Sjöstedt, E., Asplund, A., Olsson, I., Edlund, K., Lundberg, E., Navani, S., Szigyarto, C. A., Odeberg, J., Djureinovic, D., Takanen, J. O., Hober, S., Alm, T., Edqvist, P. H., Berling, H., Tegel, H., Mulder, J., Rockberg, J., Nilsson, P., Schwenk, J. M., Hamsten, M., von Feilitzen, K., Forsberg, M., Persson, L., Johansson, F., Zwahlen, M., von Heijne, G., Nielsen, J., & Pontén, F. (2015). Proteomics. Tissue-based map of the human proteome. *Science, 347*(6220), 1260419. doi:10.1126/science.1260419

Van Langenhove, T., van der Zee, J., & Van Broeckhoven, C. (2012). The molecular basis of the frontotemporal lobar degeneration-amyotrophic lateral sclerosis spectrum. *Ann Med, 44*(8), 817-828. doi:10.3109/07853890.2012.665471

Vance, C., Rogelj, B., Hortobágyi, T., De Vos, K. J., Nishimura, A. L., Sreedharan, J., Hu, X., Smith, B., Ruddy, D., Wright, P., Ganesalingam, J., Williams, K. L., Tripathi, V., Al-Saraj, S., Al-Chalabi, A., Leigh, P. N., Blair, I. P., Nicholson, G., de Belleroche, J., Gallo, J. M., Miller, C. C., & Shaw, C. E. (2009). Mutations in FUS, an RNA processing protein, cause familial amyotrophic lateral sclerosis type 6. *Science*(1095-9203 (Electronic)). doi:10.1126/science.1165942.

Vatsavayai, S. C., Nana, A. L., Yokoyama, J. S., & Seeley, W. W. (2019). C9orf72-FTD/ALS pathogenesis: evidence from human neuropathological studies. *Acta Neuropathol, 137*(1), 1-26. doi:10.1007/s00401-018-1921-0

Viodé, A., Fournier, C., Camuzat, A., Fenaille, F., , N. B. B., Latouche, M., Elahi, F., Le Ber, I., Junot, C., Lamari, F., Anquetil, V., Becher, F., Letournel, F., Vital, A., Chapon, F., Godfraind, C., Maurage, C.-A., Deramecourt, V., Meyronnet, D., Streichenberger, N., Maues de Paula, A., Rigau, V., Vandenbos-Burel, F., Duyckaerts, C., Seilhean, D., Sazdovitch, V., Milin, S., Christian Chiforeanu, D., Laquerrière, A., & Lannes, B. (2018). New Antibody-Free Mass Spectrometry-Based Quantification Reveals That C9ORF72 Long Protein Isoform Is Reduced in the Frontal Cortex of Hexanucleotide-Repeat Expansion Carriers. *Frontiers in Neuroscience, 12*. doi:10.3389/fnins.2018.00589

Watanabe, S., Inami, H., Oiwa, K., Murata, Y., Sakai, S., Komine, O., Sobue, A., Iguchi, Y., Katsuno, M., & Yamanaka, K. (2020). Aggresome formation and liquid-liquid phase separation independently induce cytoplasmic aggregation of TAR DNA-binding protein 43. *Cell Death Dis, 11*(10), 909. doi:10.1038/s41419-020-03116-2

Watson, M. L. (1959). Further observations on the nuclear envelope of the animal cell. *J Biophys Biochem Cytol, 6*(2), 147-156. doi:10.1083/jcb.6.2.147

Webster, B. M., Thaller, D. J., Jäger, J., Ochmann, S. E., Borah, S., & Lusk, C. P. (2016). Chm7 and Heh1 collaborate to link nuclear pore complex quality control with nuclear envelope sealing. *Embo j, 35*(22), 2447-2467. doi:10.15252/embj.201694574

Wen, X., Tan, W., Westergard, T., Krishnamurthy, K., Markandaiah, S. S., Shi, Y., Lin, S., Shneider, N. A., Monaghan, J., Pandey, U. B., Pasinelli, P., Ichida, J. K., & Trotti, D. (2014). Antisense proline-arginine RAN dipeptides linked to C9ORF72-ALS/FTD form toxic nuclear aggregates that initiate in vitro and in vivo neuronal death. *Neuron, 84*(6), 1213-1225. doi:10.1016/j.neuron.2014.12.010

Westergard, T., Jensen, B. K., Wen, X., Cai, J., Kropf, E., Iacovitti, L., Pasinelli, P., & Trotti, D. (2016). Cell-to-Cell Transmission of Dipeptide Repeat Proteins Linked to C9orf72-ALS/FTD. *Cell Rep, 17*(3), 645-652. doi:10.1016/j.celrep.2016.09.032

Wingo, T. S., Cutler, D. J., Yarab, N., Kelly, C. M., & Glass, J. D. (2011). The heritability of amyotrophic lateral sclerosis in a clinically ascertained United States research registry. *PLoS One, 6*(11), e27985. doi:10.1371/journal.pone.0027985

Winton, M. J., Igaz, L. M., Wong, M. M., Kwong, L. K., Trojanowski, J. Q., & Lee, V. M. Y. (2008). Disturbance of Nuclear and Cytoplasmic TAR DNA-binding Protein (TDP-43) Induces Disease-like Redistribution, Sequestration, and Aggregate Formation *journal of Biological chemistry, 283*(19), 13302-13309. doi:10.1074/jbc.M800342200

Witzel, S., Maier, A., Steinbach, R., Grosskreutz, J., Koch, J. C., Sarikidi, A., Petri, S., Günther, R., Wolf, J., Hermann, A., Prudlo, J., Cordts, I., Lingor, P., Löscher, W. N., Kohl, Z., Hagenacker, T., Ruckes, C., Koch, B., Spittel, S., Günther, K., Michels, S., Dorst, J., Meyer, T., & Ludolph, A. C. (2022). Safety and Effectiveness of Long-

term Intravenous Administration of Edaravone for Treatment of Patients With Amyotrophic Lateral Sclerosis. *JAMA Neurol, 79*(2), 121-130. doi:10.1001/jamaneurol.2021.4893

Xiao, S., MacNair, L., McGoldrick, P., McKeever, P. M., McLean, J. R., Zhang, M., Keith, J., Zinman, L., Rogaeva, E., & Robertson, J. (2015). Isoform-specific antibodies reveal distinct subcellular localizations of C9orf72 in amyotrophic lateral sclerosis. *Ann Neurol, 78*(4), 568-583. doi:10.1002/ana.24469

Xu, Z., F, P. M., Li, X., Li, Y., Shu, L., Nelson, D. L., Li, H., Hales, C. M., Gearing, M., Wingo, T. S., & Jin, P. (2013). Expanded GGGGCC repeat RNA associated with amyotrophic lateral sclerosis and frontotemporal dementia causes neurodegeneration. *Proc Natl Acad Sci U S A*(1091-6490 (Electronic)).

Yamakawa, M., Ito, D., Honda, T., Kubo, K.-i., Noda, M., Nakajima, K., & Suzuki, N. (2014). Characterization of the dipeptide repeat protein in the molecular pathogenesis of c9FTD/ALS. *Hum Mol Genet, 24*(6), 1630-1645. doi:10.1093/hmg/ddu576 %J Human Molecular Genetics

Yoshino, H., & Kimura, A. (2006). Investigation of the therapeutic effects of edaravone, a free radical scavenger, on amyotrophic lateral sclerosis (Phase II study). *Amyotrophic Lateral Sclerosis, 7*(4), 247-251. doi:10.1080/17482960600881870

Zhang, K., Daigle, J. G., Cunningham, K. M., Coyne, A. N., Ruan, K., Grima, J. C., Bowen, K. E., Wadhwa, H., Yang, P., Rigo, F., Taylor, J. P., Gitler, A. D., Rothstein, J. D., & Lloyd, T. E. (2018). Stress Granule Assembly Disrupts Nucleocytoplasmic Transport. *Cell, 173*(4), 958-971 e917. doi:10.1016/j.cell.2018.03.025

Zhang, K., Donnelly, C. J., Haeusler, A. R., Grima, J. C., Machamer, J. B., Steinwald, P., Daley, E. L., Miller, S. J., Cunningham, K. M., Vidensky, S., Gupta, S., Thomas, M. A., Hong, I., Chiu, S. L., Huganir, R. L., Ostrow, L. W., Matunis, M. J., Wang, J., Sattler, R., Lloyd, T. E., & Rothstein, J. D. (2015). The C9orf72 repeat expansion disrupts nucleocytoplasmic transport. *Nature, 525*(7567), 56-61. doi:10.1038/nature14973

Zhang, P., Fan, B., Yang, P., Temirov, J., Messing, J., Kim, H. J., & Taylor, J. P. (2019). Chronic optogenetic induction of stress granules is cytotoxic and reveals the evolution of ALS-FTD pathology. *Elife, 8*. doi:10.7554/eLife.39578

Zhang, S., Cooper-Knock, J., Weimer, A. K., Shi, M., Moll, T., Marshall, J. N. G., Harvey, C., Nezhad, H. G., Franklin, J., Souza, C. D. S., Ning, K., Wang, C., Li, J., Dilliott, A. A., Farhan, S., Elhaik, E., Pasniceanu, I., Livesey, M. R., Eitan, C., Hornstein, E., Kenna, K. P., Project Min, E. A. L. S. S. C., Veldink, J. H., Ferraiuolo, L., Shaw, P. J., & Snyder, M. P. (2022). Genome-wide identification of the genetic basis of amyotrophic lateral sclerosis. *Neuron*. doi:10.1016/j.neuron.2021.12.019

Zhang, Y.-J., Jansen-West, K., Xu, Y.-F., Gendron, T. F., Bieniek, K. F., Lin, W.-L., Sasaguri, H., Caulfield, T., Hubbard, J., Daughrity, L., Chew, J., Belzil, V. V., Prudencio, M., Stankowski, J. N., Castanedes-Casey, M., Whitelaw, E., Ash, P. E. A., DeTure, M., Rademakers, R., Boylan, K. B., Dickson, D. W., & Petrucelli, L. (2014). Aggregation-prone c9FTD/ALS poly(GA) RAN-translated proteins cause neurotoxicity by inducing ER stress. *Acta Neuropathol, 128*(4), 505-524. doi:10.1007/s00401-014-1336-5

Zhang, Y. J., Gendron, T. F., Grima, J. C., Sasaguri, H., Jansen-West, K., Xu, Y. F., Katzman, R. B., Gass, J., Murray, M. E., Shinohara, M., Lin, W. L., Garrett, A., Stankowski, J. N., Daughrity, L., Tong, J., Perkerson, E. A., Yue, M., Chew, J., Castanedes-Casey, M., Kurti, A., Wang, Z. S., Liesinger, A. M., Baker, J. D., Jiang, J., Lagier-Tourenne, C., Edbauer, D., Cleveland, D. W., Rademakers, R., Boylan, K. B., Bu, G., Link, C. D., Dickey, C. A., Rothstein, J. D., Dickson, D. W., Fryer, J. D., & Petrucelli, L. (2016). C9ORF72 poly(GA) aggregates sequester and impair HR23 and nucleocytoplasmic transport proteins. *Nat Neurosci, 19*(5), 668-677. doi:10.1038/nn.4272

Zhang, Y. J., Jansen-West, K., Xu, Y. F., Gendron, T. F., Bieniek, K. F., Lin, W. L., Sasaguri, H., Caulfield, T., Hubbard, J., Daughrity, L., Chew, J., Belzil, V. V., Prudencio, M., Stankowski, J. N., Castanedes-Casey, M., Whitelaw, E., Ash, P. E., DeTure, M., Rademakers, R., Boylan, K. B., Dickson, D. W., & Petrucelli, L. (2014). Aggregation-prone c9FTD/ALS poly(GA) RAN-translated proteins cause neurotoxicity by inducing ER stress. *Acta Neuropathol, 128*(4), 505-524. doi:10.1007/s00401-014-1336-5

Zhou, Q., Mareljic, N., Michaelsen, M., Parhizkar, S., Heindl, S., Nuscher, B., Farny, D., Czuppa, M., Schludi, C., Graf, A., Krebs, S., Blum, H., Feederle, R., Roth, S., Haass, C., Arzberger, T., Liesz, A., & Edbauer, D. (2020). Active poly-GA vaccination prevents microglia activation and motor deficits in a C9orf72 mouse model. *EMBO Mol Med, 12*(2), e10919. doi:10.15252/emmm.201910919

Zu, T., Gibbens, B., Doty, N. S., Gomes-Pereira, M., Huguet, A., Stone, M. D., Margolis, J., Peterson, M., Markowski, T. W., Ingram, M. A., Nan, Z., Forster, C., Low, W. C., Schoser, B., Somia, N. V., Clark, H. B., Schmechel, S., Bitterman, P. B., Gourdon, G., Swanson, M. S., Moseley, M., & Ranum, L. P. (2011). Non-ATG-initiated translation directed by microsatellite expansions. *Proc Natl Acad Sci U S A, 108*(1), 260-265. doi:10.1073/pnas.1013343108

Zu, T., Liu, Y., Banez-Coronel, M., Reid, T., Pletnikova, O., Lewis, J., Miller, T. M., Harms, M. B., Falchook, A. E., Subramony, S. H., Ostrow, L. W., Rothstein, J. D., Troncoso, J. C., & Ranum, L. P. (2013). RAN proteins and RNA foci from antisense transcripts in C9ORF72 ALS and frontotemporal dementia. *Proc Natl Acad Sci U S A, 110*(51), E4968-4977. doi:10.1073/pnas.1315438110

10. Annex: Draft submission to Scientific Reports

The C9orf72-derived dipeptide repeat protein poly-GA sequesters nucleoporins

Karl E.G. Richter ORCID 0000-0001-8470-3157, Maryse Romao 0000-0002-9123-2442, Brian Grabiner, Mark W. Kankel 0000-0001-7837-8044, Yuanzheng Gu 0000-0003-1493-1167, Graça Raposo 0000-0001-9590-1298, Sophie Parmentier Batteur

Abbreviations

ALS…….Amyotrophic lateral sclerosis
BAC……Bacterial artificial chromosome
C9orf72..HGNC approved gene symbol for "Chromosome 9, open reading frame 72"
C9 ALS/FTD……C9orf72-linked amyotrophic lateral sclerosis/frontotemporal dementia
CNS……Central nervous system
CSF…….Cerebrospinal fluid
DIV ……Days in vitro
DPR……Dipeptide repeat protein
ER……..Endoplasmic reticulum
fALS……Familial ALS
GA……..Glycine–alanine
GR……..Glycine–arginine
GP……..Glycine–proline
IF……..Immunofluorescence
IPS……Induced pluripotent stem
Nups.....Nucleoporins
PBS……..Phosphate buffered saline
PLA……..Proximity ligation assay
PA……..Proline–alanine
PR……..Proline–arginine
sALS……Sporadic ALS
SOD1…….Superoxide dismutase 1
SQSTM1..Sequestosome 1, also known as P62
STED……Stimulated-emission depletion (microscopy)
TBS……..Tris-buffered saline
TDP-43…..Transactive response DNA-binding protein 43

Introduction

A hexanucleotide repeat expansion in the gene C9orf72 is the most common cause of familial amyotrophic lateral sclerosis (ALS)/motor neuron disease (MND) and the cause of a spectrum of disease that includes symptoms of ALS and frontotemporal dementia[1,2]. The (G4C2) repeat lies in an intron between exon 1A and 1B and causes a reduction in canonical C9 protein expression, the accumulation of RNA foci transcribed from the repeat region, and the repeat-associated non-ATG (RAN) translation of five different dipeptide repeat proteins GA, GP, and GR (in the sense direction) and PA, PR, and GP (in the antisense direction)[3,4]. Any one or a combination of these consequences may be responsible for the disease.

In mice, expressing poly-GA, but not PR, produces an ALS-like syndrome that includes selective neuron loss in hippocampus, cortex, and spinal cord; denervation of muscle; and inflammation [5]. Expression in

mice of the entire C9 gene containing the full-length C9orf72 gene and substantial flanking sequences driven by endogenous human promoters causes the production of both sense and antisense transcripts and all 5 dipeptide repeat proteins [6]. These mice develop a phenotype that includes neurodegeneration in cortex and hippocampus, progressive loss of motor neurons resulting in motor deficits, TDP-43 inclusions in degenerating CNS regions, paralysis, and shortened lifespan [6]. In patient tissue, the most abundant of the five DPR is poly-GA [7]. An antibody against poly-GA, when administered systemically, enters the brain of the BAC transgenic mice and reduces poly-GA, GP, and GR proteins, improves behavioral deficits, decreases neuroinflammation and neurodegeneration, and increases survival [8] even without direct targeting of RNA foci. Therefore, we explored the localization and function of poly-GA in a model cellular system and in patient-derived ips motor neurons.

Results

Poly-GA accumulates in aggresomes in HEK cells

In order to study the processing of poly-GA in a cellular context, we created a cell line that produced poly-GA dipeptide repeat protein using a tet-sensitive promoter with a sequence lacking G4C2 content, precluding the possibility of G4C2-containing RNA foci. When treated with doxycycline, these cells rapidly produced poly-GA that accumulated in the cytoplasm and the nucleus of the HEK cells, without causing overt cell death (figure 1a). Aggregated poly-GA protein in the cell was highly colocalized with spots immunoreactive for SQSTM (figure1b). Vimentin and gamma-tubulin were often found close to poly-GA aggregates near the nucleus. In some instances, a single poly-GA accumulation appeared in both the nucleus and adjacent cytoplasm (figure 1c). Conventional and immuno-EM confirmed that poly-GA was found largely in aggregates that were not membrane-bound (figure 1d,e). All of these properties are characteristic of aggresomes[9].

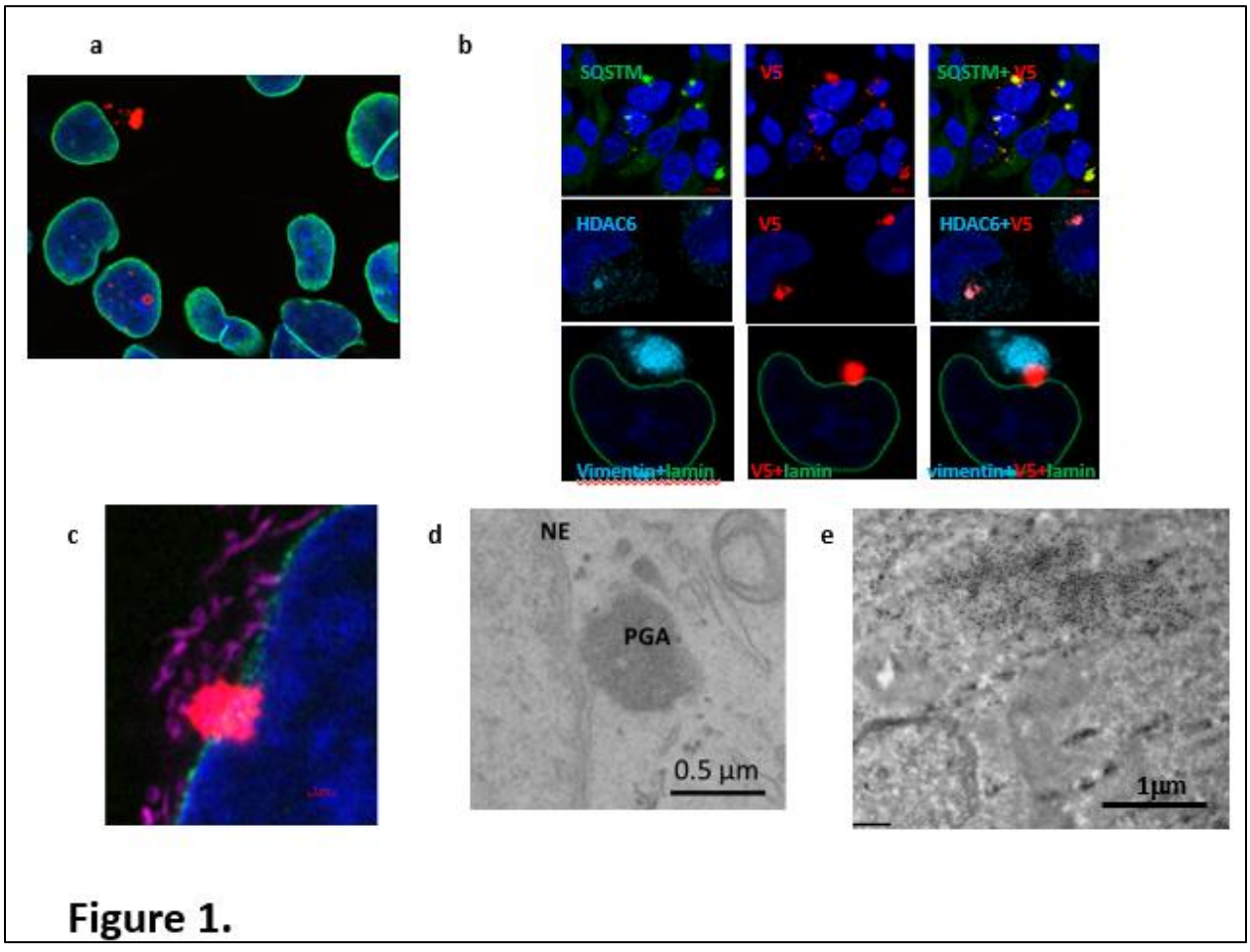

Figure 1.

Poly-GA is expressed in C9-patient-derived, but not control, ips motor neurons

In a line of ips cells from a C9ALS patient donor, poly-GA was expressed to a variable degree among neurons (figure 2a), but not in neurons from a healthy donor. A sandwich ELISA that detects poly-GA dipeptide repeat proteins[8] was used to determine apparent concentration of poly-GA in cultures of HEK and human motor neurons derived from a C9orf72 ALS patient (figure 2b).

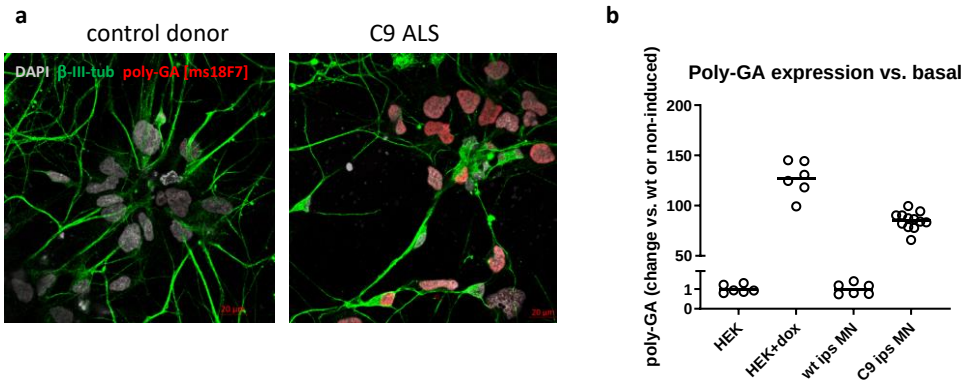

Figure 2. C9 ALS patient-derived motor neurons and HEK-GA161 express poly-GA.
a) Healthy- (left) and C9 ALS (right) patient-derived immunostained for poly-GA.
b) RIPA-soluble lysates of HEK (left) or ips motor neurons (right) contain 127 (HEK) or 85 (ips MN) fold background concentrations of poly-GA.

Poly-GA colocalizes with nucleoporins

By immunofluorescence and standard confocal microscopy, we found poly-GA aggregates colocalized with nuclear pore proteins (figure 3a). Because oxidative and other types of stress can cause the formation of stress granules, which are also known to accumulate nuclear pore proteins[10], we examined the cells for markers of stress granules to determine if the poly-GA accumulations were incorporated into such granules. Stress granules were not detected under basal conditions, but with exposure to sodium arsenite (500 µM 1 hr), we found G3BP-positive puncta in the ips motor neurons (figure 3b). Only a portion were colocalized with poly-GA aggregates (figure 3b). Higher resolution microscopy using STED confirmed colocalization of nucleoporins and poly-GA within its limit of resolution (~ 50 nm) (figure 4a) and identified apparent ectopic expression of Nup153 outside the nuclear envelope (figure 4b). Not all nucleoporins tested colocalized with poly-GA. For example, nucleoporin TPR did not (figure 4c). To confirm nucleoporin colocalization with poly-GA using a different method, we performed a proximity ligation assay using antibodies to poly-GA and to nucleoporin 98 (figure 5).

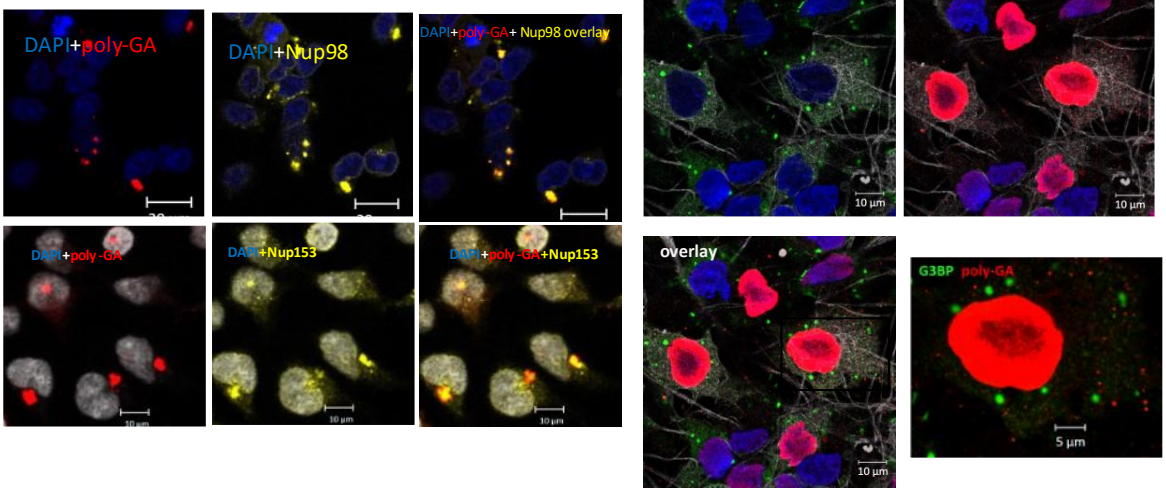

Figure 3.

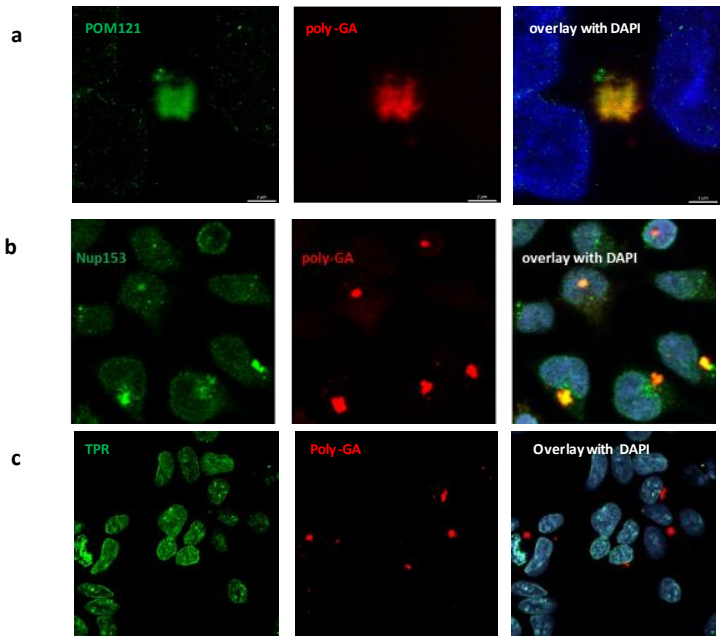

Figure 4.

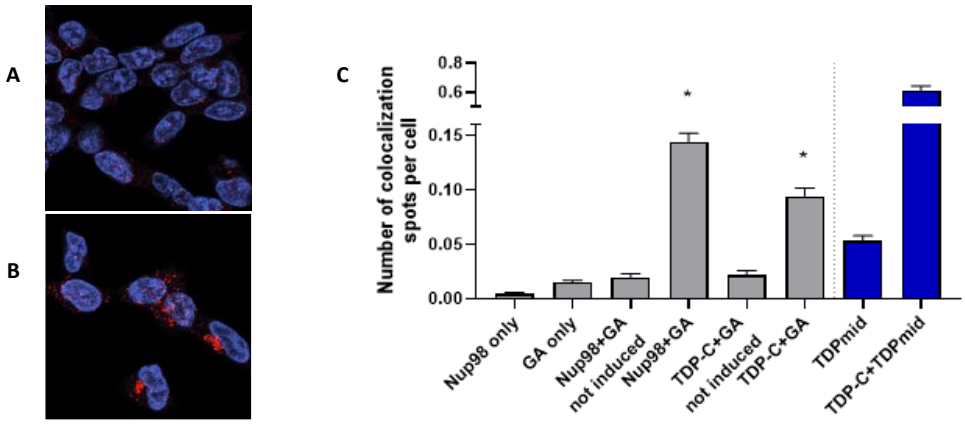

Figure 5. Proximity ligation assay detects colocalization between Nup98 and poly-GA
Proximity ligation assay produced fluorescent spots representing one or more instance of colocalization between the targets of two antibodies. **A)** Nup98 and poly-GA, not induced **B)** Nup98 and poly-GA in induced cells **C)** Quantification of PLA images. Nup98 and poly -GA colocalization signal and TDP-43 C-term and poly-GA colocalization signal were significantly greater than the highest control (both antibodies in non-induced cells), ANOVA F= 240.8 followed byŠídák's multiple comparisons test, p<0.0001 (Nup98+poly-GA vs. not induced) and p=0.0004 (TDP+poly-GA vs. not induced). Antibodies directed against two epitopes of TDP43 served as a positive control.

Poly-GA expression increases extranuclear nucleoporins in HEK-GA161

Nuclear pore proteins are typically mainly restricted to the nuclear pore complex and present in fixed ratios. We quantified the number of immunostained nucleoporin puncta found outside the nucleus. Although the number of extranuclear nucleoporin spots was not different in the parental HEK cell line and non-induced HEK with the expression cassette, induced HEK-GA161 cells expressing poly-GA had increased numbers of POM121 and Nup153 spots in the cytoplasm (figure 6).

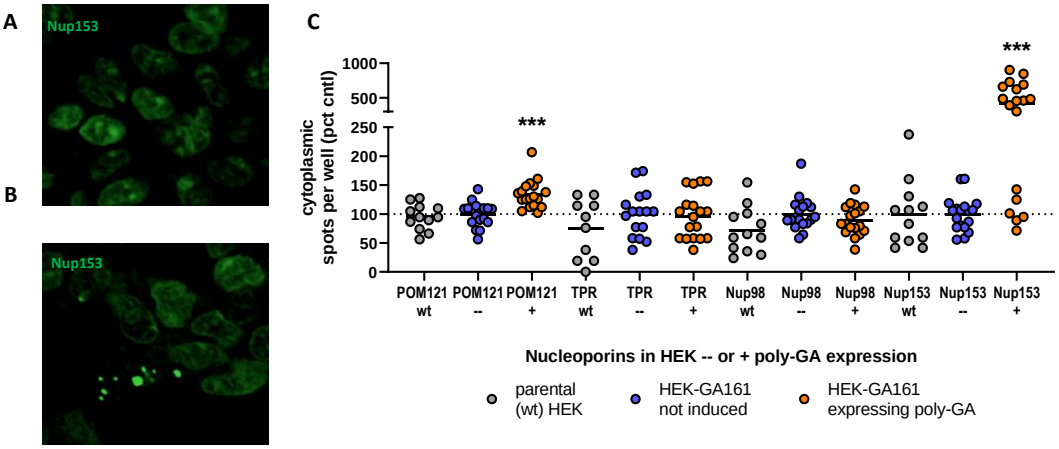

Figure 6. Expression of poly-GA causes appearance of extranuclear nucleoporins. A) Nup153 in HEK-GA161 non-induced **B)** HEK-GA161 induced **C)** Cells induced to express poly-GA had a greater number of extranuclear spots of nucleoporins POM121 (ANOVA F=14.24 followed by Tukey's, p<0.0001) and Nup153 (ANOVA F=19.68 followed by Tukey's, p<0.0001)

Poly-GA protein expression is modulated by Nup153

Because Nup153 was found both to be coaggregated with and redistributed by poly-GA, we wished to explore further the relationship between this nucleoporin and poly-GA expression. Increasing or decreasing nucleoporin expression has been found to modulate both G4C2 toxicity and dipeptide repeat protein toxicity in fly screens (Freibaum et al., 2015). Knockdown of Nup153 specifically was found to potentiate G4C2x58 RNA toxicity (Freibaum et al., 2015), although no poly-GA was reported in that model. After induction, we transfected HEK-GA161 cells with siRNA against Nup153 (OriGene) or a control si against a scrambled nucleotide sequence and measured gene expression and poly-GA 48 hrs later (figure 7). The si treatment reduced expression of Nup 153 mRNA by 75%, without changing expression of the poly-GA message (figure 7). The loss of Nup153, however, reduced the poly-GA accumulation in the cells by 40% (figure 7).

	mRNA (percent control)		
	XPO1	poly-GA	Nup153
control siRNA	100.3%	100.6%	100.5%
Nup153 siRNA A	118.7%	124.0%	25.8%
Nup153 siRNA C	108.5%	132.7%	23.5%

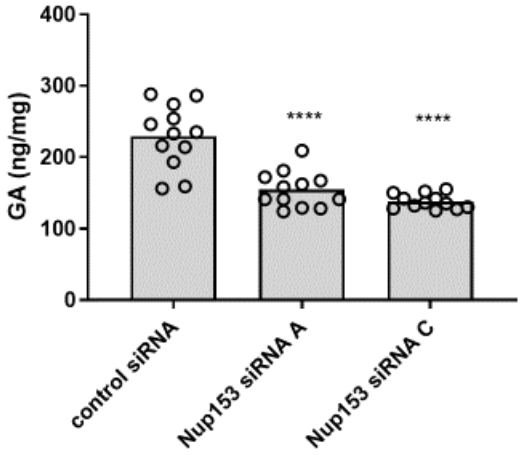

Figure 7. Nup153 knockdown reduces poly-GA
Treatment of HEK-GA161 with an siRNA against Nup153 successfully reduced Nup153 message to 26% or 24% of control, did not decrease XPO1 or poly-GA (transgene) message, but reduced poly-GA protein to 67% (siRNA-A) or 60% (siRNA-C) of control. ANOVA F=31.67 followed by Tukey's test for multiple comparisons, p<0.0001

Nup153 and POM121 expression are correlated with poly-GA expression in C9-derived ips motor neurons

Like the HEK-GA161 cells, the ips motor neurons derived from a C9 expansion carrier did not show obvious toxicity under basal conditions. Unlike the HEK-GA161 cells, poly-GA did not accumulate in aggresome-like deposits within or outside the nucleus. Instead, poly-GA was primarily found within the nucleus (figures 2, 3b). Because nucleoporins POM121 and Nup153 were mislocalized in HEK during poly-GA expression, we examined these nucleoporins in the motor neuron culture. Nuclear Nup153 was not different between the two lines, and POM121 was only slightly decreased in the C9 cells (figure 8A). However, poly-GA is very heterogeneously expressed among the cells, so the results were analyzed on a cell-by-cell basis for a random sample of wells. Both POM121 and Nup153 abundance were increased in cells

expressing more poly-GA (r-squared values of 0.686 (POM121) and 0.726 (Nup153), figure 8B). When non-poly-GA+ cells (<2000 fluorescence units in nucleus) are omitted from the analysis, the correlation is even stronger (0.809 for POM121; 0.781 for Nup153). By contrast, neurons from healthy donor cultures did not show a strong correlation between background GA-like fluorescence, suggesting that the correlation is not an artifact.

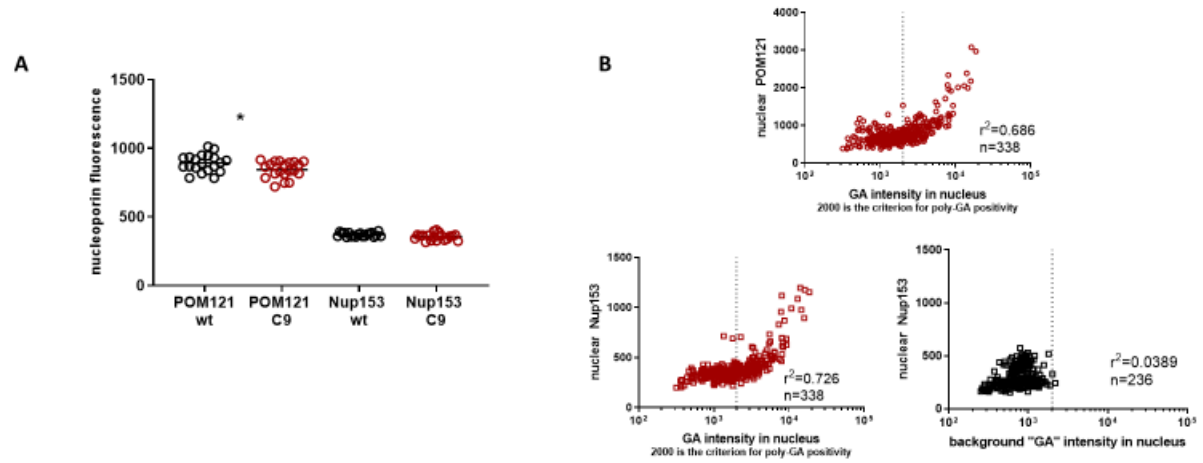

Figure 8. POM121 and Nup153 are positively correlated with poly-GA in C9-derived ips motor neurons.

A) POM121 is slightly decreased overall in the nucleus of C9 as compared with healthy donor cells and Nup153 is unchanged. One point=mean of one well. ANOVA F=816, Šídák's multiple comparisons test: (POM121) p=0.0032 (Nup153) p>0.05 **B)** Cells expressing more poly-GA also express more POM121 and Nup153, r-squared values 0.686 (POM121) and 0.726 (Nup153), in contrast to healthy donor cells, where the background fluorescence in the poly-GA channel is poorly correlated with nucleoporin expression. One point=one cell.

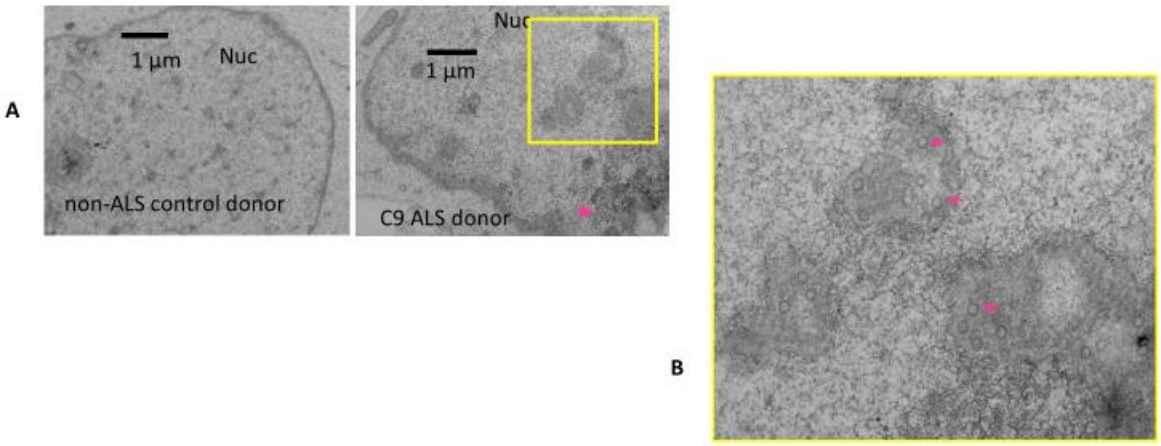

Figure 9. C9 ALS patient-derived motor neurons have disrupted nuclear membranes.
Conventional EM of ips motor neurons (30 DIV) reveals altered nuclear membrane morphology. **A)** Example of typical nuclei in cross section in healthy- vs. patient-derived ips neurons. Note atypical density and loss of membrane integrity (arrowhead). **B)** Enlarged area from A. Larger whorls suggest an indentation in the nuclear membrane in the z-dimension. Small, circular, membrane-enclosed structures suggest nuclear pores viewed in cross section (arrows).

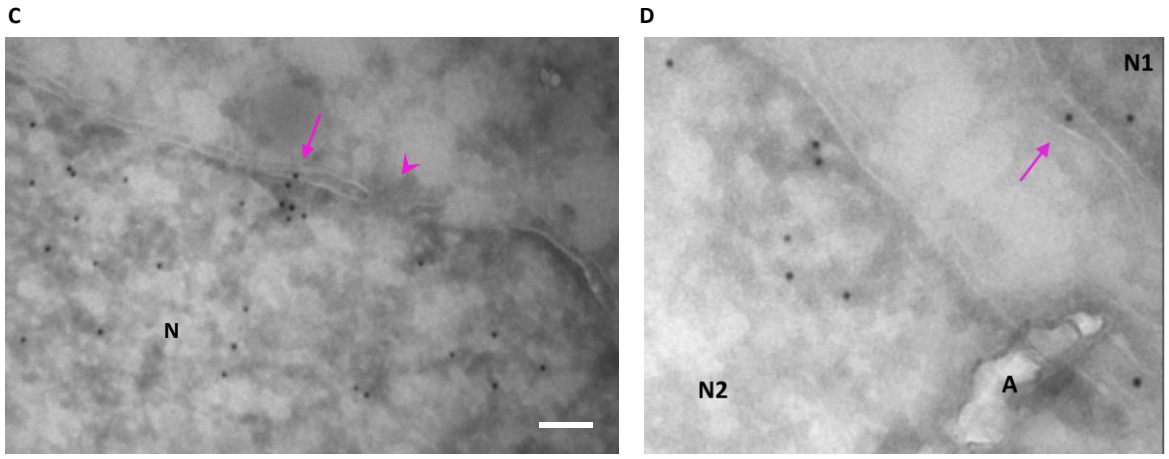

Figure 9 C, D. Poly-GA is deposited in nuclear membrane of C9 ALS patient-derived motor neurons. Immuno-EM of ips motor neurons (30 DIV) reveals poly-GA within the nuclear envelope. **C)** Arrow indicates gold-labeled αGA4 (arrow) between inner and outer nuclear membrane near a nuclear pore (arrowhead) N=nucleus. **D)** Arrow indicates example of poly-GA labeling in the nuclear envelope of nucleus (N1). N2=nucleus of another cell, A=artifact in sample.

C9-derived ips neurons have disrupted nuclear membranes

We detected poly-GA within the nucleus of the C9 patient-derived motor neurons. Therefore, we searched for possible structural consequences of this expression. By conventional EM, we found aberrant nuclear membranes in C9, but not healthy donor-derived motor neurons (figure 9A,B). In addition to disorganized nuclear membranes, we found small, circular structures resembling published images of nuclear pores from cells overexpressing Nup153[11].

Poly-GA can be found within the nuclear envelope

Nuclear membrane disruption in the C9 patient-derived motor neurons could be due to any consequences of the C9 hexanucleotide repeat expansion, not necessarily a dipeptide repeat protein. Immuno-EM confirmed that poly-GA was found within the nuclear envelope (figure 9C), thus providing evidence for one possible explanation of nuclear membrane disruption.

C9-derived ips motor neurons show increased vulnerability to puromycin

We used the protein translation inhibitor, puromycin, as a toxic insult to the ips-derived motor neurons. Puromycin has been reported to activate a set of genes similar to those upregulated in the cortex of C9 ALS-FTD patients[12]. After treatment with puromycin, 7 μM 48 hrs, cells were stained with Calcein AM/ethidium homodimer to label both live and dead cells, a sensitive measure of cell death that avoids artifacts from washing away dead cells during fixation. Puromycin killed 18.8% of the cells in the healthy donor cultures and 56.8% in the C9 ALS patient-derived cells (figure 10a).

Treating C9-derived ips motor neurons with antibody reduces poly-GA but does not protect against puromycin

Because scavenging of poly-GA with an antibody provided neuroprotection in mice expressing a repeat expansion in C9orf72 [8], the possible protective effect in the C9-patient-derived ips motor neuron culture was investigated. We treated motor neurons for 12 days beginning at DIV 30 with antibodies added every two days, using human aGA1 from Nguyen et al. and isotype control antibodies. We evaluated the number of dead cells as a percent of total and the poly-GA content of the cells in the same wells. The aGA1 treatment led to a reduction in poly-GA, whereas the isotype control antibodies did not (figure 10b). The highest concentration of aGA1, 120 nM, reduced the amount of poly-GA by 26% ($\pm$8.56%). Nevertheless, the antibody treatment did not protect the cells as measured by percent cell death (figure 10c). Similarly, the average intensity of staining for cleaved caspase, a marker of activation of apoptosis, was also unchanged by antibody treatment (10d).

Thus, we conclude that removing at least 24% of poly-GA from the C9 ALS patient-derived motor neuron cultures does not provide protection against puromycin insult.

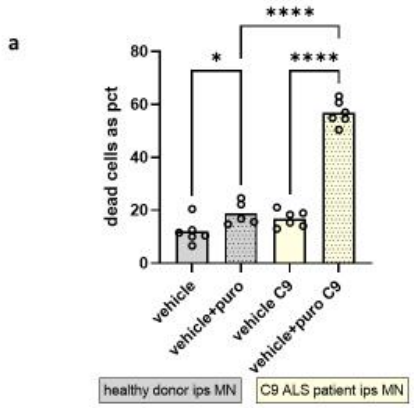

Figure 10a. Patient-derived ips motor neurons are more sensitive than control neurons to puromycin.
a) Treatment with puromycin, 7 μM, 48 hrs, killed 18.8 (±4.4)% of healthy but 56.8% (±4.6) of C9 ALS patient-derived motor neurons (ANOVA, F=143.2, followed by Šídák's multiple comparisons test, *healthy vehicle vs healthy vehicle+puromycin, p=0.0434; **** C9 vehicle vs C9 vehicle+puromycin, p<0.0001; **** healthy vehicle+puromycin vs C9 vehicle+puromycin, p<0.0001).

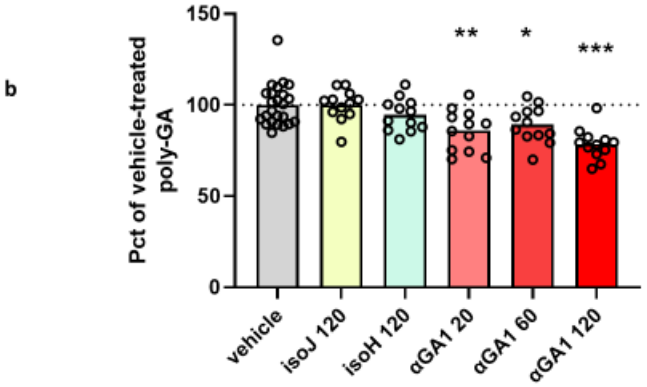

Figure 10b. αGA1 reduces poly-GA in C9-patient-derived ips motor neurons
Motor neurons were treated for 12 days beginning at DIV 30 with antibodies αGA1 and isotype control added every two days. The 120 nM αGA1 treatment reduced poly-GA by 26% (±8.56%) vs. vehicle (ANOVA, F=6.950, followed by Šídák's multiple comparisons test, **20 nM p=0.0013, *60 nM p=0.0238, ***120 nM p<0.0001)

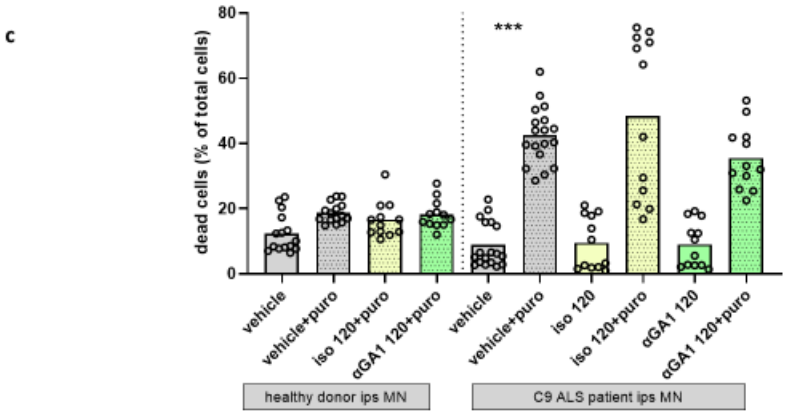

Figure 10c. αGA1 does not protect C9 ALS patient-derived motor neurons from puromycin The same motor neurons as in panel B were treated for 12 days beginning at DIV 30 with antibodies αGA1 and isotype control added every two days. Puromycin increased the number of dead C9 cells from 8.8 ±6.8% to 42.4 ±8.8% of total cells per well. Nonparametric analysis was used because of the substantial scatter in the data. (Krukal-Wallis statistic=51.2 followed by Dunn's multiple comparisons test, vehicle vs. vehicle+puro p<0.001; vehicle+puro vs. iso 120+puro p>0.999; vehicle+puro vs. αGA1 120+puro p>0.999; iso 120+puro vs. αGA1 120+puro p>0.999

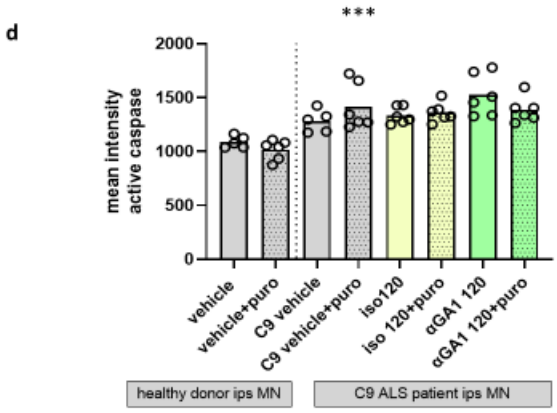

Figure 10d. αGA1 does not protect C9 ALS patient-derived motor neurons from puromycin Motor neurons were treated for 12 days beginning at DIV 30 with antibodies αGA1 and isotype control added every two days. Cleaved caspase staining was greater in the C9 than in healthy control donor neurons treated with puromycin, but none of the antibody treatments was different from C9 vehicle + puromycin. (ANOVA, F=9.570, ***vehicle+puro vs. C9 vehicle+puro, p<0.0001; C9 vehicle+puro vs. iso 120+puro p=0.9657; C9 vehicle+puro vs. αGA1 120+puro p=0.9978; iso 120+puro vs. αGA1 120+puro p=0.9991)

Discussion

In C9 patient-derived motor neurons and HEK cells, we detected a close association between poly-GA and the nuclear membrane and the appearance of disrupted nuclear membranes. In

the case of HEK, the poly-GA aggregated into SQSTM1/P62-positive, aggresome-like bodies. We confirmed colocalization of poly-GA, TDP-43 C-terminal, and nucleoporins with PLA. We identified mislocalized nucleoporins aggregated with poly-GA, including POM121, which has been identified as the earliest nucleoporin lost in C9 ips-derived motor neurons[13]. In C9 ips-derived motor neurons, we showed that the colocalizations were not due purely to stress granule formation. We detected at the ultrastructural level apparently disrupted nuclear membranes and possibly ectopic nuclear pores. Treating the motor neuron cultures with αGA1 reduced the poly-GA content of the cells but did not protect against a challenge of protein synthesis inhibition.

Although the ips-derived motor neurons model more closely than HEK the tissues of the human nervous system, they remain immature neurons, unlike the aged neurons of the aging adult human. It is possible that the HEK system, with its rapid accumulation of poly-GA into SQSTM-positive aggregates, may represent a rapid route to the type of SQSTM1-positive inclusions seen in patient tissue at autopsy.[14] It is also possible that the C9-derived ips motor neuron cultures represent a stage similar to a disease prodromal state in human, with DPR accumulating in or near the nuclear membrane, but not yet aggregated. We identified sequestration of nuclear pore proteins by poly-GA. Sequestration of Nups has been reported by others[15] [16] , but not in the context of poly-GA only expression. In vivo, Y. J. Zhang et al. [16] identified POM121 in accumulations of poly-GA in the brains of poly-GA50-expressing mice. We extended that by finding that poly-GA expression resulted in ectopic accumulation of POM121, Nup153 and TDP-43.

Parallels with disease pathology

The sequestration of nuclear pore proteins in cellular assays may provide insight into the situation in patients. Nuclear pore changes have been detected in patient tissue. For example, (Coyne et al., 2020) found a loss of POM121 in C9orf72 patient motor cortex, both in isolated nuclei extracted from cortex and in paraffin-embedded thin sections of motor cortex. After the loss of POM121, they detected the loss of an additional cohort of six nucleoporins, including TPR and Nup50. They did not, however, see such a change with Nup153. (Shang et al., 2017) found cytoplasmic upregulation of RanGAP1, GP210 and NUP50 in sALS lumbar motor neurons, and colocalization of Nup205 and TDP-43.

Nuclear membrane structure

At the microstructure level, several groups have reported apparently malformed nuclear membranes in neurons in patient tissue. Kinoshita et al. found irregular nuclear membranes in anterior horn cells of sALS patients but not control cases[17]. Distorted nuclear membranes have been reported in Alzheimer's disease[18] where they were associated with PIN1 dysfunction. Distorted nuclear membranes and cytoplasmic mislocalization of FG Nups was also reported in Alzheimer's disease by (Eftekharzadeh et al., 2018), where Nup98 was found with tau protein. The presence of nuclear membrane pathology in ips-derived neurons remains controversial.

(Paonessa et al., 2019) reported misfolded membranes in tau-associated FTD and ips neurons. (J. Chew et al., 2019) found increased nuclear membrane distortion in (G4C2)-149 mice, but others have not seen membrane changes in ips neurons specific to ALS[19], but rather to aging in general.

Poly-GA persistence

The endogenous clearance mechanism(s), if they exist, have not been determined for DPR. (Nguyen et al., 2020) also found no change in poly-GA in their HEK cell system when treated with autophagy blocker 3-MA or protease inhibitor MG-132. On the other hand, (Guo et al., 2018), found engagement with the proteasome by poly-GA; resulting in stalling of the proteasome, and (Yamakawa et al., 2014) found poly-GA inhibited its activity. In the HEK cells, the aggregated poly-GA is accumulated into aggresomes, but we did not observe its fate after such formation.

We observed poly-GA aggregates adjacent to the nuclear membrane, similar to those described by (Lee et al., 2017) in a similar context; and a striking interaction of the poly-GA aggregates with nucleoporins outside the nuclear membrane. The C-terminal region of TDP-43 has been found to interact with nucleoporins via their FG-rich regions (Chou et al., 2018), and a similar interaction may exist with poly-GA. The FG regions are important for the barrier-forming properties of the pore, but may also be responsible for pathological interactions with other hydrophobic proteins in disease. Several attempts to use poly-GA as a bait protein for co-immunoprecipitation experiments failed in our lab. However, very recently, the protein interactome of poly GA, GR and PR was investigated using a proximity labeling technique (F. Liu et al., 2022). They found the interactomes of GR and PR were quite similar, and both distinct from poly-GA. The arginine containing DPR were more associated with nuclear pore proteins, and poly-GA with proteasome components. Poly-GA did, however, associate with RANBP1 (F. Liu et al., 2022). Poly-GA has been found to sequester a variety of proteins, including HR23 (RAD23 homolog) (Y. J. Zhang et al., 2016), Unc-119 (May et al., 2014) and others. It has been reported to impair importin-α function (Khosravi et al., 2017), which may reduce TDP-43 import. Many of the same groups also find toxicity of poly-GA, but what properties are responsible for the toxicity in cell models and which may be relevant for motor neuron death are unclear.

Role of Nup153

Genetic screens have identified certain nucleoporins as regulators of either G4C2 or dpr toxicity. For example, (Freibaum et al., 2015), using a genetic screen in Drosophila expressing G4C2, identified knockdown of the following nucleoporins provided a protective effect against the neurodegeneration elicited by expression of the hexanucleotide repeats (human ortholog names): Nup107, Nup160, and Nup98. All three of these nucleoporins are pore-forming

members with FG sequences. Reduction of ALYREF, a protein coupling RNA transcription to export, also provided protection. Knockdown of Nup50, Nup153, or XPO1, on the other hand, enhanced the degeneration (Freibaum et al., 2015). Protective or pro-degenerative effects of Nups have been detected against both expression of the hexanucleotide repeat and against dpr production in the absence of potentially toxic G4C2 RNA. Nup50 and Nup153 are members of the nuclear basket and are essential for the binding and transit of mRNA to the cytosol. XPO1, however, is a transport chaperone for NES-containing proteins.

In the present work, we found knockdown of Nup153 reduced the amount of poly-GA found in the HEK-GA161. There was no effect on the mRNA (figure 7), which would have suggested an artifactual suppression of the transgene. Instead, without affecting message, poly-GA protein was diminished through an unknown mechanism. Although Nup153 plays a role in nuclear export, it is also essential for the reassembly of the nuclear pore complex after cell division (LaJoie et al., 2022). In the dividing HEK-GA161, knockdown of Nup153 for 48 hours may result in cells with incompletely assembled nuclear pores, reducing overall cell health and reducing the ability to express the large amount of poly-GA detected in the cells. In fact, recent experiments on nuclear pore function avoid the use of RNA knockdown to silence Nup153 for this reason (Li, Aksenova, et al., 2021).

It is also possible that reducing the amount of Nup153 leads to less poly-GA/nucleoporin aggregation, leaving more poly-GA in a non-aggregated state, and therefore more accessible to some form of degradation. Finally, it is known that overexpression of Nup153 alone causes Nup153 to accumulate at the inner nuclear membrane, rather than throughout the nucleus as occurs with other nuclear proteins including other nucleoporins (Bastos et al., 1996). The insertion into the membrane is driven by the amino-terminal portion of the protein, in contrast to the carboxy terminal which is critical to mRNA binding and translocation. In addition, the overexpression of Nup153 alone causes elongated nuclear membranes and the appearance of Nup153 in complex with lamins (Bastos et al., 1996). This results in ectopic nuclear pores (Bastos et al., 1996) seen by EM. Combining this information with our observation of a possible ectopic nuclear pores and the positive correlation between poly-GA and Nup153 in the ips-derived motor neurons suggests that poly-GA at the nuclear membrane may itself drive Nup153 expression, subsequently leading to formation of aberrant pores or pore-like structures. Biochemically assessing whether there is an induction of Nup153 or a redistribution of existing Nup153 will clarify whether there is indeed increased expression of the nucleoporin in the presence of poly-GA. Assessing this possible relationship is a promising area for additional research.

Effect of antibody treatment

We found an approximately 25% reduction in RIPA-extractable poly-GA after 12 days treatment with 120 nM of αGA1. This is very similar to the 31% reduction found by Nguyen et al. after 13 days of treatment with the same antibody in their ips motor neurons, although (Nguyen et al., 2020) did not show a protection against a neurotoxic insult in that system. It is

not clear why there was no protection in our model. It is possible that the poly-GA reduction was insufficient and that a higher antibody concentration or longer treatment time would provide some protection. There are alternative explanations, however. Puromycin halts protein synthesis by causing premature termination of the nascent polypeptide chain by acting as an analog of the 3'-terminal of the aminoacyl-tRNA. This produces many small, puromycylated polypeptides, which are usually targeted for degradation. One possibility is that the peptides overwhelm a proteolytic system already compromised by poly-GA. Another, similar, possibility is that the C9 genotype already means that the cells have a compromised system of protein degradation, making them more susceptible to puromycin independent of poly-GA. In fact, the partial haploinsufficiency of C9 and its role in autophagy make this a promising hypothesis.

In summary, both cell models provide information on the mechanisms by which the dipeptide repeat protein, poly-GA, disrupts cellular processes. This work confirms the effect of exogenously applied poly-GA antibody reducing poly-GA in cell culture, but does not capture the therapeutic effect suggested by the in vivo experiments in (Nguyen et al., 2020).

Methods

Generation of HEK cell line

HEK cells harboring lacZ-Zeocin fusion gene and tet repressor (Thermofisher Flp-In T-Rex) were transfected with the expression plasmid shown in the supplement including V5-tagged, codon optimized sequence encoding poly-GA161 after a CMV promoter. Clones were selected based on robust expression of the transgene with no detectable constitutive expression.

Maintenance of cultures

HEK cells were maintained at 37 °C with 5% CO_2 in Dulbecco's Modified Medium (ThermoFisher 11965-092) supplemented with 10% tet-approved fetal calf serum (Takara Bio 631106), glutaMax (ThermoFisher), antibiotic/antimycotic (Invitrogen 15240-062), Hygromycin B (GIBCO 10687010), and Blasticidin (GIBCO A11139-03). All HEK were used between passages 4 to 30.

iPSC-derived neuronal differentiation

LCLs from ALS-affected (ND09607E) or ALS-unaffected (ND70189) were obtained from Coriell, Inc. and reprogrammed using episomal reprogramming. iPSCs were cultured in mTesr1+ Media (Stem Cell Technologies 05826, 05827) on ESC-qualified Matrigel (Corning 354277), bulk passaged using ReLeSR (Stem Cell Technologies 05872) and grown until 80-90% confluency. iPSCs were treated with 0.5 mM EDTA (ThermoFisher 15575020), detached using a cell scraper and grown as embryoid body (EB) suspension for 14 days in the presence of small molecules as previously described in Maury et al. 2015 [20]. Briefly, EBs were grown in the presence of 5 uM Y-27632 (R and D Systems 1254-50MG) on differentiation day 1, 40 uM SB431542 (SIGMA 301836418) and 3 uM CHIR99021 (Tocris Biosciences 252197-06-9) on differentiation days 1-3, 0.2 uM LDN193189 (StemCell Technology 72142) on differentiation days 1-5, 1 uM Retinoic Acid (SIGMA R2625-50MG) and 0.5 uM Smoothened Agonist (Millipore 566660) on differentiation days 2-12, and 10 uM DAPT (SIGMA D5942- 25 mg) on differentiation days 8-14. At day 14, EBs were enzymatically dissociated with Papain/DNase (Worthington Biochemical LK003176, LK003170) and plated in Neurobasal medium (ThermoFisher 21103049) containing N2 supplement (ThermoFisher 17502048), B27

supplement (ThermoFisher 17504044), Knock-out serum (ThermoFisher 10828010), Y27632 (R and D Systems 1254/50), 10 ng/mL BDNF (Tocris 248-BDB-01M), 10 ng/mL GDNF (R and D Systems 212-GD-01M), 10 ng/mL CNTF (R and D Systems 257-NT-050), 10 uM DAPT (Sigma 208255805). 48 hours after plating, the medium was replaced iPSC-MN feed medium (Neurobasal medium containing N2 supplement, B27 supplement, 10 ng/mL BDNF, 10 ng/mL GDNF, 10 ng/mL CNTF). Media was replaced with 50% conditioned medium 1-2 times weekly.

Immunofluorescence

Cells were processed for immunofluorescence by washing in PBS followed by fixation with paraformaldehyde (4%)/sucrose (4%) in TBS for 15 min at room temperature, followed by permeabilization in 0.1% Triton X-100 in TBS. Cells were blocked in blocking buffer before adding antibodies diluted in blocking buffer. Blocking buffer consisted of 1% BSA (Sigma A6003) 5% goat serum (Abcam 7481) and 0.3M glycine in TBS. Secondary antibodies were anti-species-specific Ig as appropriate, coupled to AlexaFluor labels. Highly cross-adsorbed antibodies were used whenever possible.

Confocal imaging

Images were collected using either a Zeiss 710 or 980 laser scanning confocal microscope equipped with a Zeiss AxioCam 503 camera and processed with Zen software. In some instances, confocal images were acquired and processed using Zeiss' "Airyscan" hardware and software, an enhancement to ordinary confocal imaging.

High-content imaging

Cultures were imaged in 96-well Cell Carrier Ultra plates using Perkin-Elmer Opera Phenix system operating in confocal mode with a 40x NA 1.1 water-immersion objective. Fluorescence at adjacent wavelengths was collected sequentially.

STED imaging

STED images were collected using an Abberior STEDYCON device with a Zeiss Axio Observer Z1 microscope body equipped with a 100x oil-immersion objective. Images were processed using Abberior's proprietary software and ImageJ.

Proximity Ligation Assay (PLA)

Cells were processed as for immunofluorescence, followed by proximity ligation according to the manufacturer's instructions. Briefly, samples were incubated with PLA secondary antibody probes then treated with ligase at 37 degrees, followed by amplification for 100 minutes at 37 degrees before counterstaining with DAPI. Cells were imaged in a high-content imaging system for spot counting of fluorescent reaction product at Texas Red wavelengths. Images of PLA shown in this work are single z-planes.

Poly-GA ELISA

Poly-GA was measured in RIPA lysates of cells using a sandwich ELISA with Meso-Scale Discovery (MSD) electrochemiluminescent detection as described in [21]. Samples were treated with heat, SDS and reducing agent to denature any treatment antibody that might be present.

siRNA

Nucleoporin 153 was suppressed using Origene 27-mer oligonucleotide duplexes, catalog number SR322948. Duplexes were prepared in sterile buffer and mixed with Origene "siTran" transfection reagent before being added to cells at a final concentration of 2 nM. Culture medium was changed 5 hr after transfection.

Electron microscopy

For immunocytochemistry: Cell samples were fixed in a mixture of 2% PFA and 0.125% glutaraldehyde in a 0.1M phosphate buffer pH7.4 and processed for ultracryomicrotomy as described in [22]. Ultrathin cryosections were prepared with an ultracryomicrotome Ultracut FCS (Leica) and immunogold labeled with anti- Poly-GA or anti-TDP43 antibodies followed by protein A conjugated to 10 nm gold particles (Cell Microscopy Center, Department of Cell Biology, Utrecht University). Sections were analyzed on a Tecnai Spirit G2 electron microscope (FEI, Eindhoven, The Netherlands) and digital acquisitions were made with a 4k CCD camera (Quemesa, Olympus, Münster, Germany)

For conventional EM: Cell samples were fixed in 2.5% glutaraldehyde in a 0.1M cacodylate buffer, post fixed with 1% osmium tetroxide supplemented with 1.5% potassium ferrocyanide, dehydrated in in ethanol and embedded in Epon resin. Thin sectioned samples of 60-70nm were post stained with 4% aqueous uranyl acetate for 10 minutes and lead citrate for 1 minute as described [23].
Electron micrographs were acquired on a Tecnai Spirit G2 electron microscope (FEI, Eindhoven, The Netherlands) equipped with a 4k CCD camera (Quemesa, Olympus, Münster, Germany)

Antibodies used

Target protein	Clone	Vendor	Product #	Dilution	
CHMP7		Protein Tech	16424-1-AP	1:100	
COX-IV	3E11	Cell Signaling	4850	1:250	
cleaved Caspase-3		Cell Signaling	9661	1:400	
G3BP		Abcam	ab181149	1:200	
HDAC6		Cell Signaling	7558S	1:200	
Lamin A/C		Active Motif	39288	1:1000-1:250	
LC3B		Abcam	ab48394	1:5000	
b-III-tubulin		Abcam	ab107216	1:400	
Nup 153	QE5	Abcam	ab24700	1:200	
Nup 98	C39A3	Cell Signaling	2598S	1:500	
poly-GA	αGA1	Nguyen et al., 2020			
poly-GA	αGA3	Nguyen et al., 2020			
poly-GA	αGA4	Nguyen et al., 2020			
POM121		Protein Tech	15645-1-AP	1:400	
SQSTM		Abcam	ab109012	1 ug/mL	
TDP-43 (mid)		Abnova	H00023435	1:1000	
TDP-43 (C-term)		Protein Tech	12892	1:500	
TDP-43 (N-term)		Protein Tech	10782-2-AP	1:500	
TPR		Abcam	ab84516	1:200	
vimentin		Abcam	ab24525	1:1000	

Statistical analysis

Quantitative results were analyzed statistically with GraphPad Prism software using t-test or ANOVA when appropriate; nonparametric Kruskal-Wallis test when needed. Post hoc test used in most instances was Šídák's multiple comparisons test for selected group comparisons.

Acknowledgements

We acknowledge the PICT-IBiSA , Institut Curie, Paris, France, member of the France-BioImaging national research infrastructure. This work was supported by the French National Research Agency through the "Investments for the Future" program (France-BioImaging, ANR-10-INSB-04) and by the CelTisPhyBio Labex (N° ANR-10-LBX-0038) part of the IDEX PSL (N°ANR-10-IDEX-0001-02 PSL).

1 Renton, A. E. *et al.* A hexanucleotide repeat expansion in C9ORF72 is the cause of chromosome 9p21-linked ALS-FTD. *Neuron* **72**, 257-268, doi:10.1016/j.neuron.2011.09.010 (2011).

2 DeJesus-Hernandez, M. *et al.* Expanded GGGGCC hexanucleotide repeat in noncoding region of C9ORF72 causes chromosome 9p-linked FTD and ALS. *Neuron* **72**, 245-256, doi:10.1016/j.neuron.2011.09.011 (2011).

3 Ash, P. E. *et al.* Unconventional translation of C9ORF72 GGGGCC expansion generates insoluble polypeptides specific to c9FTD/ALS. *Neuron* **77**, 639-646, doi:10.1016/j.neuron.2013.02.004 (2013).

4 Zu, T. *et al.* RAN proteins and RNA foci from antisense transcripts in C9ORF72 ALS and frontotemporal dementia. *Proc Natl Acad Sci U S A* **110**, E4968-4977, doi:10.1073/pnas.1315438110 (2013).

5 LaClair, K. D. *et al.* Congenic expression of poly-GA but not poly-PR in mice triggers selective neuron loss and interferon responses found in C9orf72 ALS. *Acta neuropathologica* **140**, 121-142, doi:10.1007/s00401-020-02176-0 (2020).

6 Liu, Y. *et al.* C9orf72 BAC Mouse Model with Motor Deficits and Neurodegenerative Features of ALS/FTD. *Neuron* **90**, 521-534, doi:10.1016/j.neuron.2016.04.005 (2016).

7 Zhang, Y. J. *et al.* Aggregation-prone c9FTD/ALS poly(GA) RAN-translated proteins cause neurotoxicity by inducing ER stress. *Acta neuropathologica* **128**, 505-524, doi:10.1007/s00401-014-1336-5 (2014).

8 Nguyen, L. *et al.* Antibody Therapy Targeting RAN Proteins Rescues C9 ALS/FTD Phenotypes in C9orf72 Mouse Model. *Neuron* **105**, 645-662 e611, doi:10.1016/j.neuron.2019.11.007 (2020).

9 Kopito, R. <Kopito 2000 aggresomes T Cell Bio.pdf>.

10 Zhang, K. *et al.* Stress Granule Assembly Disrupts Nucleocytoplasmic Transport. *Cell* **173**, 958-971 e917, doi:10.1016/j.cell.2018.03.025 (2018).

11 Bastos, R., Lin, A., Enarson, M. & Burke, B. Targeting and function in mRNA export of nuclear pore complex protein Nup153. *Journal of Cell Biology* **134**, 1141-1156 (1996).

12 Klim, J. R., Pintacuda, G., Nash, L. A., Guerra San Juan, I. & Eggan, K. Connecting TDP-43 Pathology with Neuropathy. *Trends Neurosci* **44**, 424-440, doi:10.1016/j.tins.2021.02.008 (2021).

13 Coyne, A. N. *et al.* G4C2 Repeat RNA Initiates a POM121-Mediated Reduction in Specific Nucleoporins in C9orf72 ALS/FTD. *Neuron* **107**, 1124-1140 e1111, doi:10.1016/j.neuron.2020.06.027 (2020).

14 Vatsavayai, S. C., Nana, A. L., Yokoyama, J. S. & Seeley, W. W. C9orf72-FTD/ALS pathogenesis: evidence from human neuropathological studies. *Acta neuropathologica* **137**, 1-26, doi:10.1007/s00401-018-1921-0 (2019).
15 Freibaum, B. D. *et al.* GGGGCC repeat expansion in C9orf72 compromises nucleocytoplasmic transport. *Nature* **525**, 129-133, doi:10.1038/nature14974 (2015).
16 Zhang, Y. J. *et al.* C9ORF72 poly(GA) aggregates sequester and impair HR23 and nucleocytoplasmic transport proteins. *Nat Neurosci* **19**, 668-677, doi:10.1038/nn.4272 (2016).
17 Kinoshita, Y. *et al.* Nuclear Contour Irregularity and Abnormal Transporter Protein Distribution in Anterior Horn Cells in Amyotrophic Lateral Sclerosis. *Journal of Neuropathology & Experimental Neurology* **68**, 1184-1192, doi:10.1097/NEN.0b013e3181bc3bec %J Journal of Neuropathology & Experimental Neurology (2009).
18 Napoletano, F. *et al.* The prolyl-isomerase PIN1 is essential for nuclear Lamin-B structure and function and protects heterochromatin under mechanical stress. *Cell reports* **36**, 109694, doi:10.1016/j.celrep.2021.109694 (2021).
19 Coyne, A. N. & Rothstein, J. D. Nuclear lamina invaginations are not a pathological feature of C9orf72 ALS/FTD. *Acta neuropathologica communications* **9**, 45, doi:10.1186/s40478-021-01150-5 (2021).
20 Maury, Y. *et al.* Combinatorial analysis of developmental cues efficiently converts human pluripotent stem cells into multiple neuronal subtypes. *Nat Biotechnol* **33**, 89-96, doi:10.1038/nbt.3049 (2015).
21 Jambeau, M. *et al. biorxiv*, doi:10.1101/2022.01.13.475329 (2022).
22 Slot, J. W. & Geuze, H. J. Cryosectioning and immunolabeling. *Nature Protocols* **2**, 2480-2491, doi:10.1038/nprot.2007.365 (2007).
23 Hurbain, I., Romao, M., Bergam, P., Heiligenstein, X. & Raposo, G. Analyzing Lysosome-Related Organelles by Electron Microscopy. *Methods Mol Biol* **1594**, 43-71, doi:10.1007/978-1-4939-6934-0_4 (2017).

RÉSUMÉ

Chez les patients atteints de SLA familiale et porteurs d'une mutation du gène C9ORF72, cinq types de protéines à répétition dipeptidique s'accumulent dans les tissus du système nerveux. Parmi ces protéines toxiques, la plus abondante est la poly-GA, une glycine-alanine répétée amyloïdogène. Ce travail examine le poly-GA dans des modèles cellulaires de SLA et constate que le poly-GA peut entrer dans l'enveloppe nucléaire, séquestrer les protéines nucléoporines et altérer la dynamique du TDP-43. Dans les motoneurones C9 dérivés de patients atteints de SLA, des membranes nucléaires perturbées et des pores nucléaires potentiellement ectopiques ont été détectés. Le traitement avec un anticorps contre le poly-GA dans ces cellules a réduit le poly-GA soluble mais n'a pas protégé contre l'activation des caspases ou la neurodégénérescence causée par l'inhibition de la synthèse des protéines. Je discute des implications de ces résultats pour la pathophysiologie de la SLA C9 et propose de nouvelles directions de recherche.

MOTS CLÉS

sclerose laterale amyotrophique, transport nucleaire, aggregation des protéines, nucleoporin, poly-glycine-alanine

ABSTRACT

In patients with familial ALS who carry a mutation in the gene C9ORF72, five types of dipeptide-repeat proteins accumulate in nervous system tissue. Of these toxic proteins, the most abundant is poly-GA, an amyloidogenic glycine-alanine repeat. This work examines poly-GA in cellular models of ALS and finds that poly-GA can enter the nuclear envelope, sequester nucleoporin proteins, and alter TDP-43 dynamics. In C9 ALS patient-derived motor neurons, disrupted nuclear membranes and potentially ectopic nuclear pores were detected. Treatment with an antibody against poly-GA in these cells reduced soluble poly-GA but did not protect against caspase activation or neurodegeneration caused by protein synthesis inhibition. I discuss the implications of these results for C9 ALS pathophysiology and propose new directions for research.

KEYWORDS

Amyotrophic lateral sclerosis, nucleocytoplasmic transport, protein aggregation, nucleoporin, poly-glycine-alanine